2021-08-01

Sensitivity Analysis of Transportation Emissions on Near-Road Air Dispersion Using the EPA-Approved Gaussian Air Dispersion Model AERMOD

Ivan Mauricio Ramirez
University of Texas at El Paso

SENSITIVITY ANALYSIS OF TRANSPORTATION EMISSIONS ON NEAR-ROAD AIR DISPERSION USING THE EPA-APPROVED GAUSSIAN AIR DISPERSION MODEL AERMOD

IVAN MAURICIO RAMIREZ

Master's Program in Environmental Engineering

APPROVED:

Wen-Whai Li, Ph.D., P.E., Chair

Ruey Long Cheu, Ph.D., P.E.

Juan Antonio Aguilera, M.D., Ph.D., M.P.H.

Mayra Chavez, Ph.D.

Stephen Crites, Ph.D.
Dean of the Graduate School

Dedication

I dedicate the work done for this thesis to my family, friends, and mentors who constantly gave me the encouragement I desperately needed to push me outside my comfort zone. Special thanks to my parents who provided me with the tranquility, calmness, and quiet that they knew I desperately needed.

I also dedicate this thesis to two very special people who did not need to, but still took the time to push me and remind me that I was a very small step away from finishing this thesis. Dr. Wen-Whai Li and Dr. Mayra Chavez were there for me from the final days of my Bachelor's degree to the very end (not matter how long it took) of my Master's degree. Though our relationship seemed limited to academic work, I would not have been able to complete this work without you.

SENSITIVITY ANALYSIS OF TRANSPORTATION EMISSIONS ON NEAR-ROAD AIR DISPERSION USING THE EPA-APPROVED GAUSSIAN AIR DISPERSION MODEL AERMOD

by

IVAN MAURICIO RAMIREZ, BS, EIT

THESIS

Presented to the Faculty of the Graduate School of

The University of Texas at El Paso

in Partial Fulfillment

of the Requirements

for the Degree of

MASTER OF SCIENCE IN ENVIRONMENTAL ENGINEERING

Department of Civil Engineering

THE UNIVERSITY OF TEXAS AT EL PASO

August 2021

Acknowledgments

I wish to show my most sincere appreciation to my committee members who regardless of their increased workload in this chaotic time, found space in their busy schedule to share with me some of their knowledge and expertise. A very special thank you to Dr. Wen-Whai Li, my committee chairman for his eternal patience and encouragement which began before even thinking about pursuing a Master's degree even came to mind and who more than 6 years ago opened the door for my future career and interest in environmental engineering. Thank you to Dr. Ruey Long Cheu, Juan Antonio Aguilera and Mayra Chavez for committing part of your time to be part of my committee.

I would like to acknowledge the Texas A & M Transportation Institute for providing the calculations for the emission factors which proved to be an essential part of this study.

Abstract

Departments of transportation across the United States have presented concerns over making the American Meteorological Society (AMS) and U.S. Environmental Protection Agency (EPA) Regulatory Model (AERMOD) the new regulatory air dispersion model for federally funded transportations projects. Concerns arose from the lack of data presented on its use in transportation projects. AERMOD was developed to present a steady-state air dispersion model used on industrial complexes which present static emission sources unlike the dynamic sources presented by transportation projects. We used multiple analytical and statistical methods to further understand the sensitivity of the model results based on different factors and therefore create data and cases of what is expected from the model when used in dynamic transportation projects. Eight factors which were the focus of this study are surface roughness, emission type, meteorology, traffic, source characterization, environment, yearly difference, and albedo & Bowen ratio. Adjusting the different factors and comparing them with a baseline scenario made following the guidelines promulgated in the federal regulatory $PM_{2.5}$ Hot-Spot Analysis, we analyze how each of the factors affects the results produced. This study generates emission and air dispersion estimates using traffic and meteorological data from 2016 and 2015 allowing us to compare our results with already existing monitored data. Following regulatory modeling guidelines produced accurate results, it was also found that certain regulatory guidelines such as the use of 5-year offsite data can become counterproductive when compared to monitored data. We found that adjusting factors such as surface roughness, albedo, and Bowen ratio significantly affect the ultimate results. Correct calculation of these factors was found to be significant. Not only do we provide data to demonstrate how different factors affect the model but most importantly provide a guideline for the reproduction of this study in multiple areas across the world to create a deeper understanding of the use of AERMOD for transportation projects.

Table Of Contents

List of Tables

List of Figures

Chapter 1 Introduction

1.1 Mandated Air Dispersion Modeling

Air quality impact assessment for near-road communities requires air dispersion modeling of hourly exposure concentrations resulting from emissions from transportation facilities. Emissions and air dispersion models are useful tools for quantifying air quality and exposure levels and have been used for regulatory purposes involving transportation applications. Air dispersion models are used to predict the impact of pollutants on the desired site and are an essential aspect of the decision-making process of any state departments of transportation (DOT) to approve transportation impact studies. Proper understanding of air dispersion models is required in ensuring federally supported projects comply with National Ambient Air Quality Standards as set forth by the U.S. Environmental Protection Agency (EPA). These models also show significant effects on the human environment within the context of the National Environmental Policy Act (NEPA). Examples of regulatory programs in which dispersion models are essential to include New Source Review (NSR) and Prevention of Significant Deterioration (PSD) regulations. Multiple dispersion models allowed to be federally used are addressed in Appendix A of EPA's Guideline on Air Quality Models (also published as Appendix W of 40 CFR Part 51) *(*U.S. EPA, 2005). The Guideline is used by the EPA, states, tribes, and industry to prepare and review permits for new sources of air pollution and "State or Tribal Implementation Plan" revisions. The Guideline is important as it specifies models for regulatory application and provides guidance for their use.

Federal regulation has, in recent years, increased the significance of impacts caused by mobile pollutants in near-road areas. Stricter regulations have led to upgrading air dispersion models and regulations related to them. Regulation on air dispersion models has ranged from industrial to the transportation sector. The current emphasis on near-road exposure has led the EPA to change its recommended dispersion model from the California Line Source Dispersion Model (CALINE-3) to the American Meteorological Society (AMS) and U.S. Environmental Protection Agency (EPA) Regulatory Model (AERMOD) as of July 14, 2015. The change in

recommended models has affected federal, state, and private transportation agencies as the use of these models have a significant impact on federally funded transportation projects. AERMOD is typically used for industrial purposes but its ability to represent pollutant sources in various forms allows for a better representation of near-road sources.

The recent change in regulatory air dispersion models has created concern among said DOTs due to the limited validation methods of AERMOD when representing transportation sources. Despite being developed for use in industrial point sources, AERMOD has been used for modeling roadway line sources. AERMOD is recommended for a wide range of regulatory applications including highways in all types of terrain (U.S. EPA, 2005). Limited studies in the literature have mixed results thereby not pointing to a consistent trend or a pattern of the concentrations predicted by AERMOD and the real-world monitored data. The lack of real-world measurements and sufficient literary comparisons are some of the primary concerns the DOTs have cited.

1.2 Problem Statement

A recent change in regulation has made AERMOD the recommended air dispersion model for federally funded highway projects. Multiple DOTs have cited the lack of real-world measurements as a source of problems for the implementation of this new regulation. Modeling air dispersion with AERMOD is dependent on a clear understanding of various parameters such as meteorological, land cover, and vehicular density. Lack of real-world measurement comparisons with AERMOD can lead to uncertainty due to overestimation of air pollutant dispersion which can jeopardize the implementation of a new transportation project. On the other hand, underestimating the impact of the project on the environment increases the health risk posed to the nearby population. Since approximately 45 million people are living near high-capacity highways in the United States, a good understanding of the sensitivity of various modeling parameters on AERMOD concentration predictions is fundamental for transportation project planners to minimize the impacts a transportation project may have on residents living near the projects.

1.3 Objective

This research aims to provide a clearer understanding between observed and AERMOD predicted air concentrations by evaluating the effects of data variability in meteorology and other modeling options using $PM_{2.5}$ as the primary pollutant of interest for near-road receptors. The use of $PM_{2.5}$ for this study stems from the growing concern over the adverse health effects produced by black carbon such as inflammation of the respiratory system. Black carbon pollution falls under the category of $PM_{2.5}$ due the particle size as well as its ability to easily infiltrate the inner human lungs. Black carbon emissions are typically attributed to heavy duty vehicles such as 18 wheelers or heavy transportation trucks. Vehicular density and meteorological variables are ever-changing parameters that need to be properly understood for efficient air dispersion modeling. A sensitivity analysis is conducted to provide a clear comparison between the monitored and the AERMOD modeled concentrations resulting from the variability in modeling parameters. By creating various scenarios with parameters of different values in each scenario, the model produces various results that can be used for comparison with monitored data.

Chapter 2 Background Knowledge

2.1 Importance of near-road air pollution to human health

Traffic-related air pollution has a significant impact on human health because of the number of pollutants emitted and the relative proximity between the source and the population. Prior studies have documented the adverse impacts of traffic-related air pollution on respiratory health via acceleration of atherosclerosis or cardiovascular health in adults (Adar et al., 2013; Hoffman et al., 2007). Emerging evidence suggests that close residential proximity to traffic is particularly harmful to children. Schoolchildren living 30-300 meters from a major roadway have been found to have increased arterial stiffness (Iannuzi et al., 2010), increased carotid intima-media thickness (Armijos et al., 2015), and increased clinical asthma symptoms (Wendt et al., 2014) all of which could lead to a decreased academic performance (Gilliland et al., 2001) potentially due to increased absenteeism (Chen et al., 2000). According to a recent national household survey (AHS, 2015), 15.06 million households in the U.S. lived within 1/2 block from a 4-or-more-lane highway, railroad, or airport in 2010. This implies that approximately 43.5 million people were exposed to a high level of traffic emissions in 2011, using an average number of people per household of 2.58 for that year. The numbers are consistent with a widely quoted statistic of 22 million total housing units and 45 million of the population living near traffic facilities (U.S. EPA 2010; Weinstock et al 2013).

The U.S. EPA recognized the potentially detrimental effects of air pollution on public health and required national ambient air monitoring networks to i) provide air pollution data to the general public promptly; ii) support compliance with ambient air quality standards and emissions strategy development, and iii) support for air pollution research studies. In 2006, the U.S. EPA finalized a requirement to conduct an assessment of these networks every five years. In 2010, the U.S. EPA further established requirements for a new national air quality monitoring network that include the characterization of nitrogen dioxide (NO_2) in the near-road environment. Specifically, Title 40 CFR Part 58, Appendix D, Section 4.3.2 requires microscale near-road NO_2 monitors for

core-based statistical areas (CBSAs) with populations of 500,000 or more persons. An additional near-road NO_2 monitoring station is required for any CBSA with a population of 2,500,000 persons or more, or in any CBSA with a population of 500,000 or more persons that has one or more roadway segments with 250,000 or greater annual average daily traffic (AADT). The requirement to install near-road nitrogen dioxide (NO_2) monitoring stations in CBSAs having populations between 500,000 and 1 million by January 1, 2017, was removed by EPA on December 30, 2016 Revision to the Near-road NO2 Minimum Monitoring Requirements, 2016) because i) current near-road monitoring shows that air quality levels, in urban areas with larger populations, are well below the National Ambient Air Quality Standards for NO_2 issued in 2010; and ii) near-road NO_2 concentrations are not expected to be above the health-based national air quality standards in smaller urban areas. However, this action does not change the requirements for near-road NO_2 monitors in more populated areas, area-wide NO_2 monitoring, or monitoring of NO_2 in areas with susceptible and vulnerable populations. The near-road NO_2 monitoring stations are selected by ranking all road segments within a CBSA by AADT and then by identifying a location or locations adjacent to those highest-ranked road segments, considering fleet mix, roadway design, congestion patterns, terrain, and meteorology, where maximum hourly NO_2 concentrations are expected to occur and siting criteria can be met per Title 40 CFR Part 58, Appendix D (EPA, 2016). In addition, measurements at required near-road NO_2 monitor sites utilizing chemiluminescence federal reference methods (FRMs) must include at a minimum: NO, NO_2, and NO_X. Appendix D, 4.2.1 and 4.7.1(b)(2) further requires that at least one $PM_{2.5}$ monitor and one CO monitor be collocated at a near-road NO_2 station.

Recent studies have concluded from reviews of near-road air monitoring data that only PM (PM_{10} or $PM_{2.5}$) in the near-road environment may exceed the annual or 24-hr average NAAQS (De Winter et al., 2018 and Ginzburg et al., 2015). Furthermore, it was concluded that the contribution of traffic-related emissions to the near-road PM pollution is less than 15% (De Winter et al., 2018, Keuken et al., 2013 and Vallamsundar et al., 2013) and near-road PM

pollution does not decrease as rapidly as other pollutants once off the highway (Karner et al., 2010). Traffic $PM_{2.5}$ pollution was reported to dilute slowly to a background level in approximately 1 km (Karner et al., 2010) or remain essentially undiluted at distances well beyond 200 m (Cahill et al., 2016). These studies may not seem to agree well with the estimates derived from a typical Gaussian line source model. For instance, Venkatram showed that the concentration of an inert pollutant decays rapidly to less than 1/5 of its initial strength in 100 m in the direction normal to the roadway (Venkatram et al., 2013). The discrepancy could be attributed to many uncontrollable factors, such as the existence of sound walls for at-grade freeways, elevated or filled sections of a freeway, canopy vegetation, and classification of atmospheric stability conditions. Nevertheless, this gross mismatch between the downwind concentrations and the model estimates shows the need for further model improvement.

2.2 Transportation Hot-spot Analysis for Installing Transportation Facilities

In a typical hot-spot transportation conformity study, Gaussian air dispersion models, such as AERMOD or CAL3QHCR, are performed to provide estimates of the increased pollutant concentrations in space and time resulting from various sources of emissions. CAL3QHCR is a Gaussian dispersion model that in 2015 together with AERMOD was considered a preferred model for pollutant predictions in new federally funded projects. As of 2017 CAL3QHCR has been completely replaced as the preferred air dispersion model by the EPA. Depending on the purposes of the assessment, it may or may not be critical to accurately account for the spatial and temporal variations in the prediction (Wood et al., 2014). For example, the focus of a transportation air quality compliance assessment is to determine whether the incremental impacts due to traffic emissions will result in noncompliance with National Ambient Air Quality Standards (NAAQS) for the criteria pollutants. Under such circumstances, a model is deemed more appropriate than others if it can conservatively, yet realistically, predict the worst 1-hr, 8-hr, 24-hr, or annual averages. An over-conservative estimate used in the determination of air quality compliance could severely hinder or disrupt the implementation of a transportation project, not to mention that an

unbiased prediction of pollutant concentrations in space and time is of pivotal importance for a sound human exposure and health assessment.

A vast amount of effort has been focused on how to improve the accuracy of vehicle emissions and air dispersion models and how to address the sensitivities of various parameters (traffic, emissions, meteorological, topographic, behavioral, etc.) in the models. Model validation requires a good agreement between concentration estimates and data observed at a near-road monitor where more than 85% of the PM is attributed to background emissions from sources other than the road segment immediately adjacent to the monitor.

Air dispersion models are used to predict the impact of pollutants on near-road receptors. The current emphasis on near-road exposure has led the Environmental Protection Agency (EPA) to change its recommended dispersion model from the California Line Source Dispersion Model (CALINE-3) to the American Meteorological Society (AMS) and U.S. Environmental Protection Agency (EPA) Regulatory Model (AERMOD) as of July 14, 2015. The change in recommended models from CALINE-3 to AERMOD has affected federal, state, and private transportation professional as the use of these models have a significant impact on federally funded transportation projects. AERMOD is typically used for industrial purposes but its ability to represent pollutant sources in various forms allows for a better representation of near-road exposure sources.

2.3 Transportation Air Quality

Vehicular transportation is often considered one of the most significant aspects of declining air quality. Heavy-duty diesel vehicles and passenger vehicles are the main contributors to declining air quality related to urban transportations sources (Hodan et al, 2004). Said contributors increase the concentrations of pollutants such as carbon monoxide (CO), carbon dioxide (CO_2), volatile organic compounds (VOCs), hydrocarbons (HCs), nitrogen dioxides (NO_X), and particulate matter (PM) among others. Pollutants emitted from mobile sources are typically created through the incomplete combustion of fossil fuel most often gasoline and diesel. An increase in pollution from mobile sources significantly increases the

health risk primarily of households in close proximity to high-density highways. Epidemiological studies have found that vehicular emissions are an important factor when looking at the exacerbation of asthma, especially in young children (Araujo, 2011).

2.4 Near-Road Air Monitoring

Near-road is a term used to describe areas closer than about 150-200 meters to a high-traffic highway of an annual average daily traffic (AADT) higher than 250,000 in a core-based statistical area (CBSA) (40CFR Part 58, Appendix D.1). Around 45 million people live, work or attend school within 300 feet from a major highway many of them being low-income families. Near-road air monitoring exposure has recently been shown to have an array of adverse health effects. Near-road monitoring began when the EPA promulgated a new national ambient air quality standard for 1-hour nitrogen dioxide (NO_2) in February 2010. Creating a new primary objective, EPA called for the creation of a monitoring network to be used to illustrate near-road exposure to ambient NO_2. A secondary objective of the monitoring network included the monitoring of fine particulate matter ($PM_{2.5}$) and CO. Currently, there are six near-road air monitoring stations in Texas, one in San Antonio, one in Austin, two in the Dallas/ Fort Worth area and 2 in Houston. Out of over 200 monitoring sites only the mentioned six are considered Near-Road according to the EPA mandate on near-road air monitoring. The air monitoring station CAMS 1052 of Houston belongs to the six near-road air monitoring station networks and the data collected from this station is used in this study for comparison with AERMOD concentration predictions.

2.5 Hot-Spot Analysis

The hot-spot analysis is the estimation of future pollutant concentrations as well as a comparison of concentrations relevant to the National Ambient Air Quality Standards (NAAQS). Hot-spot analyses assess the impacts caused by air pollutants within a much-localized area that is usually called an air regulation attainment area which typically covers whole cities. On May 10, 2006, the EPA established a rule creating transportation conformity requirements that are used for the analysis of particulate matter impacts that could arise from new transportation projects.

The use of hot-spot analysis is not confined to only highway projects, any localized projects that could produce new air quality regulations are required to be analyzed using hot-spot analyses.

2.6 Background Concentration

Pollutant concentrations found in near-road monitors include an incremental pollutant concentration from adjacent roadways known as background concentration. It has been found that the $PM_{2.5}$ impacts of traffic emission are not noticeable at 150 meters from the source. Approximately 14% of $PM_{2.5}$ found at near-road sites is produced in the monitored sector (Ginzburg, 2015). Roadway contribution of emissions varies considerably due to changes in the area's microscale meteorology, vehicular fleet, or land classification. Background concentrations are used to represent the concentration of air pollutants already affecting the areas of a new project. This is done by looking at already existent monitored pollutant data from the surrounding air monitoring stations. It is estimated that these concentrations can be up to 95% of the total air pollutant present in the proposed new project pollutant impact (Vallamsundar, 2013). EPA's transportation conformity hot-spot analysis requires the use of background concentration for use in air dispersion modeling.

Background concentrations are important for obtaining the design value of a project. A design value is the addition of the predicted pollutant concentration impact of the new project added to the background concentration. The design value combined with the modeled concentration is of importance given the value calculated being used for compliance by comparing it to the respective pollutant found in the NAAQS. Using the hot-spot analysis regulations, an overestimation of background concentrations can result in an overestimation of air emissions presented whereas underestimation produces misjudged air quality impacts which increase the risk of adverse health effects. Therefore, inappropriate use of background concentrations can negatively affect the approval of the project. It is recommended when analyzing background concentration data to use statistical and mapping methods.

Li and colleagues have evaluated seven background $PM_{2.5}$ concentration estimation methods, 4 of them suggested by the U.S. EPA, using 2 years of hourly urban-scale background

air monitoring data available at 11 sites in 2 Texas cities (Li, 2019). The performance of the methods was assessed by comparing the observations at one site to those estimated from the surrounding sites. The seven methods are listed below.

i) Single station (based on distance, upwind location, and similar surface parameters)

ii) Arithmetic mean from multiple stations

iii) Inverse distance weighing from multiple stations

iv) Inverse distance squared weighing from multiple stations

v) Normalized arithmetic mean from multiple stations

vi) Normalized inverse distance weighing from multiple stations

vii) Normalized inverse distance squared weighing from multiple stations

Method 1 looks at the air pollution from the closest most similar air monitoring station to the area of the project, specifically looking at similarities in land use, meteorology, and main pollutant source.

$$y_{i,j}^{s} = x_{k,j} \ (k \neq i) \tag{2-1}$$

Method 2 estimates the concentration by taking an average of all available background air monitoring stations.

$$y_{i,j} = \frac{1}{m-1}[(\sum_{k=1}^{m} x_{k,j}) - x_{i,j}] \tag{2-2}$$

Method 3 uses a weighted average by the inverse of the distance to the project site.

$$Weight1_{i,k} = \frac{\frac{1}{Distance_{i,k}}}{\sum_{\substack{k=1 \\ k\neq i}}^{m} \frac{1}{Distance_{i,k}}}, k \neq i \tag{2-3}$$

$$Weight1_{i,k} = 0, \quad if\ k = i \tag{2-4}$$

$$z_{i,j} = \sum_{k=1}^{m}(x_{k,j} \cdot Weight1_{i,k}) \tag{2-5}$$

Method 4 is a weighted average but unlike method three the inverse squared distance to the project site is used.

$$Weight2_{i,k} = \frac{\frac{1}{(Distance_{i,k})^2}}{\sum_{\substack{k=1 \\ k\neq i}}^{m} \frac{1}{(Distance_{i,k})^2}}, k \neq i \tag{2-6}$$

$$Weight2_{i,k} = 0, \quad if\ k = i \tag{2-7}$$

$$w_{i,j} = \sum_{k=1}^{m}(x_{k,j} \cdot Weight2_{i,k}) \tag{2-8}$$

Method 5 through 7 are identical to methods 2 through 4 with the only difference being that the time series of each monitoring station is normalized. Method 5 normalizes the estimates of the concentration by taking an average of all available background air monitoring stations.

$$X_{i,j} = \frac{x_{i,j}}{\frac{1}{n}\sum_{j=1}^{n} x_{i,j}},\ i = 1, \cdots, m,\ j = 1, \cdots, n \tag{2-9}$$

$$Y_{i,j} = \frac{1}{m-1}[(\sum_{k=1}^{m} X_{k,j}) - X_{i,j}] \tag{2-10}$$

$$y_{i,j}^{N} = Y_{i,j} \cdot (\frac{1}{n} \cdot \sum_{1}^{n} y_{i,j}) \tag{2-11}$$

Method 6 normalizes the weighted average by the inverse of the distance to the project site.

$$Z_{i,j} = \sum_{k=1}^{m}(X_{k,j} \cdot Weight1_{i,k}) \tag{2-12}$$

$$z_{i,j}^{N} = Z_{i,j} \cdot (\frac{1}{n} \cdot \sum_{1}^{n} z_{i,j}) \tag{2-13}$$

Method 7 is a normalization of the weighted average using the inverse squared distance to the project site is used.

$$W_{i,j} = \sum_{k=1}^{m}(X_{k,j} \cdot Weight2_{i,k}) \tag{2-14}$$

$$w_{i,j}^{N} = W_{i,j} \cdot (\frac{1}{n} \cdot \sum_{1}^{n} w_{i,j}) \tag{2-15}$$

It was found that the 24-hour and annual average background $PM_{2.5}$ concentrations at a site can be best estimated by the normalized inverse squared distance weighted average of the concentrations measured at surrounding background sites. This method was thus used to develop hourly as well as 24-hr average background $PM_{2.5}$ concentrations for CAMS 1052. A detailed description of the algorithms and analyses is included in "Determination of Background PM2.5 Concentrations at Near-road Air Monitors" (Li et al, 2019).

2.7 AERMET

AERMET is a preprocessor for AERMOD, it is primarily used to combine different data sets and create the meteorological data inputs that AERMOD requires. AERMET requires raw hourly surface observations, raw upper air soundings, and the optional raw hourly onsite data.

AERMET merges the files and creates the surface and profile dataset required for AERMOD. AERMET was used in this study to develop on-site and off-site meteorological data for use in AERMOD. Procedures for developing the necessary meteorological files are included in Appendix A. Data input and output for AERMET are briefly discussed in Chapter 3.

2.8 AERMOD

Air dispersion models are used to predict various characteristics of airborne pollutants emitted from stationary sources like power plants or mobile sources like diesel trucks. The characteristics predicted with air dispersion models describe the transportation and dispersion in the atmosphere. Pollutant dispersion is influenced by the inputs on the model which can range from the meteorological condition, type of source, surface, or pollutant characteristics. There are four primary types of air dispersion models called: Gaussian plume dispersion, atmospheric box, source apportionment, and computational fluid dynamics (Holmes, 2006). The most used model type is the Gaussian plume dispersion model due to its accessibility of use. Gaussian models like AERMOD are applicable for distances less than 50 km due to its assumption that emissions and meteorological conditions are not able to consider the Coriolis force and mesoscale meteorology.

AERMOD is a steady-state Gaussian air dispersion model that began development in 1991 through a collaboration of AMS and EPA. The goal of the collaboration was to introduce planetary boundary layer concepts into regulatory air dispersion models. During its development, other issues were found such as plume interaction with terrain, surface releases, urban dispersion, and building downwash. Said issues were prominent in air dispersion models created during the 1990s. As previously mentioned AERMOD was created to model short-range dispersion making it ideal for industrial use. Detailed discussions on the modeling parameters and values utilized are discussed in Chapter 3.

Chapter 3 Study Approach

This study was conducted by modeling the $PM_{2.5}$ emissions and air dispersion from traffic-related activities on a section of an interstate highway, I-610, and by comparing model predictions to data collected from a near-road monitor CAMS 1052 located in Houston, Texas. The modeling domain, emission estimates, meteorology, and AERMOD modeling are discussed in this chapter. A separate study was performed to evaluate all near-road monitors available in Texas prior to this study. CAMS 1052 was selected based on this study (see Appendix A).

3.1 Site Description and Model Domain

The Houston North Loop continuous air monitoring station CAMS 1052 (EPA AQS Site Number: 482011052) is located north of the I-45 Highway in Harris County, Houston, Texas, and was activated on April 13, 2015. The location of this site is at 822 North Loop, Houston with coordinates of 29.81453, -95.38769. Equipment to acquire air pollution data includes CO, $NO/NO_2/NOx$, $PM_{2.5}$, outdoor temperature, wind direction, and wind speed monitors. The monitoring objective of all these samplers is to find maximum precursor emissions impact at a microscale. The distance of this site to the nearest traffic lane is 15 meters and has a sampling probe height of 4 meters. Figure 3-1 shows the locations of the station in relation to the city of Houston, Figure 3-2 shows an image of the station looking to I-610, and Figure 3-3 shows houses adjacent to I-610.

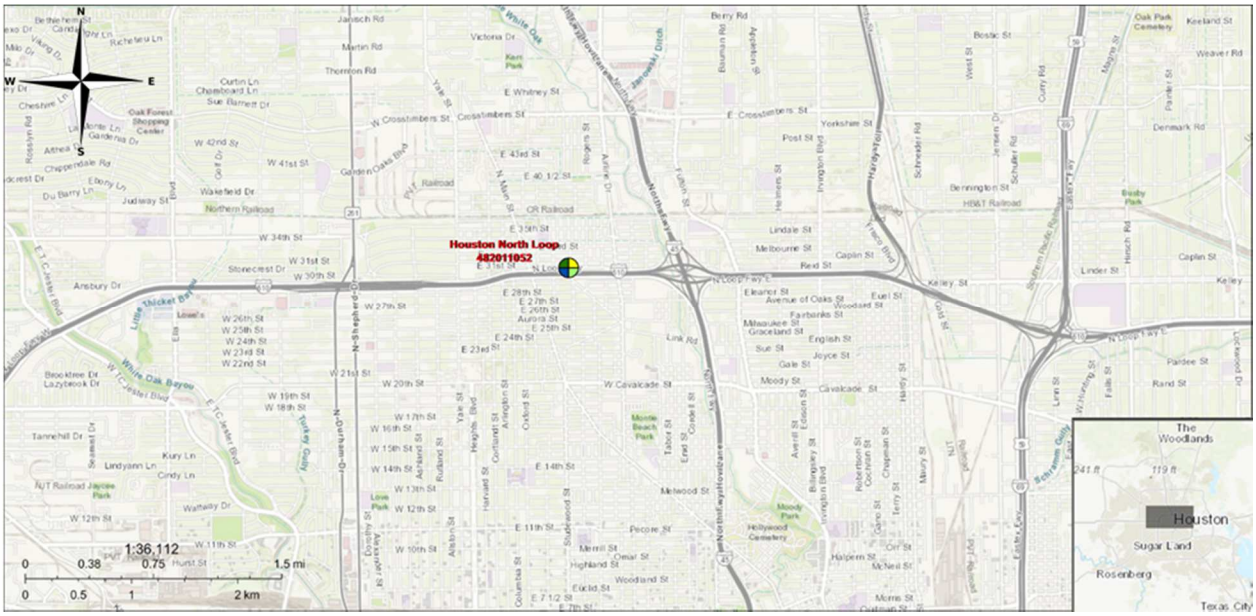

Figure 3-1 CAMS 1052 Mapped Location

Figure 3-2 CAMS 1052 South View

Figure 3-3 CAMS 1052 North View

3.2 Emission Estimation

The Clean Air Act federally regulates on-road and off-road air emissions and defines responsibilities for the EPA to protect public health and improve air pollution. As part of the Clean Air Act, the EPA must constantly revise and update emission rates and estimation models. An emission rate or emission factor is basically the amount of pollutant produced based on the amount of fuel or raw materials consumed. EPA's newest emission model, Mobile Source Emission Simulator (MOVES) was used for this project as it has a model-based approach and for

its capability to estimate both emissions and emission rates at different geographical scales. A model-based approach is important in the creation of emission factors since the use of already tabulated EPA emission factors can appear too general for a very specific study such as ours. MOVES is a model whose primary purpose is the estimation of pollutants created by mobile emission units in the case of this study it was used to produces an estimation of pollutants creates by traffic in I-610. The Emission factors required for air dispersion modeling in this study were processed by the Texas Transportation Institute (TTI). TTI developed the emission data through emission modeling using the EPA's MOVES2014a emission model which was the most current version of the model as of the start of the study. Whenever there is an update to the MOVES model its name is changes based on when or what update it is, at the beginning of this study the most current update to MOVES was made in 2014 hence why the complete name of the model is MOVE2014a. MOVES requires information for 72 vehicle types, ages, fuel types, and the emissions parameters to estimate emission factors. TTI used the latest MOVES2014a inputs in combination with TTI's State Implementation Plan-quality inventory development methodology to develop the emission factors for Interstate Highway 610 to be used in this study. MOVES RunSpecs or MRS provides instructions for how and what data to be used for estimating emission factors. Re-suspended dust emissions factors from paved roads were estimated separately using the dust emission model provided by the U.S. EPA (AP-42, Section 13.2.1) (U.S. EPA 1985). The emission factors calculated by MOVES for vehicular emissions are combined with the re-suspended emission rates for each emission point for each time period and season for I-610 in this study (TTI 2019). This set of data was then processed for use in AERMOD air dispersion modeling. As part of the study, each model run consisted of 29 emission points (source links) used to roughly represent the area of study. Running MOVES scenarios required the input of the following information:

- Description: a summary of the purpose of the modeled scenario
- Scale: definition of the level of analysis (project-scale in this case)

- Periods and aggregation level: Years, months, days, hours, and aggregation by a specified time unit
- Geographic bound: location (e.g., the county where the roadway links modeled is located)
- Vehicle types: vehicle types as specified by engine type, fuel type, and other vehicle technologies (e.g., gasoline passenger car and gasoline passenger truck)
- Road types: on-road roadway link or off-network link in urban/rural environment
- Pollutants and processes: each chemical compound that would be generated by one or more emission processes (e.g., running exhaust oxides of nitrogen).
- Additional User Databases: other user-specified information.

Sixteen MOVES2014a runs were conducted to generate emission rate factors representing four weekday periods and four weather seasons. The four time periods are morning (6 a.m. to 9 a.m.), midday (9 a.m. to 4 p.m.), evening peak (4 p.m. to 7 p.m.), and overnight (7 p.m. to 6 a.m.). The four weather seasons were represented by three months with January through March being Winter, April through June being spring, July through September being summer, and October through December being fall. The results of all runs were extrapolated to represent a whole year of created emissions. It is expected for weekend peak traffic to be at different periods than on weekdays however for this study and due to the complexity of requiring another sixteen MOVES2014a runs only to calculate weekend emission factor, it was decided to uses the same emission factors for the weekend and weekday traffic.

3.3 Meteorology

Meteorological data required for AERMOD was created using the AERMET preprocessor. The AERMET processor requires surface observations, upper air soundings, and minute data which was all acquired from the National Climatic Data Center (NCDC). The on-site

data was acquired from the Texas Commission on Environmental Quality (TCEQ), this is done to have data that accurately represents CAMS 1052 data such as wind speed and direction. To better understand the meteorology of the study area appropriate land use data is required. Land use data was downloaded from the United States Geological Survey. Li, 2019, Determination of Background PM2.5 Concentrations at Near-road Air Monitors describes details of the procedures of how the input files were obtained and processed to develop the necessary meteorological files for AERMOD inputs.

3.4 Model Scenarios

To efficiently run AERMOD and be able to analyze the results for sensitivity a Baseline scenario that provides a neutral reference is necessary. The Baseline scenario for use in the study was created following the PM hot-spot analysis in which peak traffic was used for the calculation of emission rate factors. The emissions factors used for the Baseline represent regional emission rate factors for a bigger area of study than the area of this study. Regional data is meant to be a representation of the Houston area as opposed to only representing the highway sector that is the study area. Three baseline-related scenarios were created, all modeling parameters were kept the same as in the Baseline except for surface roughness. The difference in surface roughness is meant to represent how plain the area is, the difference in the surface roughness is important as the way air and therefore pollutants travel can vary greatly between plain areas and on areas with multiple hills. Three different surface roughness classifications (low, medium, and high) were modeled to examine how the results vary from the Baseline. Scenarios named with the first digit being 0 (Scenario 0) represent model runs equal to the Baseline with only the surface roughness being different among them using the previously mentioned classifications as opposed to the calculated roughness used for the Baseline. Scenarios named with the first digit being 1 (Scenario 1) were designed to evaluate the sensitivity of site-specific emissions on AERMOD concentration estimates. It contains 4 runs for the evaluation of different surface roughness classifications and site-specific emission rate factors on AERMOD outputs. Scenarios named with the first digit being 2 through 4 (Scenarios 2 – 4) differed from the Baseline in the use of

regional meteorological data and surface roughness classification. As required by U.S. EPA in the guidelines for hot-spot analysis, the use of regional meteorological data must include the most recent five years of data, which means data from 2012 to 2016 in our study. Scenarios 2 through 4 use regional meteorological data but different surface roughness: low surface roughness for Scenario 2, medium for Scenario 3, and high for Scenario 4. Scenario named with the first digit being 5 and 6 (Scenarios 5 and 6) differ from the Baseline in the emission rate factor used, scenario 5 uses average traffic, and scenario 6 use hourly traffic. Scenario named with the first digit being 8 (Scenario 8) is used to evaluate the difference in dispersion if the study area was in a rural environment versus an urban environment. Source characterization is evaluated in Scenarios named with the first digit being 7 and 9 (Scenarios 7 and 9). Scenarios 7 and 9 examine the variation in volume source characterization, Scenario 9 applies one row of volume sources with a width of greater than 8 m for simulating the interstate highway emissions Scenario 7 follows the guidance provided in the U.S. EPA hot-spot analysis and uses three rows of volume source to represent a single highway line source, two rows of volume source for frontage line sources and a single row of volume sources for inlet and outlet ramp line sources. Scenario named with the first digit being 10 (Scenario 10) is similar to the Baseline and scenario 0 in the use of the different categories of surface roughness, the only difference being the use of 2015 onsite meteorological data. The purpose of Scenario 10 is to test how consistently AERMOD can produce accurate data based on regulated guidelines. The effects of the Bowen ratio and albedo value are evaluated in Scenarios named with the first digit being 11 through 13 (Scenarios 11 – 13). Sensitivity in AERMOD model outputs resulting from the two parameters is assessed using two extreme values being high (1.0) and low (0.0), to provide the upper and lower bounds for the model outputs and 1 site-specific value obtained from the AERSURFACE (AER) processor. Scenario 11 uses low surface roughness and all variations of Bowen ratio and albedo using all classifications (low, high, and AER). Scenarios 12 and 13 are similar to scenario 11 with the primary difference being that scenario 12 uses medium surface roughness and scenario

13 uses high surface roughness. Table 3-1 summarizes all model scenarios and parameters used in this study.

Table 3-1 AERMOD Scenario Matrix

Scenario	Traffic	Emissions	Meteorology	Environment	Roughness	Bowen Ratio	Albedo	Source
Baseline	Peak	Regional	Onsite-16	Urban	AER	AER	AER	Line
0-1	Peak	Regional	Onsite-16	Urban	Low	AER	AER	Line
0-2	Peak	Regional	Onsite-16	Urban	Medium	AER	AER	Line
0-3	Peak	Regional	Onsite-16	Urban	High	AER	AER	Line
1-1	Peak	Site-Specific	Onsite-16	Urban	AER	AER	AER	Line
1-2	Peak	Site-Specific	Onsite-16	Urban	Low	AER	AER	Line
1-3	Peak	Site-Specific	Onsite-16	Urban	Medium	AER	AER	Line
1-4	Peak	Site-Specific	Onsite-16	Urban	High	AER	AER	Line
2 5 yr.	Peak	Regional	Offsite 12-16	Urban	Low	AER	AER	Line
2-1	Peak	Regional	Offsite 12	Urban	Low	AER	AER	Line
2-2	Peak	Regional	Offsite 13	Urban	Low	AER	AER	Line
2-3	Peak	Regional	Offsite 14	Urban	Low	AER	AER	Line
2-4	Peak	Regional	Offsite 15	Urban	Low	AER	AER	Line
2-5	Peak	Regional	Offsite 16	Urban	Low	AER	AER	Line
3 5 yr.	Peak	Regional	Offsite 12-16	Urban	Medium	AER	AER	Line
3-1	Peak	Regional	Offsite 12	Urban	Medium	AER	AER	Line
3-2	Peak	Regional	Offsite 13	Urban	Medium	AER	AER	Line
3-3	Peak	Regional	Offsite 14	Urban	Medium	AER	AER	Line
3-4	Peak	Regional	Offsite 15	Urban	Medium	AER	AER	Line
3-5	Peak	Regional	Offsite 16	Urban	Medium	AER	AER	Line
4 5 yr.	Peak	Regional	Offsite 12-16	Urban	High	AER	AER	Line
4-1	Peak	Regional	Offsite 12	Urban	High	AER	AER	Line
4-2	Peak	Regional	Offsite 13	Urban	High	AER	AER	Line
4-3	Peak	Regional	Offsite 14	Urban	High	AER	AER	Line
4-4	Peak	Regional	Offsite 15	Urban	High	AER	AER	Line
4-5	Peak	Regional	Offsite 16	Urban	High	AER	AER	Line
5	Average	Regional	Onsite-16	Urban	AER	AER	AER	Line
6	Hourly	Regional	Onsite-16	Urban	AER	AER	AER	Line
7	Peak	Regional	Onsite-16	Urban	AER	AER	AER	Volume
8	Peak	Regional	Onsite-16	Rural	AER	AER	AER	Line
9	Peak	Regional	Onsite-16	Urban	AER	AER	AER	Volume width ≤ 8
10-1	Peak	Regional	Onsite-15	Urban	AER	AER	AER	Line
10-2	Peak	Regional	Onsite-15	Urban	Low	AER	AER	Line
10-3	Peak	Regional	Onsite-15	Urban	Medium	AER	AER	Line
10-4	Peak	Regional	Onsite-15	Urban	High	AER	AER	Line
11-1	Peak	Regional	Onsite-16	Urban	Low	Low	AER	Line
11-2	Peak	Regional	Onsite-16	Urban	Low	Low	Low	Line
11-3	Peak	Regional	Onsite-16	Urban	Low	Low	High	Line
11-4	Peak	Regional	Onsite-16	Urban	Low	High	AER	Line
11-5	Peak	Regional	Onsite-16	Urban	Low	High	Low	Line
11-6	Peak	Regional	Onsite-16	Urban	Low	High	High	Line
11-7	Peak	Regional	Onsite-16	Urban	Low	AER	Low	Line
11-8	Peak	Regional	Onsite-16	Urban	Low	AER	High	Line
12-1	Peak	Regional	Onsite-16	Urban	Medium	Low	AER	Line
12-2	Peak	Regional	Onsite-16	Urban	Medium	Low	Low	Line
12-3	Peak	Regional	Onsite-16	Urban	Medium	Low	High	Line
12-4	Peak	Regional	Onsite-16	Urban	Medium	High	AER	Line

Scenario	Traffic	Emissions	Meteorology	Environment	Roughness	Bowen Ratio	Albedo	Source
12-5	Peak	Regional	Onsite-16	Urban	Medium	High	Low	Line
12-6	Peak	Regional	Onsite-16	Urban	Medium	High	High	Line
12-7	Peak	Regional	Onsite-16	Urban	Medium	AER	Low	Line
12-8	Peak	Regional	Onsite-16	Urban	Medium	AER	High	Line
13-1	Peak	Regional	Onsite-16	Urban	High	Low	AER	Line
13-2	Peak	Regional	Onsite-16	Urban	High	Low	Low	Line
13-3	Peak	Regional	Onsite-16	Urban	High	Low	High	Line
13-4	Peak	Regional	Onsite-16	Urban	High	High	AER	Line
13-5	Peak	Regional	Onsite-16	Urban	High	High	Low	Line
13-6	Peak	Regional	Onsite-16	Urban	High	High	High	Line
13-7	Peak	Regional	Onsite-16	Urban	High	AER	Low	Line
13-8	Peak	Regional	Onsite-16	Urban	High	AER	High	Line

Chapter 4 Meteorological Processing/AERMET

AERMOD requires two MET input files, a surface and a profile file, which are created using AERMET. AERMET consists of three different stages. The first stage extracts the input data and processes them through various quality checks. The second stage merges all the inputs and creates a single file. Stage three creates both the surface and profile files to be used for AERMOD.

4.1 Raw Data Acquisition

For more accurate results from the MET file, there are a total of five input files use to create the MET file. The files created are called Surface, Onsite, Upper Air, AERMINUTE, and AER.

4.1.1 Surface Data

The surface input is acquired from the NCDC which is owned by the National Oceanic and Atmospheric Administration (NOAA). The data placed in a file transfer protocol server at the following link; ftp://ftp.ncdc.noaa.gov/pub/data/noaa/, the year of the desired data is be chosen from the provided list. Once choosing the year of the desired data it is necessary to look at the station code of the desired data. The list containing the code of the desired stations is located in the link called *isd_history.csv* found after the list of data years.

4.1.2 Onsite Data

The output file has to be created from scratch based on what parameters are desired to be used based on Table B-3 in the EPA's AERMET user manual. Each column of the created dataset should represent one parameter. For the case of this project the parameters to be used are day, month, year, hour, precipitation amount, temperature, dew point temperature, wind speed, wind direction, standard deviation horizontal wind, and relative humidity. The data for these parameters can be acquired as a CSV file, from NOAA's Local Climatological Data at the link https://www.ncdc.noaa.gov/cdo-web/datatools/lcd. For more specific data of Texas, all the parameters can also be found using the Texas Air Monitoring Information System (TAMIS) tool on the Texas Commission on Environmental Quality (TCEQ) website.

4.1.3 Upper Air Data

The data for upper air was downloaded in NOAA's Radiosonde Database at the following link; https://ruc.noaa.gov/raobs/. The data format required from Breeze's AERMET is FSL. Once the data is formatted correctly it is then converted to a text file for use in AERMET.

4.2 AERMINUTE

This minute data can be found in the NDCD, the data can be found using the same link as the surface data. As the minute files are too big they will have to be downloaded by month instead of by year. Easier access to the folder is done by copying the following link onto the file explorer search bar; ftp://ftp.ncdc.noaa.gov/pub/data/asos-onemin/6405-2016/. In creating a MET file, the data used should start with the code for the station used for this study which is 6405, followed by the four-letter abbreviation of the desired monitoring station (the abbreviated name for these stations can be found in the link *isd_history.csv* found in ftp://ftp.ncdc.noaa.gov/pub/data/noaa/) and the date in the format; *yyyymm*.

4.3 AERSURFACE

The data from AERSURFACE can be created or simplified by dividing the area of study into different sectors and giving each sector an albedo, Bowen ratio, and surface roughness. In this study, the AERSURFACE program was run using National Land Cover Data from 1992 (NLCD 1992) from the United States Geological Survey (USGS), accessible at https://www.mrlc.gov/viewerjs/. Once the land cover for the area and the latitude and longitude coordinates for the four corners of an area are defined USGS produces a TIFF type file (NLCD 1992).

4.3.1 Running AERSURFACE

AERSURFACE is a scarcely updated processor which requires knowledge of an MS-DOS environment. To run the program more efficiently, the program and the land cover input file need to be in the same folder. The first step required is to write the file name of the TIFF data file followed by a .tif. Naming the file is done to tell the processor which from to obtain data. Following the name of the input, it is necessary to name the output file as a .out file. A choice is

given between which type of coordinate to use, Universal Transverse Mercator or Latitude and Longitude. Upon choosing the type of coordinate system to use, AERSURFACE will allow the user to input the coordinates of the center of the area of study. After the coordinates, the user is prompted to choose a horizontal datum between NAD83 and NAD27. Using the center of the area of study find the radius of the area of study and input it when asked to do so. Similar to Breeze's AERMET the area of study can be divided into different sectors between 1 and 12 sectors. If more than one sector is chosen AERSURFACE allows the user to input the starting and ending polar coordinates. A temporal distribution is select between annual, season, or monthly and can be set up based on preferences. Annual is used if the change in local climatology is negligible. Using the seasonal variation chosen for this study the temporal distribution is divided into winter, spring, summer, and autumn each lasting three months with winter covering from December to February. Monthly variation allows the user to reassign the months in each season. If snow cover is believed to be an important factor in the area of study it must also be set up by choosing which months have snow cover. Much like snow cover, it is also necessary to define if there is an average, high or low amount of moisture in the area. It is also important to know if the area is near an airport. Upon setting all parameters for the area of study, AERSURFACE will create two files, one is a text file and the other is an output file. The output file created is required for AERMET.

4.4 Breeze AERMET

Breeze's AERMET contains five tabs called surface, onsite, upper air, land use, and quality assurance. There is also an option where you may place data that has already been processed by AERMET that allows the user to make changes. Creating an AERMET dataset can be very time-consuming which is why a tool that allows the user to simply update sections of the dataset is fundamental.

4.4.1 Surface Tab

The first tab when looking from top to bottom called surface is divided into different sections called data, station information, options, and ASOS wind data. The first section, data, is

where the surface wind data input will be added to the program, once added the user may select the data format, ISHD is the format used for wind data files. The date of the data will be automatically populated as well as the station information added. The only part of the station information that will not automatically be changed is the time difference from LST. The section called options is where the wind direction can be randomized, substitute surface data for onsite surface data, and adjust surface friction velocity. The ASOS wind data will give the option of applying the ASOS wind speed adjustment, use a threshold for one-minute wind speed, and get the options of using one-minute ASOS wind data. If it is desired to use one-minute data AERMET gives the option of using a created AERMINUTE data file or run AERMINUTE with the acquired minute data which will be placed in the ASOS one-minute data section under ASOS wind data.

4.4.2 Onsite Tab

The onsite tab allows the user to use more specific data from the desired area of study, and this is where the created onsite data will be added. Unlike the surface window, the station information and the date of the data will have to be automatically populated. The options section gives the user the ability to customize the different measurement levels as well as using Bulk Richardson stable layer processing. The format definitions section allows the user to specify how the program will read the added onsite data such as telling it what each information each column contains as well as how many numbers or digits to count before the next column can be read, in the case of the created data there should be eleven different parameters and it should be easier if the first columns are reserved for the date. Data may be placed in either the surface tab or the onsite tab but not both at the same time. The primary difference between the tabs is that onsite data is typically created by the user and the data from the surface tab is downloaded.

4.4.3 Upper-Air Window

The upper air window is very similar to the surface window in that the data added automatically changes the station information as well as the date. When the upper air data acquired is added to the program, the data format must be changed to FSL. The sounding section

is the area where the user can adjust the sounding data, use local sunrise for preferred sounding selection and search for valid sounding.

4.4.4 Land Use Window

The land use window is where data created using AERSURFACE can be added for both the surface and onsite data. There is an option to not use AERSURFACE accessed by selecting to use custom surface characteristics which allows the setting of frequency, soil condition, and the number of sectors the area of study will be divided into which is an AERSURFACE like processor already embedded in Breeze's AERMET. The dialog box where the different land sectors appear can be edited with the angle of the sector and the category. On the window next to surface roughness called albedo/ Bowen ratio, the coverage per land category can be changed representing different percentages. The section called site characteristics will show the calculated albedo, Bowen ratio, and surface roughness and under the section, there is a box that by being checked allows the user to manually change these values.

4.4.5 Quality Assurance

Breeze's AERMOD includes a quality assurance processor. The quality assurance window is designed to allow the user to do an extra quality check based on the limit the user desires to place on every parameter for both the upper air and the surface added data.

Once each window has been changed to the user's preference, on the upper left corner click the run AERMET button which will run all three stages of AERMET producing message and reports files for each stage as well as the surface and profile inputs requires for AERMOD.

4.5 Meteorological Model Scenarios

According to PM hot-spot analysis guidelines, the latest five years of data must be processed when using the regional dataset for air dispersion modeling. Only the most current one-year data should be processed when using onsite data. As part of this project, a single onsite year was created for the years 2015 and 2016 and a five-year regional data file containing data from 2012 to 2016. In addition to yearly data, the Breeze AERMOD graphical interface unit (GUI) allows for the manual input of surface characteristics such as albedo, surface roughness,

and Bowen ratio. Using the manual editing tool allowed for the creation of categories for the three surface characteristics. AERMET stores data per project which does not allow for the user to make parameter changes. This fact made it so that each scenario with a parameter difference stemming from AERMET had to have an individual AERMET project made for it. 35 individual AEMRET runs were produced to be used for the scenarios created through AERMOD the constant in each run was the use of Houston International Airport for surface data and Lake Charles for upper air data. To keep track of all AERMET runs a naming standard was used as follows using *ONSITE_IAH_LCH_16_HLT* as an example note that not all runs require an adjustment of Bowen ratio and albedo making it unnecessary to specify which classification is used in the name of the file.

Regional Data = Onsite or Offsite

Surface Data = IAH (Houston International Airport)

Upper Air Data = LCH (Lake Charles)

Year = 15, 16 or 12-16

Surface Roughness = H (High), L (Low), M (Medium), AER (AER)

Bowen Ratio = H (High), L (Low), AER (AER)

Albedo = H (High), L (Low), AER (AER)

the list below shows the parameters used for each run.

Table 4-1 AERMOD File Creation

Name	Year of Study	Surface Roughness	Bowen Ratio	Albedo	Scenario Use
OFFSITE_IAH_LCH_12-16_H	2012 - 2016	High	N/A	N/A	4 5 yr., 4-1, 4-2, 4-3, 4-4, 4-5
OFFSITE_IAH_LCH_12-16_L	2012 - 2016	Low	N/A	N/A	2 5 yr., 2-1, 2-2, 2-3, 2-4, 2-5
OFFSITE_IAH_LCH_12-16_M	2012 - 2016	Medium	N/A	N/A	3 5 yr., 3-1, 3-2, 3-3, 3-4, 3-5
ONSITE_IAH_LCH_15_AER	2015	AER	N/A	N/A	1-1, 10-1
ONSITE_IAH_LCH_15_H	2015	High	N/A	N/A	1-4, 10-4
ONSITE_IAH_LCH_15_L	2015	Low	N/A	N/A	1-2, 10-2
ONSITE_IAH_LCH_15_M	2015	Medium	N/A	N/A	1-3, 10-3

Name	Year of Study	Surface Roughness	Bowen Ratio	Albedo	Scenario Use
ONSITE_IAH_LCH_16_AER	2016	AER	N/A	N/A	Baseline, 5, 6, 7, 8, 9
ONSITE_IAH_LCH_16_H	2016	High	N/A	N/A	0-3
ONSITE_IAH_LCH_16_HAERH	2016	High	AER	High	13-8
ONSITE_IAH_LCH_16_HAERL	2016	High	AER	Low	13-7
ONSITE_IAH_LCH_16_HHAER	2016	High	High	AER	13-4
ONSITE_IAH_LCH_16_HHH	2016	High	High	High	13-6
ONSITE_IAH_LCH_16_HHL	2016	High	High	Low	13-5
ONSITE_IAH_LCH_16_HLAER	2016	High	Low	AER	13-1
ONSITE_IAH_LCH_16_HLH	2016	High	Low	High	13-3
ONSITE_IAH_LCH_16_HLL	2016	High	Low	Low	13-2
ONSITE_IAH_LCH_16_L	2016	Low	N/A	N/A	0-1
ONSITE_IAH_LCH_16_LAERH	2016	Low	AER	High	11-8
ONSITE_IAH_LCH_16_LAERL	2016	Low	AER	Low	11-7
ONSITE_IAH_LCH_16_LHAER	2016	Low	High	AER	11-4
ONSITE_IAH_LCH_16_LHH	2016	Low	High	High	11-6
ONSITE_IAH_LCH_16_LHL	2016	Low	High	Low	11-5
ONSITE_IAH_LCH_16_LLAER	2016	Low	Low	AER	11-1
ONSITE_IAH_LCH_16_LLH	2016	Low	Low	High	11-3
ONSITE_IAH_LCH_16_LLL	2016	Low	Low	Low	11-2
ONSITE_IAH_LCH_16_M	2016	Medium	N/A	N/A	0-2
ONSITE_IAH_LCH_16_MAERH	2016	Medium	AER	High	12-8
ONSITE_IAH_LCH_16_MAERL	2016	Medium	AER	Low	12-7
ONSITE_IAH_LCH_16_MHAER	2016	Medium	High	AER	12-4
ONSITE_IAH_LCH_16_MHH	2016	Medium	High	High	12-6
ONSITE_IAH_LCH_16_MHL	2016	Medium	High	Low	12-5
ONSITE_IAH_LCH_16_MLAER	2016	Medium	Low	AER	12-1
ONSITE_IAH_LCH_16_MLH	2016	Medium	Low	High	12-3
ONSITE_IAH_LCH_16_MLL	2016	Medium	Low	Low	12-2

Datasets refer to different meteorological files processed for 4 different surface roughness classifications, namely, site-specific (AERSRUFACE), low (0.05 m), medium (0.5 m), and high (1 m). The high, medium and low classifications are used by TCEQ to generally categorize the surface characteristics in the state of Texas. The 2016 single-year files were also created to categorize albedo with the values of 0.01 for low classification and 0.75 for high classification, Bowen ratio with values of 0.01 for low classification and 10 for high classification, and surface roughness with the same values as the five-year data files. Note that for the albedo and Bowen ratio there is not a medium classification defined and instead there is the calculated value. The

high and low values are designed to provide the upper-bound and lower-bound values for the parameter to evaluate their impacts on AERMOD modeled concentrations. Incidentally, the albedo and Bowen ratio computed under the AERSURFACE run land around the midpoint of the classifications. Using similar nomenclature as the surface roughness, albedo and Bowen ratio values were categorized as low, AERSURFACE (medium), and high. A total of 36 different AERMET files were created, including the 28 files created for the 2016 onsite single year.

Chapter 5 Air Dispersion Modeling/AERMOD

5.1 Source Characterization

Two types of source representation methods were used to model the Interstate 610 and frontage road study area, namely, line and volume sources. 29 line sources were used to characterize the highway links of I-610 in all model scenarios except Scenarios 7 and 9. Scenario 7 was elected to evaluate the model sensitivity to the source type selection. Scenario 7 emissions from I-610 were simulated with 3,454 small volume sources following EPA's hot-spot analysis guidelines. The impact on the AERMOD concentration estimates was further evaluated by representing the highway link with fewer volume sources of larger dimensions. This resulted in a total of 704 volume sources for Scenario 9.

5.1.1 Line Sources

Characterization of a line source requires inputs of (1) beginning and ending coordinates (meters), (2) elevation (meters), (3) emission rate ($\frac{g}{sm^2}$), (4) release height (meters), (5) width (meters), (6) initial vertical dimension (meters) and (7) emission rate factor ($\frac{\frac{g}{s}}{m^2}$). Beginning and ending coordinates, in x-y Cartesian coordinates, were input to the file according to the UTM coordinates. The elevation is set as zero for all links, the base elevation for AERMOD is 13.5 meters, the same base elevation as the CAMS 1052 station. Assuming a flat terrain, all sources are set to have a base elevation similar to the CAMS station. Source emission rates can be treated as constant throughout the modeling period. Emission rate factors may be varied by month, season, hour-of-day, or other optional periods of variation and may be specified for a single source or a group of sources. A generic unit emission rate ($1\ \frac{\frac{g}{s}}{m^2}$)was set for all sources in AERMOD such that the true emission rate could be obtained by multiplying the unit emission rate by the variable emission rate factors developed from MOVE2014a for each source link. The variable emission rate factors for each source link were calculated using MOVES14a by season and by hour of day. The width is calculated based on the number of lanes; a single highway lane is designed to be 12 feet or 3.6 meters. The release height and initial vertical dimension for

heavy-duty vehicles is 3.4 meter and for light-duty vehicles is 1.3 meters as developed per EPA's guidelines for hot-spot analysis. Following EPA's guidelines, the release height and initial vertical dimension are calculated by adding the product of the percentage of light-duty traffic (LDT) and 1.3 to the product of the percentage of heavy-duty traffic (HDT) and 3.4 as shown in the equation below giving the value used of 1.487 meters.

$$Source\ Release\ Hight = (LDT \times 1.3) + (HDT \times 3.4) \quad (5\text{-}1)$$

A computer-generated line source representation of the I-610 highway sections was created for use in conjunction with the MOVES model to create the emission sources. The line source representation of the highway initially contained 28 different source links. After adjusting, deleting, and adding new source links, 29 sources were used to better represent the roadway. Adjustments had to be made to the source configurations to accommodate the actual configurations of the highway. For example, a curved section of the highway, such as ramps, will have to be split into at least two links to better represent the curve. Consequently, the emissions will need to be calculated separately for each link accordingly. The final set-up of the line sources represented by purple rectangles for the I-610 section can be seen in Figure 5-1 whereas Figure 5-2 shows the same image superimposed over a map of the area of study.

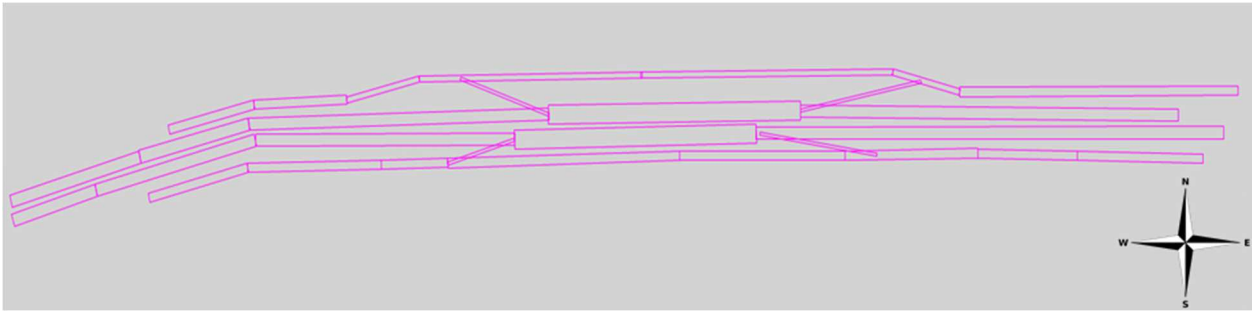

Figure 5-1 Line Source Arrangement Without Map

Figure 5-2 Line Source Arrangement With Map

5.1.2 Volume Sources

Volume source characterization requires inputs of (1) x and y coordinate (meters), (2) elevation (meters), (3) emission rate ($\frac{g}{s}$), (4) release height (meters), (5) initial vertical dimension (meters) and (6) emission rate factor ($\frac{g}{s}$). The x and y coordinate necessary for a volume source represents the center of the source. Elevation, emission rate, release height and initial vertical dimension are identical values as the line sources. The width does not need to be input into the model however it is necessary to calculate the initial lateral dimension, which is an input not present in line sources. The initial lateral dimension is calculated by dividing the width of the source by 2.15. The width is the same as the line source width unless the volume source is divided into more rows of sources, for example when representing the highway sector the line source is turned into three rows of volume sources, the total width of the highway must be divided by three to represent the width of each row, this is then divided by 2.15 to get initial lateral dimension. Width is also necessary for converting emission rate factors from line source to volume source, line source emission rate factors have units of $\frac{\frac{g}{s}}{m^2}$ and volume source emission rate factors have units of $\frac{g}{s}$. Volume sources are represented by squares, in order to get the area covered by the source, the value is squared, the area of the volume source is then multiplied by the linear emission rate factor to convert into a volumetric emission rate factor.

Volume sources are used to simulate a line source and represent the same area. Volume sources were created following this guideline by graphically adjusting them in the same manner as a line source making sure that the center point of each volume source is placed where the line source originally was. The first step to convert line sources into volume sources is to find the

total length of the line source. Using the length of the line source, the amount of volume sources that will replace the line source is found dividing by any value less than 8 meters. If the width is not less than 8 meters an extra row of sources will have to be created to represent the line source in Scenario 7, for instance, if the width of the source is 10.8 meters the width would have to be divided into 5.4 meters making two rows of volume sources equal to one line source. Having found the appropriate width of the volume sources, divide the length of the line source by the width of the volume sources, this is done to approximate the number of volume sources per row that will represent the line source. The center coordinates of each volume source were transformed from the coordinates of the line source using the orientation, width, and length of the corresponding line source. Note that the first volume source in each row must be placed at 0.5 its width from the original line source starting point, this is done so its center lies right in the middle of its width. When the line source is represented by 2 or 3 rows of volume sources, the placement of sources must be adjusted. To do the adjustment the first step is to make a triangle where the line source is the hypotenuse and finding the smallest angle in said triangle. No line source is completely aligned with the east-west trending of the Cartesian plane meaning that translating sources requires the angle to be taken into account for every single line source. Using the center of the first volume source one must find the translation of any subsequent source by finding its translation in the horizontal and vertical direction. Figure 5-3 shown below displays the difference between the setup of 1, 2, and 3 row volume sources as well as being the setup for scenario 7, the sources a represented by red squares.

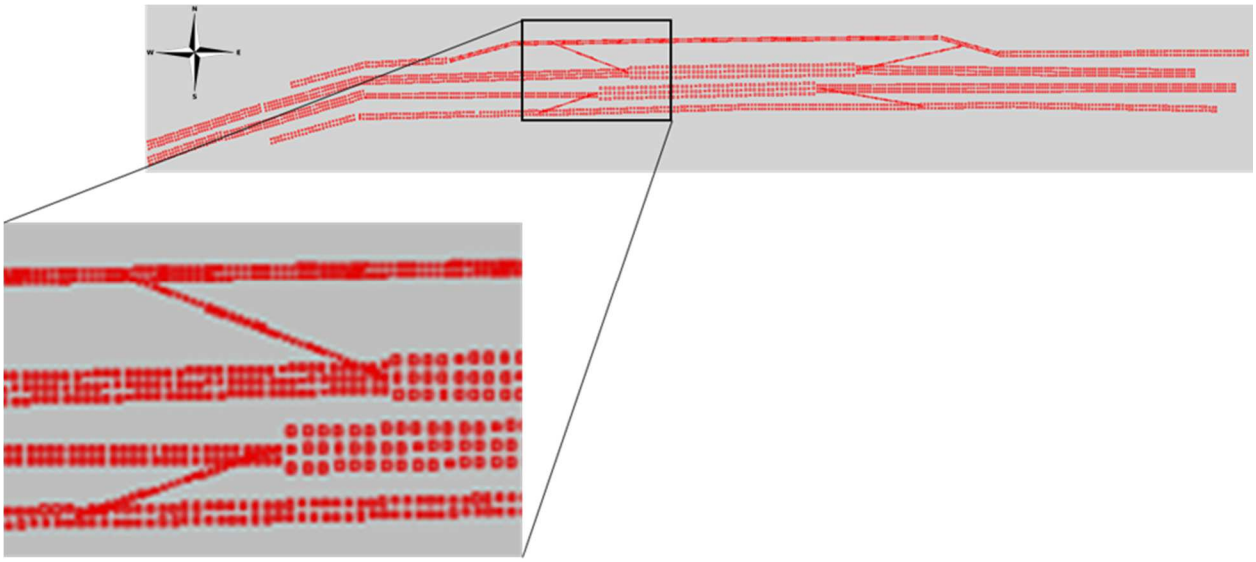

Figure 5-3 Volume Sources Following Hot-Spot Analysis

5.2 Receptor

Two sets of receptors were utilized in this study. The primary receptor for the study is a discrete receptor positioned at the same coordinates as the CAMS 1052 station. A network of grid receptors was generated to provide detailed concentration distributions in the study domain. Two additional sets of receptor networks were created: the first set of receptors is placed on the sources links meant to represent the eastward and westward flowing highway sectors nearest to CAMS 1052 which represent the east and west traffic on Interstate 610 and the second set of receptors is placed north of the source meant to represent CAMS 1052. The receptor network spread out from 5 meters to 500 meters away from the CAMS 1052 receptor. Both sets of receptors represented by yellow dots can be seen in Figure 5-4. A spacing between 15 to 100 meters as shown in Table 5-1 was used to create a grid of receptors to better be able to observe the dispersion of the pollutant particles. The grid setup can be seen in Figure 5-5 where each receptor in the grid is represented by a yellow dot. Each receptor is meant to capture the concentration of $PM_{2.5}$ pollutants at each specific distance from the source. It is expected that the father the pollutant moves form its source there will be a decrease in the amount of said pollutant. When the average value captured by each receptor is plotted it shows a contour around

the source of the pollutant that explains how far and where the pollutant is being dispersed faster of slower.

Table 5-1 Receptor Grid Spacing

Distance (Meters)	5	15	30	45	50	100	200	300	400	500
Spacing (Meters)	15	15	15	15	50	50	100	100	100	100

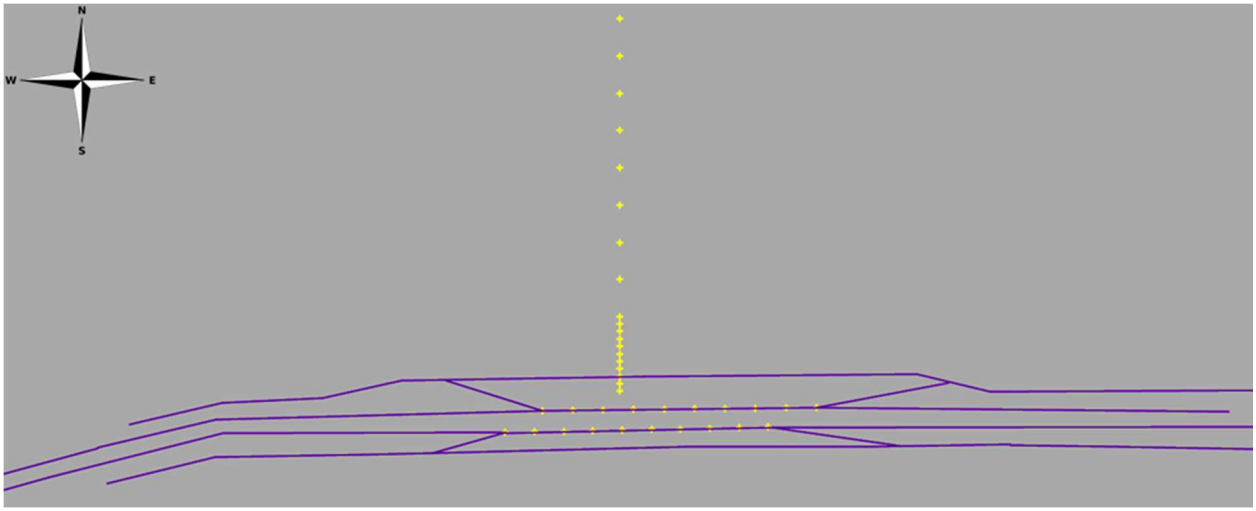

Figure 5-4 In Road and Parallel Receptor Set-Up

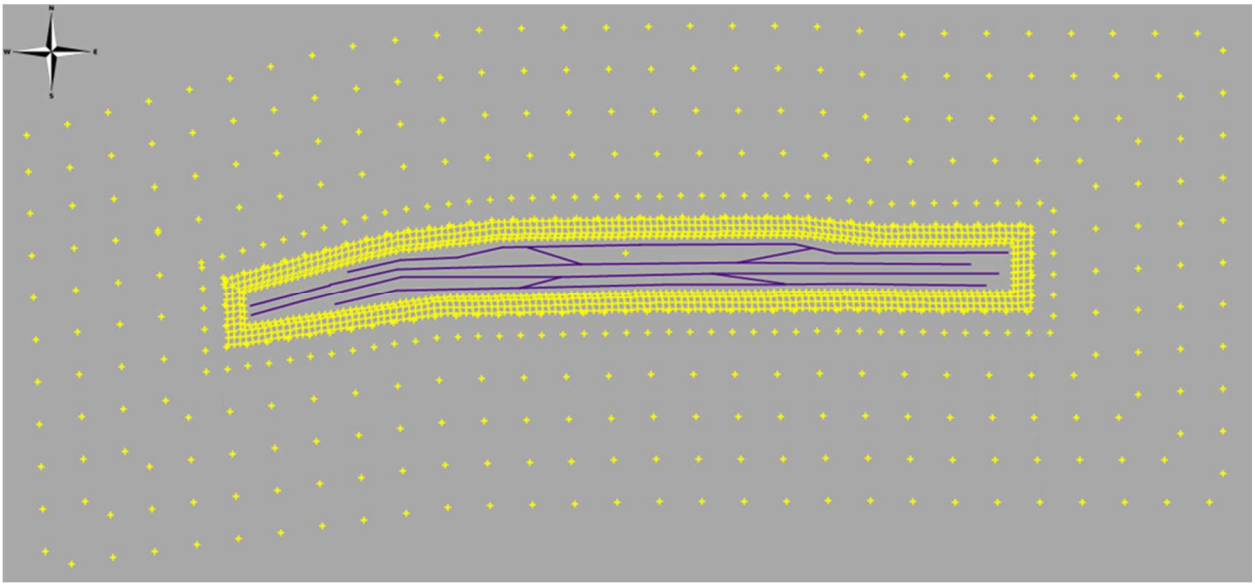

Figure 5-5 Receptor Set-Up for Contour Creation

5.3 Modeling Options

This study follows closely the AERMOD modeling recommendations made in the PM hot-spot analysis. The six primary parameters analyzed as part of the sensitivity analysis are as follows:

- Urban vs. Rural
- Line Source vs. Volume Source
- Meteorology
- Surface Roughness
- Bowen Ratio
- Albedo

AERMOD allows modifications of these parameters which form the basis for this sensitivity analysis. Certain options remained constant across each scenario such as the use of Universal Transverse Mercator (UTM) zone 15 as a projection and World Geodetic System 84 (WGS 84) as the datum. The projection parameters remained constant due to there not being a need in moving the study area, moving the area of study would not allow for an appropriate sensitivity analysis. Version 18081 of AERMOD was released at the same time in which the EPA made AERMOD the preferred air dispersion model for transportation projects. Breeze AERMOD had not implemented this version on its GUI, making version 16216r the most current version in the GUI and the version used for all scenarios. All but one scenario uses an urban environment, AERMOD requires the urban environment to specify the population urban roughness on the study site. The population of the greater Houston area based on the 2017 census was approximately 6,892,427. The urban roughness of 1 meter was used as it is the default value for regulatory purposes. In this study, the outputs required from Breeze's AERMOD were plot files which allow are allowed as input for Breeze 3D Analyst. 3D Analyst creates a graphical representation of the contour created from the network of receptors, to be used to visualize the PM dispersion.

Chapter 6 Results

6.1 Meteorological and Air Pollution Data at the Houston North Loop Site, CAMS 1052

Before being able to create a sensitivity analysis around CAMS 1052 it is necessary to first understand the area's pollution and wind data. The analyzed data was acquired from TCEQ's TAMIS.

6.1.1 Meteorological Data

Meteorology has a strong impact on pollutant dispersion. Figure 6-1 shows wind rose plots that represent the frequency of occurrence of wind direction and wind speed categories for CAMS 1052 in both 2015 and 2016. The predominant wind direction for both stations is from the southwest to the northeast, and the monitoring station is found downwind of I-610 for approximately 47.28 and 43.97 percent of the time on 2015 and 2016 monitoring years respectively as seen in Figure 6-1. The I-610 sector of highway used for this project is situated south of the monitoring station showing that wind is likely to drive pollutants toward the monitoring station and the nearby communities.

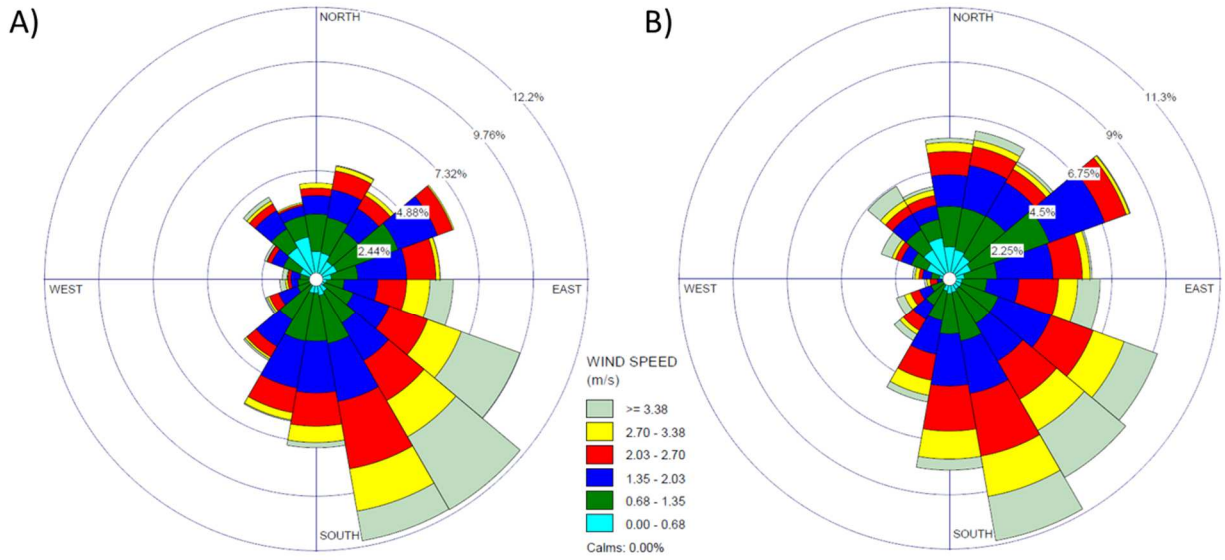

Figure 6-1 Annual CAMS 1052 A) 2015 and B) 2016 Wind Rose

Looking at the 5-year offsite wind data we found that the wind's predominant wind direction is from the southwest to the northeast approximately 45.49 percent of the time. However, there is a significant portion of wind throughout the 5 years that is coming from the north to the south as shown in Figure 6-2.

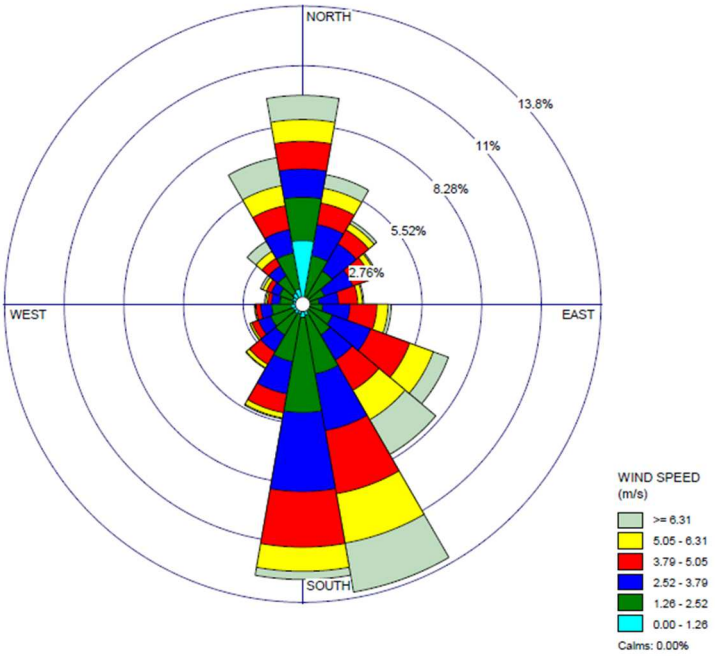

Figure 6-2 CAMS 1052 2012 – 2016 Wind Rose

6.1.2 Air Quality Data

Polar concentration plots that present the frequency of occurrence of pollutant concentrations categorized by wind direction and $PM_{2.5}$ concentration can be seen in Figure 6-2 for CAMS 1052 for the years 2015 and 2016. $PM_{2.5}$ is distributed primarily in the southeast and southwest quadrant, suggesting that $PM_{2.5}$ pollutants come from the general direction of I-610. It is safe to assume that vehicular emissions have a big impact on the population north of I-610 as a majority of the $PM_{2.5}$ concentration comes from the direction of I-610. In 2016 approximately 40 percent of the $PM_{2.5}$ concentration comes from the southeast sector alone. This distribution is more focused than what is seen in 2015 where approximately 50 percent of $PM_{2.5}$ concentrations come from the southern direction.

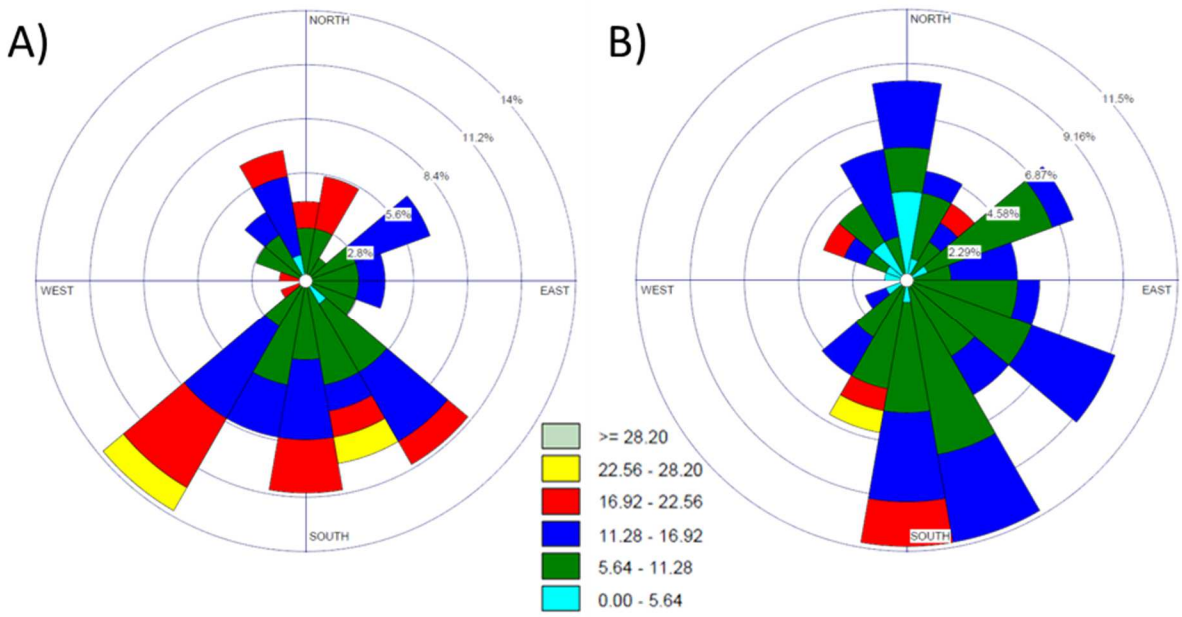

Figure 6-3 Annual CAMS 1052 A) 2015 and B) 2016 Concentration Rose

6.2 Background Concentrations for CAMS 1052

$PM_{2.5}$ background concentrations for CAMS 1052 were developed by taking a normalized inverse distance squared weighted average from multiple regional background stations (Li, 2019). A total of 7 $PM_{2.5}$ monitoring stations not considered to be part of the EPA mandated near-road stations. These 7 monitoring stations were found within a 50-mile radius from CAMS 1052 and the data was used as part of the background concentration calculations using the seven methods discussed in Chapter 2.6 and further in Li, 2019, Determination of Background PM2.5 Concentrations at Near-road Air Monitors. The background concentration study covered data years 2015 and 2016. Calculating the annual average using all 7 methods found that results vary no more than 10 percent between stations and no more than 15 percent between data years. Only 252 days of data from each background station were used for the 2015 data year due to a significant amount of time in 2015 that the $PM_{2.5}$ monitor at CAMS 1052 was either not in operation or under maintenance. Using various statistical analysis methods, it was found that the normalized inverse distance squared weighting method was more accurate at

predicting background concentrations (Appendix C). Figure 6-4 presents a comparison prepared by Dr. Wen Whai Li of all seven calculation methods vs. the observed data of a Fort Worth station being studied in conjunction with CAMS 1052 in the same background concentration study whose results were used for this study. The figure represents how using any estimation method could represent background concentration similarly hence why using any of the 7 methods is seen as acceptable by federal regulation.

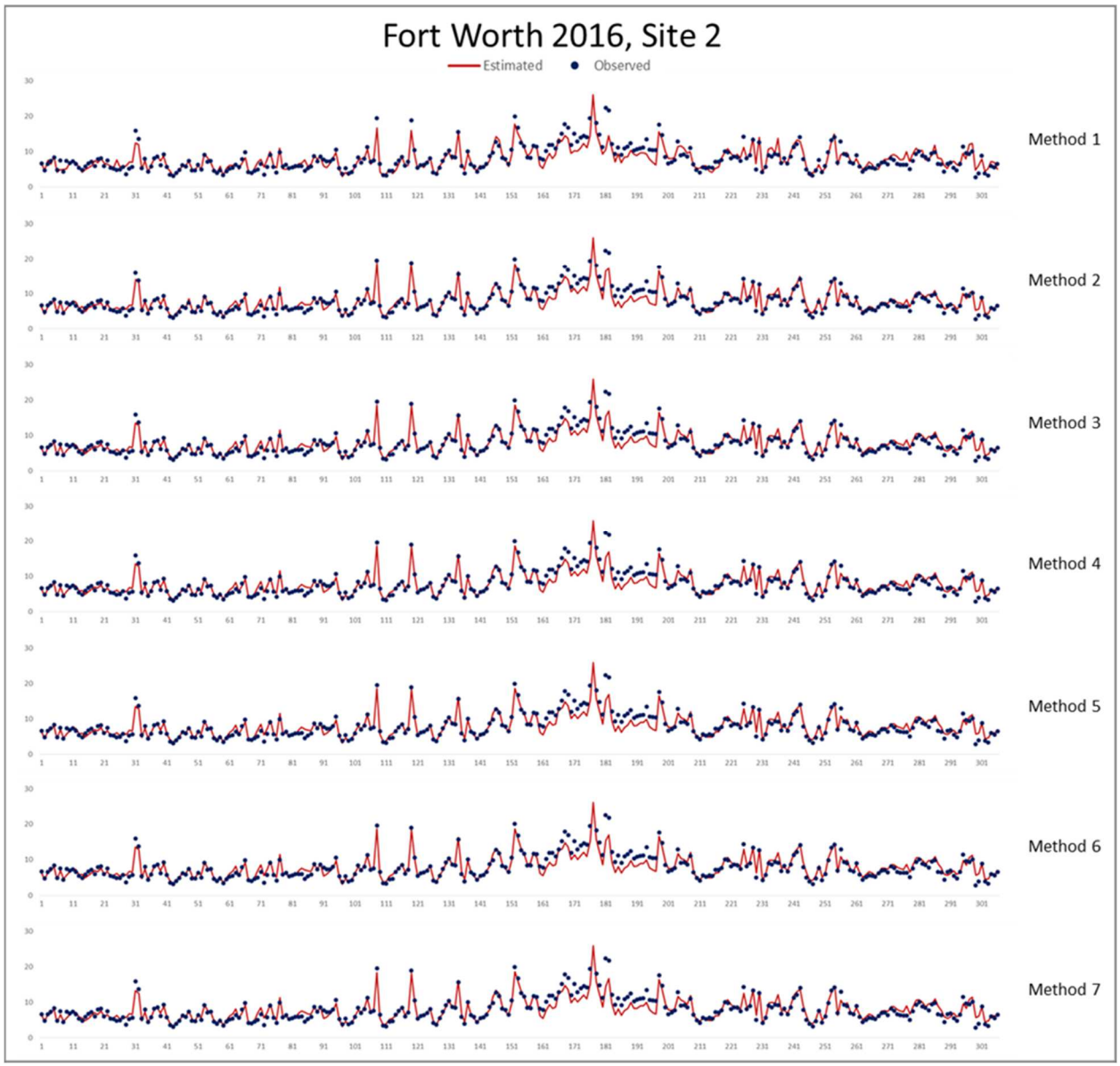

Figure 6-4 Comparison of Predicted vs Observed $PM_{2.5}$ Concentrations by Different Methods

6.3 Model to Monitor Comparison

Using the network of receptors, we were able to create a contour to display the $PM_{2.5}$ dispersions around CAMS 1052. Thanks to the captured concentration of $PM_{2.5}$ pollutants of each receptor shown in figures 5-4 and 5-5 we could clearly visualize how the pollutant concentration is dispersing in regards to its source. Higher $PM_{2.5}$ concentrations were found near the entrance/ exit between I-610 and I-45. Higher concentrations of pollutants can be seen to last farther from traffic going westward than eastward although initial concentrations are higher in eastward traffic. Figure 6-5 represents a dispersion contour created for the Baseline scenario however every other scenario produced a similar trend in dispersion and location of higher pollutant concentrations. Thank to the captured concentration of $PM_{2.5}$ pollutants of each receptor shown in figures 5-4 and 5-5 we could clearly visualize how the pollutant concentration is dispersing in regards to its source.

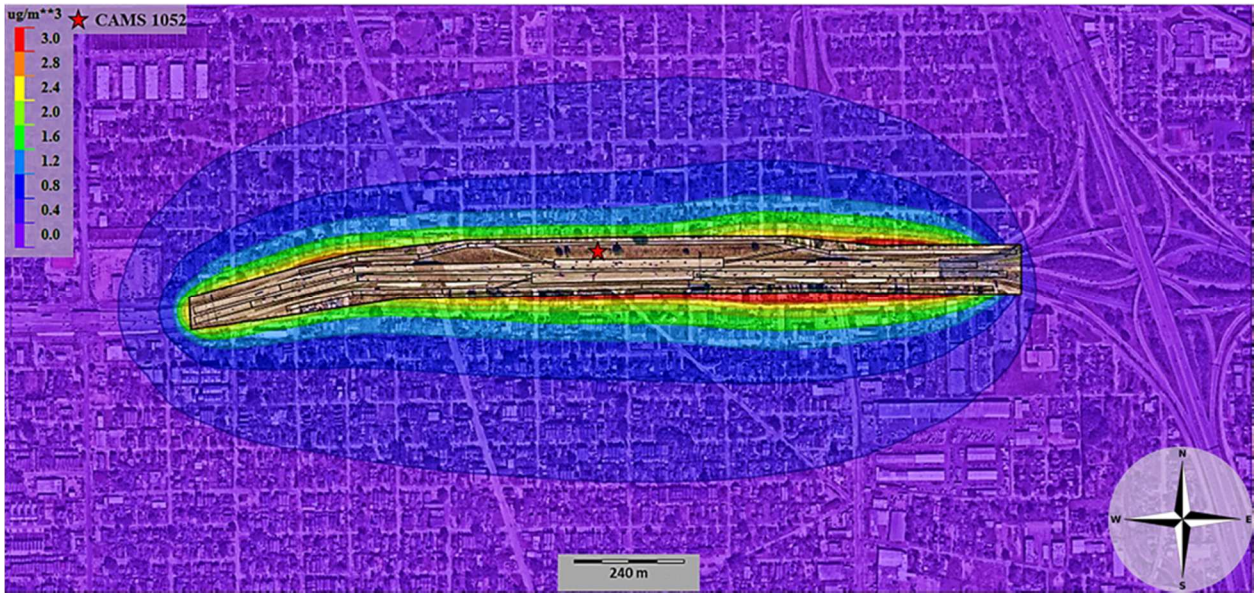

Figure 6-5 Baseline PM2.5 Concentration Dispersion Around CAMS 1052

Analysis of results was done by looking at all scenarios, adding the background concentrations, finding the mean, median, 98th percentile, standard deviation, and comparing the

modeled results with the monitored data from CAMS 1052. Three primary steps were taken to be able to identify the model scenarios that mirrors monitored data with less discrepancy.

The first step in the analysis consisted of comparing the annual mean of all scenarios with the monitored CAMS 1052 data. Most scenarios were compared with 2016 mean values of 10.12 $\mu g/m^3$, scenarios 2-4, 3-4, 4-4, and all the different runs in Scenario 10 were compared with the 2015 mean value of 12.54 $\mu g/m^3$. Scenarios 2 – 4 produced results from 5 years of data, to have a better comparison the mean of both 2015 and 2016 monitored data was calculated to be a mean of 11.09 $\mu g/m^3$. Annual averages of each scenario were presented in comparison with the year of data that it is meant to represent. Quantification of the difference between the scenario and the monitored data was done by calculating the difference between monitored and modeled. Scenario 4-4 was the only scenario to predict lower emissions than its monitored counterpart. Scenario 3-4 has a difference of 0.14 $\mu g/m^3$ from 2015 CAMS 1052 monitored data, making it the most accurate model scenario in terms of the annual average. Scenarios produced using 5-year data produced some of the most accurate results when compared to monitored data. When considering only scenarios containing 1 year of data, the best-modeled results came from scenario 10 runs for which the difference was not higher than 2 $\mu g/m^3$, except for scenario 10-1. Scenario 10 produced modeled emissions for 2015 and was divided into scenarios to look at the calculations when using different surface roughness however the most accurate results among Scenario 10 runs came from the scenario using AERSURFACE calculated roughness. Focusing on scenarios meant to represent the year 2016, Scenarios 5 and 6 which use average and hourly traffic receptively to calculate emission rate factors are the scenarios with the lowest annual average difference from the 2016 CAMS 1052 data with the difference being of 2.08 $\mu g/m^3$ and 2.09 $\mu g/m^3$ respectively. All other scenarios use max traffic to calculate the emission rate factors. Of all the scenarios using max traffic, not including the previously mentioned, the most accurate scenario was 0-3 which uses high surface roughness with a mean difference of 2.8 $\mu g/m^3$ from the monitored data. The remaining 0 scenarios have a difference of 3.86 $\mu g/m^3$ for the scenario 0-2 using medium surface roughness and 5.05 $\mu g/m^3$ for scenario 0-1 using low surface

roughness. A comparable trend can be seen in scenario 1 in which scenario 1-3 which uses high surface roughness has the lowest difference of 2.82 $\mu g/m^3$ from the monitored data. The difference in the remaining Scenario 1 runs is higher than the difference found in the baseline compared with monitored data which was 3.55 $\mu g/m^3$. Scenario 1 using calculated surface roughness had a difference of 3.58 $\mu g/m^3$, scenario 1-2 produced results with a difference of 3.9 $\mu g/m^{3,}$ and scenario 1-1 had a difference of 5.22 $\mu g/m^3$. Scenarios 7 and 9 which use volume sources produced very similar mean values and when compared with CAMS 1052 data the difference was 3.31 for scenario 9 $\mu g/m^3$ and 3.41 $\mu g/m^3$ for scenario 7 for with volume sources were created following federal hot-spot analysis regulations. Scenario 8 produced a difference of 4.34 $\mu g/m^3$ when compared with the monitored data of 2016. Scenario 8 assumed that the area of study was in a rural area which in reality is an urban center. A summary of the mean comparisons of all scenarios is presented in Figure 6-6.

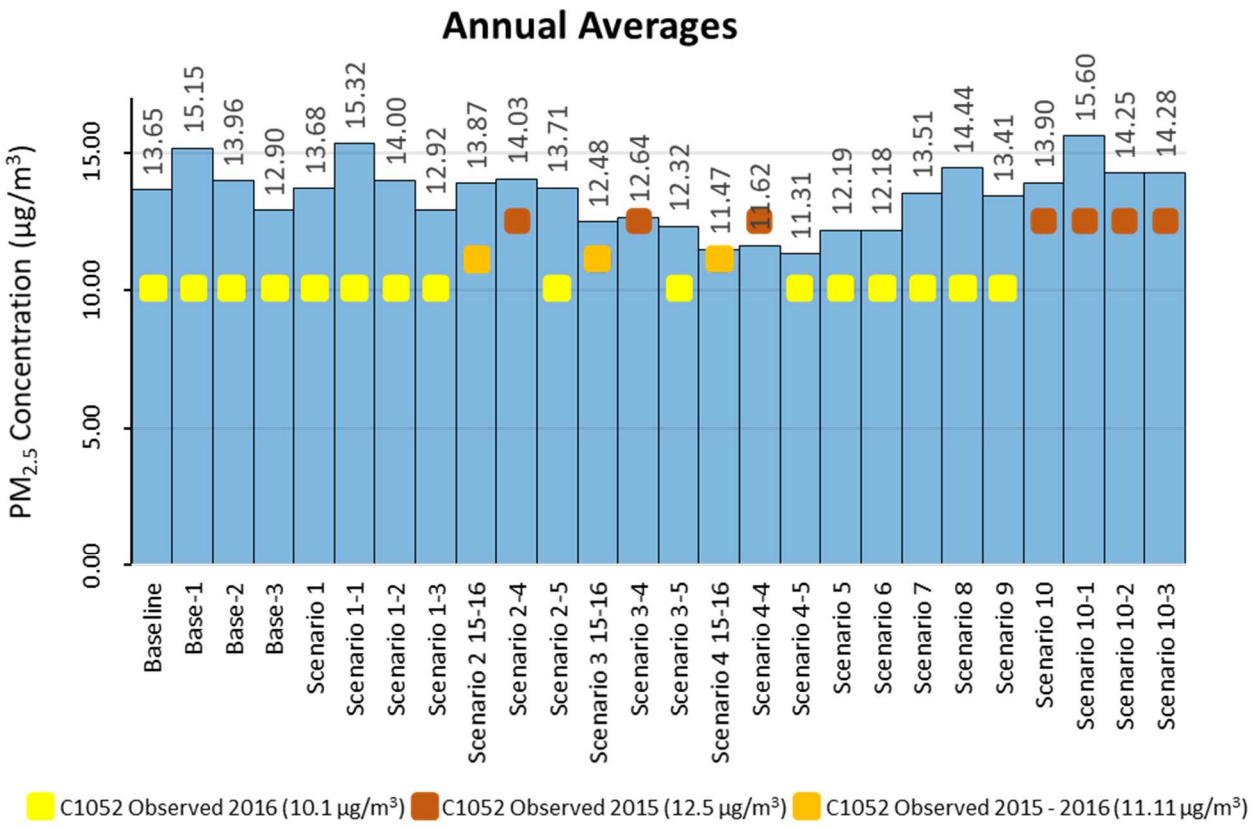

Figure 6-6 Annual Averages Comparison Baseline-Scenario 10

Focusing only on scenarios 11 – 13, Table 6-6 roughly shows that as the surface roughness increases the difference between annual means decreases. Scenario 11 produces the highest annual mean followed by scenario 12 and scenario 13. The difference in modeled and monitored means for scenario 11 ranges from 5.55 µg/m^3 as the highest to 4.4 µg/m^3 as the lowest difference. Ranges in difference from CAMS 1052 and scenario 12 go from 4.15 µg/m^3 to 3.44 µg/m^3. The lowest range of difference between scenarios 11 to 13 is found in scenario 13 going from 2.94 µg/m^3 to 2.51 µg/m^3. The lowest difference in each scenario was produced in the fifth run meaning that scenarios 11-5, 12-5, and 13-5 produced the lowest annual mean difference for their respective scenario. The opposite can be said for scenarios 11-3, 12-3, and 13-3 which produced the highest difference among their scenario. The fifth run in scenarios 11 –

13 uses a high Bowen ratio and low albedo and the third run is created using a low Bowen ratio and high albedo. The highest overall difference in annual means was created by scenario 11-3.

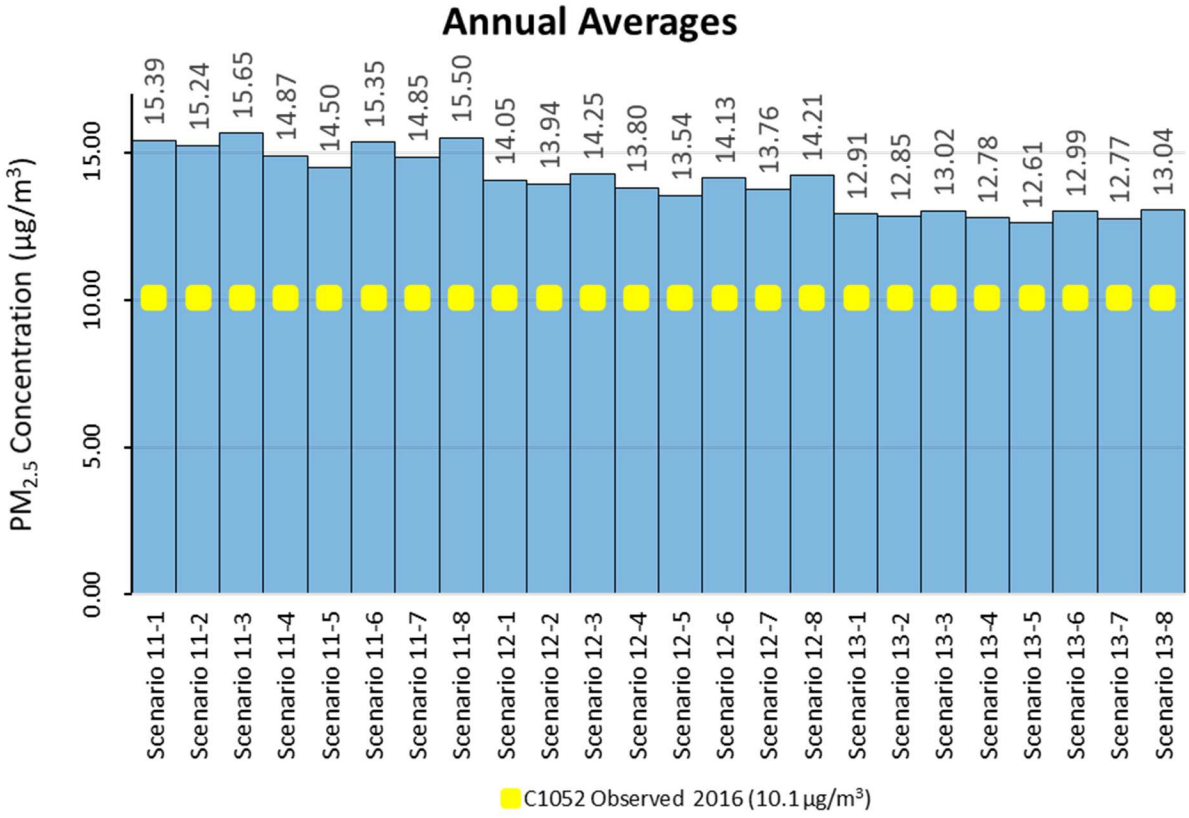

Figure 6-7 Annual Averages Comparison Scenario 11 to Scenario 13

The second analysis focused on evaluating data distribution and much like in the analysis of annual means the results showed that a majority of the scenarios produced higher values than those detected by CAMS 1052. Data distribution analysis was done by creating box plots for the data, a simple analysis was made to recognize the scenarios that better mirrored the monitored data. Analyzing all scenarios was made simpler by separating all scenarios based on similar characteristics. The comparison of data using box plots was made by dividing the dataset based on the four types of surface roughness used meaning that all scenarios were divided into low, high, medium, and AER source roughness. Low surface roughness scenarios show a slightly larger distribution of emissions calculated than the other three categories. Similar to the medium and high categories, the last three box plots represent CAMS 1052 monitored data. CAMS 1052

data is plotted for 2016, 2015, and 2015 together with 2016 to allow for a proper comparison with scenario 10 which produces 2015 data, and scenarios 2, 3, and 4 which produce 2015 and 2016 data. Comparing scenarios that produce only 2016 data show that the distribution of data is constant among all scenarios except 11-4 to 11-6 which were created using a high Bowen ratio. 2016 monitored data was found to have the lowest distribution among the monitored data which is very different from all scenarios producing 2016 data. Among all 2016 scenarios, the distribution from 11-4 to 11-6 were the datasets to most closely reproduce 2016 monitored data. Scenario 10 closely mirrors the distribution of data between the 25^{th} and 75^{th} percentile found in CAMS 1052 for the 2015 year however the scenario shows the distribution with a higher concentration of pollutants than was recorded by monitoring. Combining 2015-2016 data does not show as much distribution as what was found in scenario 2 which produced data from 5 years. In general monitored data was found to record much smaller values and distributions than all scenarios which were modeled with low surface roughness which is displayed in the graph of Figure 6-8.

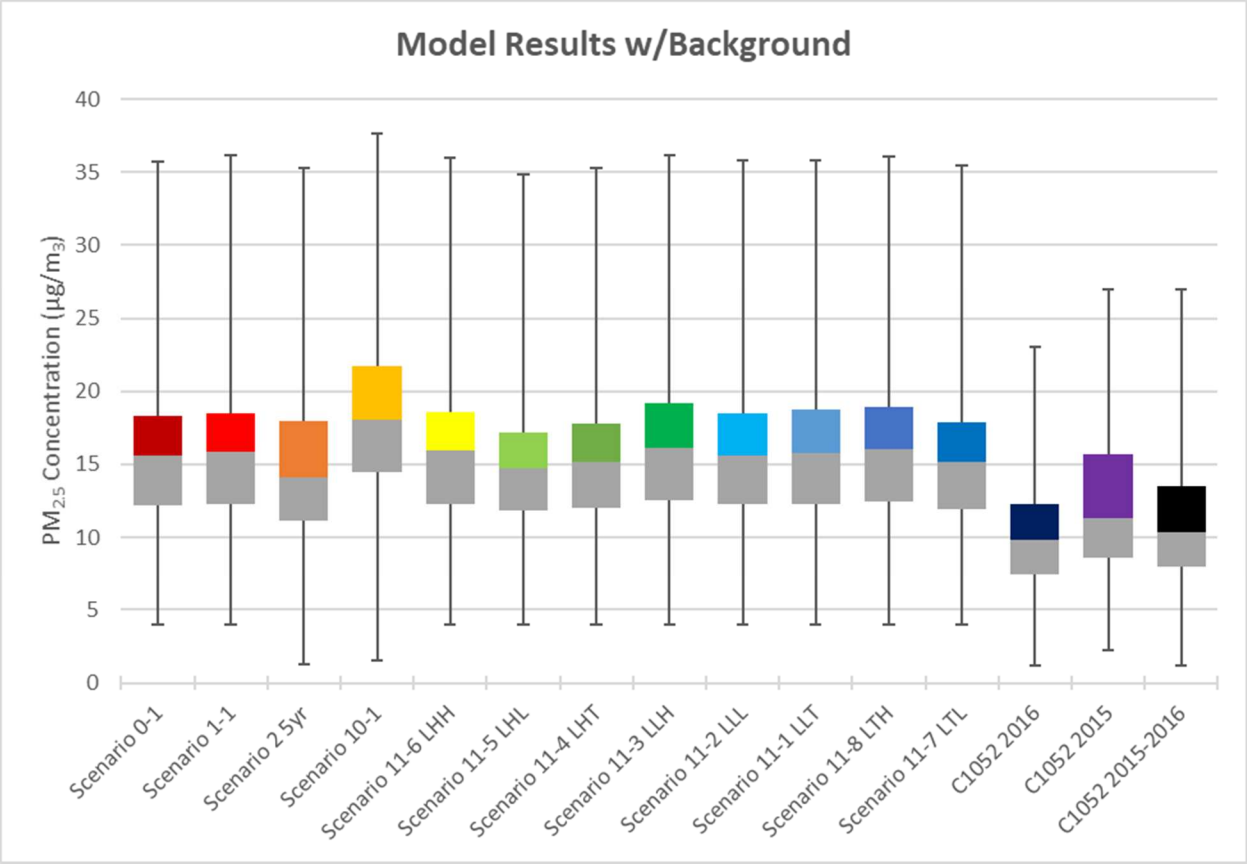

Figure 6-8 Low Surface Roughness Scenario Box Plot

A trend similar to the one found in low surface roughness can be seen in the medium surface roughness scenarios. In general, the values of medium surface roughness scenarios are lower than what is produced by the low surface roughness scenarios, this, in turn, shows a closer resemblance to the values monitored. 2016 scenarios mirror monitored data distribution between the 25th and 75th percentile closer than low surface roughness but still produce higher pollutant concentration. The same can be noted in scenario 10, in which the distribution is similar to the monitored 2015 data, but the values are still much higher. The distribution among the 2016 dataset is slightly more uniform than low surface roughness scenarios except for scenarios12-4 and 12-5 among 2016 datasets which produce the lowest values in all the medium surface roughness scenarios but have a very similar distribution to the 2016 monitored data. The data distribution found for scenario 3 is smaller than the distribution in scenario 2, making it slightly more similar to monitored 2015-2016 data. By comparing the values found in Figure 6-9 and

Figure 6-7 the trend of lower distribution and overall pollutant concentration created by the model scenarios is apparent.

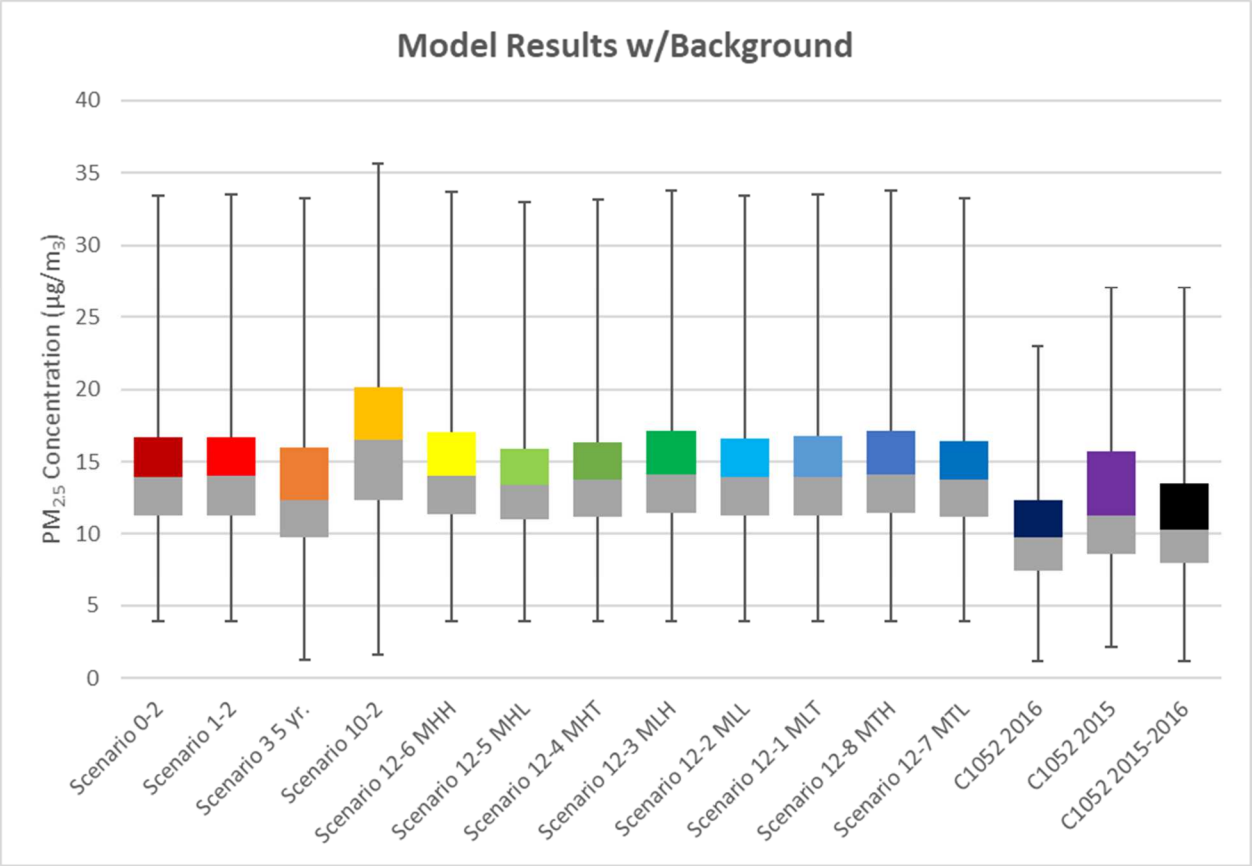

Figure 6-9 Medium Surface Roughness Scenario Box Plot

High surface roughness scenarios produced the lowest pollutant concentration values which when compared to monitored data showed an improvement compared to other surface roughness scenarios. Using pure visualization of data, all 2016 scenarios produce a very similar distribution of data to CAMS 1052 data and each other. The values produced by each 2016 scenario are higher than monitored but are the closest to the 2016 CAMS 1052 data. Similarly, scenario 4 shows a very similar dataset to CAMS 1052 2015-2016 data in terms of both distribution and concentration values. The biggest discrepancy in data sets found in high surface roughness scenarios is found in scenario 10 which produced much higher values than those detected for 2015. 25 percent of the concentration values produced by scenario 10-3 are within

75 percent of the values found by monitoring. The lower values found by analysis of high surface roughness scenarios can be found in Figure 6-10.

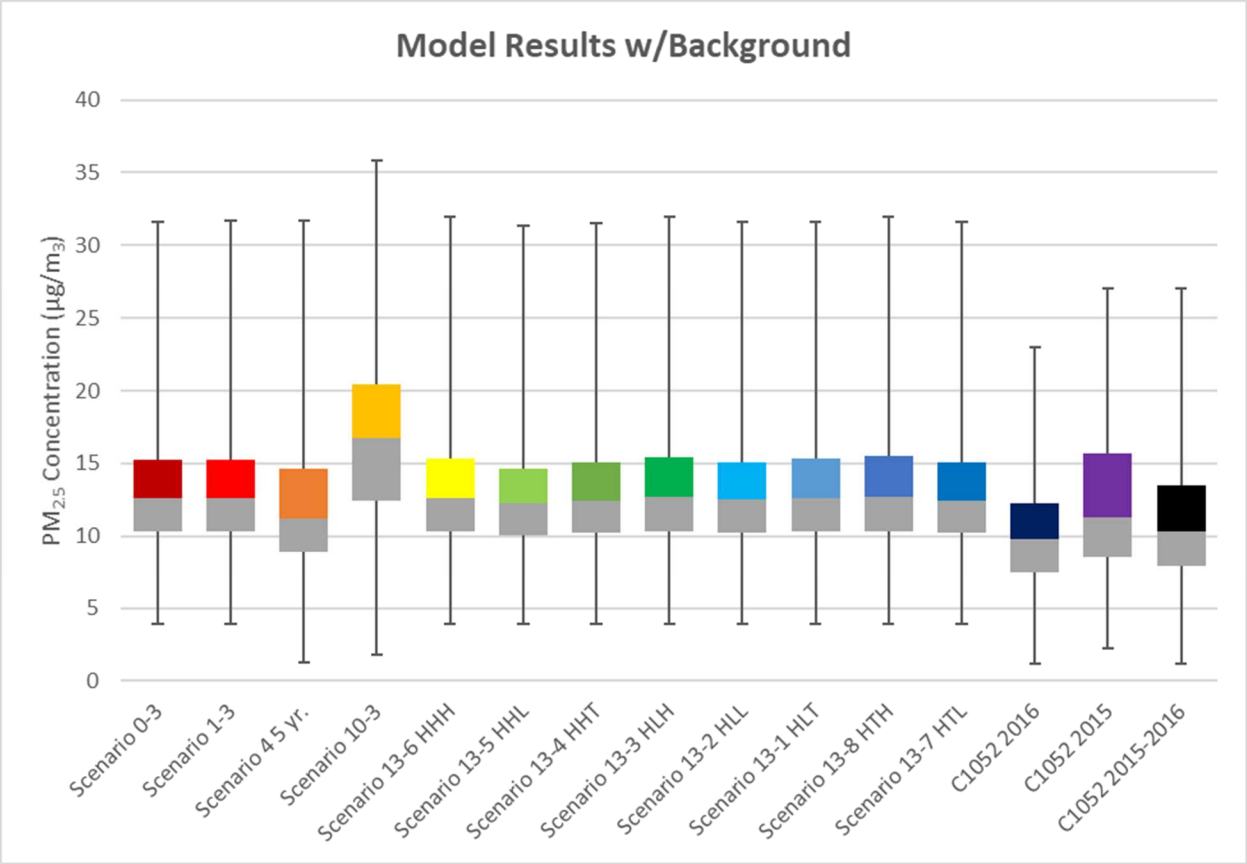

Figure 6-10 High Surface Roughness Scenario Box Plot

The low, medium and high surface roughness scenarios are similar among the three surface roughness classifications, the only difference being the surface roughness. The use of calculated surface roughness is used primarily for comparison of different source, environment, and emission factor calculation types. Emissions produced by the baseline, 1 and 10 are similar to the one produces by their medium surface roughness counterpart which are scenarios 0-2, 1-2, and 10-2. The values were higher than the produced in the high surface roughness scenarios of 03, 1-3 and 10-3 most likely due to the AER values used for surface roughness falls around the range of the medium surface roughness. Likewise, scenarios 7 and 9 which use volume sources, produce slightly higher emissions than the CAMS 1052 monitored data but at similar data

distributions. Scenario 8 which uses a rural environment created some of the highest emission values on all scenarios and its distribution of data is much higher than the monitored 2016 data. Figure 6-11 showcase the comparison of all scenarios that use AR surface roughness with their monitored counterparts.

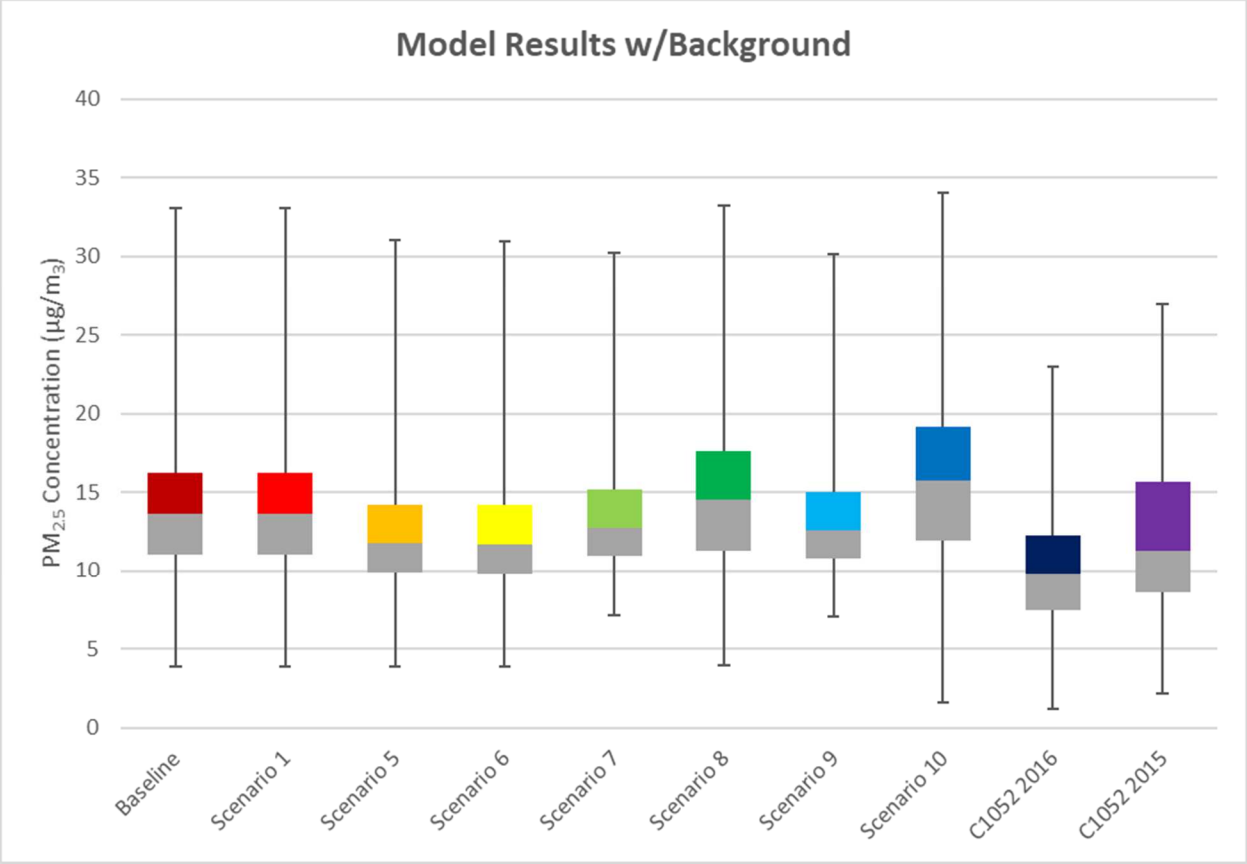

Figure 6-11 AER Surface Roughness Scenario Box Plot

The third analysis uses the findings of the previous 2 analyses to find the ten modeled scenarios closest to CAMS 1052 monitored data. The ten closest scenarios to monitored data are scenarios 4 5 year, 5, 6, 7, 9, 13-1, 13-2, 13-4, 13-5, and 13-7. The ten scenarios have the lowest distribution and annual mean difference to CAMS 1052 from all scenarios, the Table below shows the different annual mean and distribution values of the top ten scenarios.

Table 6-1 Annual Mean and Distribution of 10 Modeled Scenarios Nearest to CAMS 1052

SCENARIO NUMBER	ANNUAL MEAN ($\mu g/m^{3)}$	DISTRIBUTION ($\mu g/m^3$)
4 5-YEAR	0.4362	4.6000
5	2.0923	5.3916
6	2.0766	5.2555
7	3.4123	1.3038
9	3.3066	1.2715
13-1	2.8112	5.9408
13-2	2.7458	5.9342
13-4	2.6834	5.8229
13-5	2.5080	5.7045
13-7	2.6702	5.8871

The reduction of scenarios from 59 to 10 for examination made the analysis more efficient when looking at the data comparison as a whole years' worth of data.

Chapter 7 Discussion

7.1 Sensitivity Factors

Following the use of three different analyses of data produced 10 scenarios out of the 59 were chosen as the closest representation of monitored data. Each scenario is unique in the sensitivity factors that were chosen to represent said scenario and will be discussed by comparing it to scenarios using similar factors. Eight significant sensitivity factors were found to have the most impact on produced results. The eight sensitivity factors are classified as follows:

1. Surface Roughness
2. Emission Type
3. Meteorology
4. Traffic
5. Source Characterization
6. Environment
7. Yearly Difference
8. Albedo and Bowen Ratio

All scenarios were created to fall into one of the eight classifications. Using the results produced and statistical metrics, each factor will be discussed. The top 10 scenarios are discussed by comparing with similar ones and not monitored data hence all values shown in the tables below do not include the addition of background data. When comparing all scenarios with the regulation created Baseline scenario we did not include any background concentrations due to it being the exact same value for every scenario including the Baseline.

7.1.1 Surface Roughness

Surface roughness scenarios focus on 4 different classifications of surface roughness going from the lowest to the highest possible roughness to produce accurate results. As shown in Table 7-1, scenarios 0-1 to 0-3 use different surface roughness and like all other sensitivity factors, they are compared to the baseline scenario. Scenario 0-3 which uses high surface

roughness produces the lowest values in all different study metrics. It has been found in previous studies that there is an increase in pollutant concentrations for reduced surface roughness (Barnes et al, 2014). Surface roughness is a measurement of how smooth the texture of a surface is (in this case the highway). The smoother the surface the less fraction on the surface and the easier it is for particles to disperse allowing for the higher dispersion shown by the results in table 7-1.

Table 7-1 Surface Roughness Sensitivity Factor Model Statistics (in $\mu g/m^3$)

Scenario	Roughness	Mean	Median	SD	98th Percentile
BASE	AER	4.44809	4.67795	2.24284	8.03000
0-1	Low	5.94586	6.50744	3.30820	10.92859
0-2	Med	4.76051	5.11511	2.42734	8.65294
0-3	High	3.69871	3.82794	1.76941	6.79892

Using only statistical metrics it may seem that the base and 0-2 scenarios produce similar values most likely due to the similarities in the surface roughness used for both scenarios. Looking at the ten highest values in each scenario it can be seen that results produced by scenario 0-2 are the most similar to the baseline. Table 7-2 demonstrates the similarities between the baseline and scenario 0-2 as well as how the results compare to the vastly different scenarios 0-1 and 0-3.

Table 7-2 Surface Roughness Sensitivity Factor Highest Ten Values (in $\mu g/m^3$)

Scenario	1st	2nd	3rd	4th	5th	6th	7th	8th	9th	10th
BASE	9.19024	8.91737	8.75931	8.37899	8.37481	8.24306	8.13177	8.03178	8.00257	8.00038
0-1	12.8538	11.7479	11.6639	11.5085	11.3436	11.1973	11.0397	10.9286	10.9210	10.8639
0-2	10.1352	9.37839	9.04919	8.94169	8.81452	8.79961	8.66855	8.65294	8.6246	8.55638
0-3	7.94822	7.88164	7.08169	7.05833	6.91736	6.89411	6.82868	6.79892	6.75443	6.73219

7.1.2 Emission Type

Emission type focuses on where the data used to calculate the emission factor was acquired. For the regional emission factors, the data used to calculate it came from regional Houston traffic data and site-specific uses traffic data found only in the area of study. Focusing solely on regional versus site-specific emission factors turned out to be too simple a comparison. To get a better comparison the surface roughness factor is also included essentially comparing scenarios all four different surface roughness classifications and site-specific emission factors

against the baseline which uses regional emission factor and AER surface roughness. There was a narrow difference between the different emission factors used for both regional and site-specific which can be seen by the little difference between the metric of the baseline scenario and scenario 1-0 shown in table 7-3. Scenarios 1-1 to 1-3 follow the trend found when focusing only on surface roughness which helps cement the fact that higher surface roughness produces lower dispersion. Based on our analysis it is safe to say that the use of different emission factors does not affect the results much when both factors are calculated using data from the same general area.

Table 7-3 Emission Type Sensitivity Factor Model Statistics (in $\mu g/m^3$)

Scenario	Emission	Roughness	Mean	Median	SD	98th Percentile
BASE	Regional	AER	4.44809	4.67795	2.24284	8.03000
1-0	Site-specific	AER	4.48453	4.71570	2.26135	8.11000
1-1	Site-specific	Low	6.11608	6.69991	3.41082	11.23233
1-2	Site-specific	Med	4.80431	5.16533	2.44956	8.73558
1-3	Site-specific	High	3.71554	3.84896	1.77664	6.82185

Table 7-4 further helps point out the similarities between using regional and site-specific emissions. Regional emission factors are simpler to calculate due to the larger availability of data, consequently making the use of them recommendable and with little effect on the overall results produced.

Table 7-4 Emission Type Sensitivity Factor Highest Ten Values (in $\mu g/m^3$)

Scenario	1st	2nd	3rd	4th	5th	6th	7th	8th	9th	10th
BASE ($\mu g/m^3$)	9.19024	8.91737	8.75931	8.37899	8.37481	8.24306	8.13177	8.03178	8.00257	8.00038
1-0 ($\mu g/m^3$)	9.2501	8.97188	8.80186	8.45483	8.45318	8.30659	8.18547	8.11222	8.07239	8.05659
1-1 ($\mu g/m^3$)	13.0009	11.9842	11.9591	11.6724	11.6212	11.3724	11.3420	11.2323	11.1864	11.1863
1-2 ($\mu g/m^3$)	10.1828	9.43552	9.09602	9.02954	8.88828	8.86623	8.76237	8.73558	8.6847	8.63848
1-3 ($\mu g/m^3$)	7.98223	7.95789	7.11425	7.08989	6.9533	6.92255	6.8523	6.82185	6.78323	6.76058

7.1.3 Meteorology

Following EPA's regulations, when using regional meteorological data instead of onsite, the AERMOD run must include the previous 5 years of data (EPA, 1998). Table 7-5 compares the results from the 5-year data, each year from 2012 to 2016, and the baseline. The primary focus of the analysis in Table 7-5 is the comparison of 1-year versus 5-year data but similarly to the emission type analysis there is also an analysis of surface roughness. When including

background concentration scenario 4 5-yr was found to be the scenario most similar to monitored CAMS 1052 data. Scenario 4 5-yr uses high surface roughness which according to AERSURFACE calculations is not the correct roughness for the area of study, meaning that using 5 years of data significantly affects the results of the model run especially as the top results most often use AERSURFACE of mid surface roughness. Comparing baseline to scenarios 2 to 4 find that the values closest to the baseline are found in scenario 2 which use low surface roughness.

Table 7-5 Meteorology Sensitivity Factor Model Statistics (in $\mu g/m^3$)

Scenario	Meteorology	Roughness	Mean	Median	SD	98th Percentile
BASE	Onsite-2016	AER	4.44809	4.67795	2.24284	8.03000
2 5-YR	Offsite 2012-2016	Low	4.83223	5.26234	2.69407	9.18569
2-1	Offsite 2012	Low	5.27328	5.93476	2.72023	9.27798
2-2	Offsite 2013	Low	4.67497	4.97080	2.66467	9.16129
2-3	Offsite 2014	Low	4.86925	5.29080	2.72938	9.46495
2-4	Offsite 2015	Low	4.83386	5.26617	2.76404	9.40432
2-5	Offsite 2016	Low	4.50979	5.06000	2.53150	8.61992
3 5-YR	Offsite 2012-2016	Med	3.39433	3.56850	1.92013	6.80065
3-1	Offsite 2012	Med	3.72105	4.02750	1.94502	7.14663
3-2	Offsite 2013	Med	3.25143	3.36839	1.89413	6.72671
3-3	Offsite 2014	Med	3.43412	3.53319	1.93938	6.99682
3-4	Offsite 2015	Med	3.44093	3.55118	1.99978	6.95242
3-5	Offsite 2016	Med	3.12411	3.44248	1.76678	6.18066
4 5-YR	Offsite 2012-2016	High	2.34618	2.37549	1.29870	4.80074
4-1	Offsite 2012	High	2.58685	2.66846	1.32953	5.18716
4-2	Offsite 2013	High	2.25521	2.27147	1.29680	4.85490
4-3	Offsite 2014	High	2.35578	2.37240	1.29989	4.71806
4-4	Offsite 2015	High	2.41893	2.40276	1.37394	5.02912
4-5	Offsite 2016	High	2.11414	2.25963	1.13747	4.21446

Using 5 years of data appears to be an efficient way of averaging out regional data which helps in representing the area of study when using offsite meteorology. As can be seen in table 7-6, year-to-year predictions can vary wildly, skewing results towards non-accurate results however this is expected as no two years are the same meteorologically wise. Looking at the

years 2012 to 2016 it would seem that the use of 5-year data is not efficient, perhaps due to the varying meteorology found in the Houston or other bay areas, primarily due to the uncertainty of natural disasters such as Hurricanes and heavy rainfall. Table 7-6 shows this uncertainty by displaying how the 2013 (scenarios 2-2, 3-2, and 4-2) model runs compared to a 2016 model run, in which the 2013 scenarios have the higher pollutant dispersion results of the 5 years and 2016 scenarios produce the lowest results of the 10 highest values in each scenario.

Table 7-6 Meteorology Sensitivity Factor Highest Ten Values (in $\mu g/m^3$)

Scenario	1st	2nd	3rd	4th	5th	6th	7th	8th	9th	10th
BASE	9.19024	8.91737	8.75931	8.37899	8.37481	8.24306	8.13177	8.03178	8.00257	8.00038
2 5-YR	10.7465	10.4245	10.0329	9.92534	9.69021	9.51866	9.29630	9.18569	9.11208	9.05789
2-1	11.4954	10.5976	10.5702	10.5647	9.90991	9.70343	9.39458	9.27798	9.27113	9.2205
2-2	11.1125	11.0866	10.0784	9.97293	9.61127	9.59573	9.4262	9.16129	9.13752	9.0607
2-3	10.5271	10.5118	10.3984	10.0966	10.0817	9.79369	9.4673	9.46495	9.2959	9.26083
2-4	11.1590	11.0878	10.3422	10.2397	10.1240	9.81128	9.54679	9.40432	9.39099	9.3675
2-5	9.43849	8.83884	8.77519	8.75277	8.72419	8.68917	8.64666	8.61992	8.46485	8.37994
3 5-YR	8.01908	7.67078	7.51277	7.27215	7.14850	6.93458	6.8958	6.80065	6.72868	6.66464
3-1	8.23584	7.99104	7.63295	7.58591	7.50968	7.20463	7.18747	7.14663	7.00351	6.91635
3-2	8.5635	7.52358	7.4055	6.99365	6.88678	6.85374	6.80603	6.72671	6.64955	6.63448
3-3	8.14157	8.01328	7.86055	7.48968	7.36578	7.07593	7.05768	6.99682	6.9713	6.86717
3-4	8.30717	8.03678	7.96208	7.70934	7.49113	7.16938	7.08708	6.95242	6.8634	6.80978
3-5	6.8473	6.78921	6.70275	6.58217	6.48915	6.36925	6.34074	6.18066	6.15565	6.09544
4 5-YR	5.76623	5.59526	5.39263	5.17377	5.06547	4.99030	4.88749	4.80074	4.76592	4.71216
4-1	5.75327	5.65121	5.57557	5.39819	5.31946	5.30968	5.21359	5.18716	5.18129	5.03957
4-2	6.28584	6.25933	5.5797	5.14414	4.96328	4.8707	4.86045	4.8549	4.781	4.76678
4-3	6.08699	5.77965	5.70523	5.33832	5.23511	5.11454	5.02837	4.71806	4.67485	4.64354
4-4	5.75922	5.58903	5.55627	5.45608	5.38538	5.25976	5.08964	5.02912	5.02882	4.9503
4-5	4.94584	4.69708	4.5464	4.53211	4.42408	4.39686	4.24544	4.21446	4.16362	4.1606

7.1.4 Traffic

Another important factor of the vehicle data used for the calculation of emission factors is the type of traffic used. Throughout the study the type of traffic used was peak, meaning that emission factors were calculated using the highest vehicle density throughout the year during the space of one hour. Table 7-7 shows the significant difference in results from the baseline and scenarios 5 and 6. Both scenarios 5 and 6, which tested the sensitivity of the model to varying traffic data, are among the best representations compared to CAMS 1052 monitored data.

Table 7-7 Traffic Sensitivity Factor Model Statistics (in µg/m^3)

Scenario	Traffic	Mean	Median	SD	98th Percentile
BASE	Peak	4.44809	4.67795	2.24284	8.03000
5	Observed-Avg	2.99226	3.18314	1.53276	5.70478
6	Observed-Hourly	2.97657	3.2204	1.52686	5.69902

At first hand, both scenarios 5 and 6 seem to be closely related due to the little difference between their respective statistical metrics. Table 7-8 clarifies the differences between the results of scenarios 5 and 6 also further displaying the difference of both scenarios to the baseline. Scenario 6 appears to have the least difference between values, which is expected as hourly traffic can be very constant during certain times of the day an example being the little difference in traffic during daily peak hours as compared to the average traffic density day by day.

Table 7-8 Traffic Sensitivity Factor Highest Ten Values (in µg/m^3)

Scenario	1st	2nd	3rd	4th	5th	6th	7th	8th	9th	10th
BASE	9.19024	8.91737	8.75931	8.37899	8.37481	8.24306	8.13177	8.03178	8.00257	8.00038
5	7.22607	6.13999	6.02894	5.91328	5.89745	5.84423	5.74412	5.70478	5.65018	5.59958
6	6.83414	6.56678	6.5312	6.01734	6.01083	5.80083	5.75456	5.69902	5.56379	5.53567

7.1.5 Source Characteristic

Much like the traffic sensitivity factor, source characteristic sensitivity also demonstrates improvements in the quality of data produced by AERMOD when compared to monitored data. Scenarios 7 and 9 are part of the ten closest scenarios to monitored data. Table 7-9 does not show a significant difference between the statistical metric of the baseline when compared with scenarios 7 and 9.

Table 7-9 Source Characteristic Sensitivity Factor Model Statistics (in µg/m^3)

Scenario	Source	Mean	Median	SD	98th Percentile
BASE	Line	4.44809	4.67795	2.24284	8.03000
7	Volume, small	4.31232	4.40526	0.91000	5.92540
9	Volume, large	4.20655	4.29473	0.88917	5.79319

The focus on the ten highest values that are in display in Table 7-10 clarifies why scenarios 7 and 9 are among the best representations of monitored data. Looking at the statistical metric the mean of all three scenarios present in Table 7-9 varies from 4.21 to 4.45, which does

not appear to big a significant difference. By looking at the ten highest values it is found that the values for the baseline range from 9.2 to 8 and for scenarios 7 and 9 the results of the ten highest values range from 6.7 to 5.8 which is a much more significant comparison than the mean.

Table 7-10 Source Characteristic Sensitivity Factor Highest Ten Values (in $\mu g/m^3$)

Scenario	1st	2nd	3rd	4th	5th	6th	7th	8th	9th	10th
BASE	9.19024	8.91737	8.75931	8.37899	8.37481	8.24306	8.13177	8.03178	8.00257	8.00038
7	6.70925	6.34083	6.28471	6.25068	6.1734	6.01703	6.01696	5.9254	5.91329	5.91069
9	6.54478	6.18909	6.12817	6.10062	6.02976	5.86702	5.86554	5.79319	5.78093	5.77263

7.1.6 Environment

The purpose of the environment sensitivity factor was to see if the dispersion of pollutants would be as expected when comparing urban with rural areas. Assuming for this study that a rural area has the same traffic as an urban sector, it is expected for a higher air pollutant dispersion to happen due to the largely missing obstructions in a rural area, primarily buildings. Table 7-11 shows the expected results of a higher air dispersion in a rural area when compared to the urban modeling done by the baseline with overall higher study metric values.

Table 7-11 Environment Sensitivity Factor Model Statistics (in $\mu g/m^3$)

Scenario	Environment	Mean	Median	SD	98th Percentile
BASE	Urban	4.44809	4.67795	2.24284	8.03000
8	Rural	5.24043	5.21976	3.18803	11.57065

Table 7-12 presents the bigger difference between urban and rural dispersion as seen by the 10 highest values produced in each scenario. On average the rural scenario (scenario 8) air dispersion is approximately 42% higher on the highest ten values than the baseline which assumes the study area is an urban center.

Table 7-12 Environment Sensitivity Factor Highest Ten Values (in $\mu g/m^3$)

Scenario	1st	2nd	3rd	4th	5th	6th	7th	8th	9th	10th
BASE	9.19024	8.91737	8.75931	8.37899	8.37481	8.24306	8.13177	8.03178	8.00257	8.00038
8	15.8148	15.5452	13.8479	13.1391	13.0167	11.7880	11.5977	11.5707	11.5194	11.3601

7.1.7 Yearly Difference

Regarding the differing results found in the surface and meteorology sensitivity factors, it was decided to take another look at the difference year and surface roughness data can produce.

Scenario 10-0 is a replica of the baseline scenario with the exception that the data acquired is from the year 2015. Results found in table 7-13 can be interpreted as there not being an unexpected difference between the two years of data according to their statistical metrics. Scenarios 10-1 to 10-3 can be used as further proof of the findings that the lower the surface roughness the higher the dispersion, similar results can also be found in the surface roughness analysis.

Table 7-13 Yearly Sensitivity Factor Model Statistics (in $\mu g/m^3$)

Scenario	Meteorology	Roughness	Mean	Median	SD	98th Percentile
BASE	Onsite-2016	AER	4.44809	4.67795	2.24284	8.03000
10-0	Onsite-2015	AER	4.70414	5.11052	2.12445	7.84386
10-1	Onsite-2015	Low	6.40126	7.28064	3.11775	10.62146
10-2	Onsite-2015	Med	5.04638	5.46297	2.30209	8.51661
10-3	Onsite-2015	High	5.08496	5.27868	2.37697	8.58842

In a similar way as in previous sensitivity factor tables, table 7-14 exemplifies how the different surface roughness affects the results. The table also shows the similarities found between the 2016 and 2015 years of data. Both scenario 10-0 and the baseline do not appear to show a significant difference even though they represent different years, however, mentioned before the climate instability of the Houston area does not allow for confidence when using multiple years of data. The instability primarily comes from the uncertainty of their natural disasters, primarily hurricanes which can be extremely powerful and lengthy one year and nonexistent the next.

Table 7-14 Yearly Sensitivity Factor Highest Ten Values (in $\mu g/m^3$)

Scenario	1st	2nd	3rd	4th	5th	6th	7th	8th	9th	10th
BASE	9.19024	8.91737	8.75931	8.37899	8.37481	8.24306	8.13177	8.03178	8.00257	8.00038
10-0	9.73969	9.45229	8.58405	8.44988	8.31443	8.17758	8.05791	7.84386	7.82309	7.75852
10-1	12.4813	12.2867	12.0856	11.1917	10.7803	10.6908	10.6731	10.6215	10.4808	10.4651
10-2	10.2998	9.78457	9.17941	8.778	8.73793	8.6368	8.59719	8.51661	8.43152	8.23363
10-3	9.38684	9.22416	8.96658	8.84115	8.82455	8.79364	8.77349	8.58842	8.55965	8.28263

7.1.8 Albedo and Bowen Ratio

Though important to test the sensitivity of the albedo and Bowen ratio, they are not as significant as surface roughness due to there not being much variability in surrounding areas.

The low variability of the albedo and Bowen ratio make the two factors make them less significant for the study of sensitivity. TCEQ uses one value for albedo and one value for Bowen ratio per city for their modeling purposes even when using varying surface roughness values. Nonetheless, it is important to understand the effect both factors can have on the air dispersion of an area when doing a sensitivity analysis. Table 7-15 displays multiple scenarios with various combinations of albedo, Bowen ratio, and surface roughness which was also included to further showcase the results found thus far being that the lower the surface roughness used the higher the pollutant concentration. Focusing on only one surface roughness classification the same effect found in surface roughness can be found in the Bowen ratio of higher results produced by lower Bowen ratio, however, the opposite is true for albedo. The amount of lost surface heat calculated by the Bowen ratio varies primarily to the sun exposure of the surface (Lin et al., 2016) meaning that days with less sun create a lower Bowen ratio allowing for higher dispersion. Albedo is a measure of the diffusion of solar radiation on the surface meaning that in an area with low surface roughness there is a higher diffusion of solar radiation which ultimately allows for less radiation to affect the dispersion of air pollutants, this fact helps explain the opposite effects albedo and surface roughness have on the results.

Table 7-15 Albedo and Bowen Ratio Sensitivity Factor Model Statistics (in $\mu g/m^3$)

Scenario	Roughness	Bowen Ratio	Albedo	Mean	Median	SD	98th Percentile
BASE	AER	AER	AER	4.44809	4.67795	2.24284	8.03000
11-1	Low	Low	AER	6.19192	6.75585	3.42807	11.39883
11-2	Low	Low	Low	6.03855	6.47148	3.33759	11.24463
11-3	Low	Low	High	6.44735	7.03608	3.57966	12.00342
11-4	Low	High	AER	5.67440	6.15234	3.16586	10.80091
11-5	Low	High	Low	5.30245	5.88803	2.97218	10.18656
11-6	Low	High	High	6.14782	6.70863	3.42862	11.32080
11-7	Low	AER	Low	5.65296	6.18022	3.14582	10.58450
11-8	Low	AER	High	6.29780	6.87313	3.51430	11.73565
12-1	Med	Low	AER	4.85075	5.14032	2.45277	8.82514
12-2	Med	Low	Low	4.73980	5.00694	2.39547	8.53079
12-3	Med	Low	High	5.04878	5.27185	2.55830	9.24327
12-4	Med	High	AER	4.59619	4.88237	2.34589	8.41053
12-5	Med	High	Low	4.34194	4.65118	2.22689	8.12226
12-6	Med	High	High	4.93173	5.25508	2.51455	9.06841
12-7	Med	AER	Low	4.55806	4.86601	2.32694	8.29077
12-8	Med	AER	High	5.01422	5.28107	2.55981	9.23636
13-1	High	Low	AER	3.71118	3.84675	1.74912	6.78243
13-2	High	Low	Low	3.64575	3.77885	1.71264	6.59966
13-3	High	Low	High	3.82154	3.93180	1.80328	6.83615
13-4	High	High	AER	3.58336	3.72254	1.71065	6.44849
13-5	High	High	Low	3.40802	3.59286	1.62863	6.25126
13-6	High	High	High	3.78810	3.92320	1.80635	6.85360
13-7	High	AER	Low	3.57024	3.70901	1.70436	6.45871
13-8	High	AER	High	3.83638	3.94613	1.83705	7.07736

Scenarios 13-1, 13-2, 13-4, and 13-5 are in the ten best-representing scenarios to the monitored data. Neither of the four scenarios uses high albedo which increases the results produced. All four of the scenarios stand out in table 7-16 as having some of the lowest values produced in the albedo, Bowen ratio sensitivity factor. The best representation of monitored data in these four scenarios is produced by scenarios 13-1 and 13-2 which both have high surface roughness and low Bowen ratio and the only variability comes from the use of low and AERSURFACE calculated albedo.

Table 7-16 Albedo and Bowen Ratio Sensitivity Factor Highest Ten Values (in µg/m^3)

Scenario	1st	2nd	3rd	4th	5th	6th	7th	8th	9th	10th
BASE	9.19024	8.91737	8.75931	8.37899	8.37481	8.24306	8.13177	8.03178	8.00257	8.00038
11-1	13.5478	12.0197	11.978	11.9116	11.8929	11.6648	11.663	11.3988	11.3814	11.2741
11-2	12.8758	11.8863	11.8301	11.6391	11.4734	11.4551	11.3352	11.2446	11.1236	11.0815
11-3	14.0310	12.8869	12.4477	12.4204	12.2565	12.2465	12.1503	12.0034	11.8592	11.7798
11-4	12.5089	11.3762	11.1256	11.1157	10.9555	10.9434	10.9306	10.8009	10.7142	10.6753
11-5	12.1576	11.1445	10.6906	10.5811	10.2879	10.2727	10.2296	10.1866	10.1458	10.1394
11-6	13.4744	12.8093	12.1335	11.8828	11.6566	11.5988	11.3983	11.3208	11.3153	11.2640
11-7	11.9432	11.3550	10.9919	10.9434	10.8938	10.7882	10.7744	10.5845	10.5509	10.4778
11-8	13.6763	12.8481	12.2683	12.1957	12.0339	11.8977	11.8136	11.7357	11.6819	11.6721
12-1	10.4097	9.60249	9.23161	9.09037	9.08662	8.97631	8.86565	8.82514	8.79066	8.78845
12-2	9.84063	9.58624	9.16733	9.08163	8.99182	8.81379	8.73498	8.53079	8.48519	8.42775
12-3	10.8002	10.0546	9.69362	9.66243	9.64403	9.46188	9.28546	9.24327	9.22382	9.0863
12-4	9.94618	9.00179	8.91724	8.76319	8.69652	8.60951	8.59984	8.41053	8.39157	8.3543
12-5	9.56216	8.90964	8.63527	8.53558	8.22309	8.19782	8.19579	8.12226	8.07524	8.00884
12-6	10.5898	10.0327	9.53906	9.39139	9.12642	9.0961	9.07147	9.06841	8.98475	8.96842
12-7	9.4355	9.09261	8.99883	8.69794	8.59058	8.36568	8.31484	8.29077	8.25729	8.2545
12-8	10.6833	10.0430	9.7689	9.59642	9.38917	9.29217	9.24485	9.23636	9.16126	9.14373
13-1	7.99651	7.9311	7.2806	7.20938	6.93388	6.92658	6.85352	6.78243	6.65171	6.64009
13-2	7.93267	7.56889	7.20489	6.92192	6.80086	6.74133	6.60761	6.59966	6.57616	6.54575
13-3	8.24816	7.95331	7.73981	7.6539	7.16508	6.97508	6.86336	6.83615	6.82055	6.80293
13-4	7.79602	7.60449	7.16899	6.89423	6.80515	6.77764	6.61814	6.44849	6.44519	6.35448
13-5	7.58766	7.37821	6.84509	6.63083	6.45227	6.31971	6.29917	6.25126	6.23536	6.13029
13-6	8.16215	7.95331	7.52551	7.44966	7.15582	6.92336	6.89322	6.8536	6.80183	6.73999
13-7	7.74005	7.41343	6.96557	6.88544	6.80048	6.48951	6.47592	6.45871	6.44261	6.43546
13-8	8.21168	8.19337	7.64525	7.55401	7.16007	7.13881	7.09006	7.07736	7.03652	6.97999

The first analysis was divided into scenarios focusing on each of the distinct sensitivity factors. The analysis consisted of looking at the annual mean of every scenario and compare it to CAMS 1052. By looking at the first part of the first analysis which consisted of scenarios with variability in environment, traffic, surface roughness, and modeling year it was found that in general scenarios with 2015 data are closer to the CAMS 1052 2015 annual mean which was not the same when comparing 2016 data scenarios and CAMS 1052 2016. AERMOD constantly produces higher values to what is seen through monitoring, based on our data 2015 is an especially high vehicular pollution year as the monitored values are closer to what is produced by the model. However, scenario 4-4 with an average concentration of 11.62 µg/m^3 is a rare example of a scenario that produced a lower annual mean than the monitored which is 12.50 µg/m^3 for 2015. EPA's hot-spot analysis specifies the use of maximum traffic for calculating emission rate factors but looking at scenarios 5 and 6 we found that using average and hourly traffic creates emissions closer to the found annual mean in CAMS 1052 for 2016. Both

scenarios 5 and 6 with annual mean concentrations of 12.19 μg/m^3 and 12.18 μg/m^3 produced the lowest difference in annual mean from 2016 only scenarios. Scenario 0 and scenario 1 look at all the surface roughness classification and the results are very similar with the difference between scenarios being the emission rate factors used. By looking at both scenarios, we found the first example showing that as the surface roughness increases the annual mean becomes closer to the CAMS 1052 annual mean with the closest values produced when using high surface roughness. As expected, the values from medium surface roughness and AER calculated are similar due to the proximity of the surface roughness values used. Following scenarios 5 and 6 in the ten closest scenarios to monitored based on annual mean, scenarios 0-3 and 1-3 with concentrations of 12.90 μg/m^3 and 12.92 μg/m^3 have the closest annual mean to the CAMS station. Both scenarios 0-3 and 1-3 are produced using high surface roughness. A trend found when focusing on surface roughness can be seen in scenarios 1 and 0 with scenarios labeled with a -3 generating emissions closest to the monitored followed by higher difference in scenarios labeled with -2 and -1 which have medium and low surface roughness respectively. Scenarios using volume sources produced a high annual means they were still among the closest values to those monitored with scenario 9 having a slightly lower annual mean of 13.41 μg/m^3 compared to scenario 7 which has an annual concentration of 13.51 μg/m^3. Oddly enough scenario 7 was produced following EPA's hot-spot analysis guidelines and scenario 9 was not. As expected, the biggest difference between monitored and modeled was generated by scenario 8 which changes the environment from urban to rural. The annual concentration produced by scenario 8 was 15.60 μg/m^3 compared to the 10.1 μg/m^3 concentration on monitored data. Dispersion of pollutants is more prevalent in rural areas as there are not as many obstructions for the pollutant to disperse as in an urban environment. We have found that high surface roughness causes lower concentrations which assimilate closer to monitored data, said findings are followed by scenarios 11 to 13. From scenarios 11 to 13 it was found that not only does surface roughness have a big impact on $PM_{2.5}$ emission dispersion, other significant parameters are also Bowen ration and albedo. Identical to surface roughness, the increase in Bowen ratio there is also a decrease in $PM_{2.5}$ concentrations

that ultimately makes the model closer to CAMS 1052 monitored data. On the other hand, when the albedo value used is lowered the concentrations produced are lowered.

Following the already found trend of scenarios with higher surface roughness, said scenarios also have a lower distribution of $PM_{2.5}$ concentration making it similar to CAMS 1052. The analysis looking into the distribution of data was separated primarily by surface roughness classification, of which high surface roughness classification shows a clearer similarity to the monitored station data. Focusing on the 25^{th} and 75^{th} percentile of values for data distribution it was found that scenarios 5, 6, 7, 9, 13-4, 13-5, and 13-7 had a similar distribution to CAMS 1052, these scenarios are important as they also generated the closest annual mean concentrations to the monitoring station. Exclusively focusing on the distribution of data, both volume source scenarios produced data with a difference in the distribution of CAMS 1052 data of 1.3 $\mu g/m^3$ for scenario 7 and 1.27 $\mu g/m^3$ for scenario 9 which were the lowest differences found. The next closest difference in the distribution of data came from scenario 4 representing the 5 years of data with a distribution difference from CAMS 1052 of 4.6 $\mu g/m^3$. Following both analyses a top ten list of scenarios was found by choosing the closest similarity to monitored data from annual mean and data distribution and it was found that of the top ten, six scenarios were created using high surface roughness, and the remaining 4 having parameter changes in source characterizations and emission rate factor.

Chapter 8 Conclusion And Future Work

The multiple model scenarios created as well as analyzing data using statistical metrics such as mean, median standard deviation and 98th percentile we have found that following guidelines presented in the $PM_{2.5}$hot-spot analysis produce accurate results especially if following the source characterization procedures for the use of volume sources. Hot-spot analysis requires the use of maximum traffic data for the calculations of emission factors, however, we found that using average and hourly traffic produces more accurate results. Using hourly traffic can be a tedious task in calculating and entering into the model which is why if the regulations were to be updated based on this study the use of average traffic data would be preferable due to its simplicity. Based on our findings the difference between results is not significant enough to make hourly traffic a preferable choice in the calculating of emission factors. We have also found the trend that lowering the input value for Bowen ratio and surface roughness as well as increasing the albedo value produces better results when compared to monitored data which could mean that the calculation of surface roughness is not as accurate and for the Bowen ratio and albedo we could have calculated the values instead of using pre-existent TCEQ values. Finding the mentioned trend as well as testing hot-spot analysis procedures has helped in the understanding of AERMOD for vehicular emissions. Having a very limited area of study can only expand our understanding up to a certain limit, however, during this study we have developed a set of procedures for analyzing AERMOD data for vehicular sources that may be replicated for a similar study in any city with readily available traffic and meteorological data. As a future study, we could develop a similar study procedure for other areas in the city of Houston, Texas to compare results between different areas or even in multiple cities across Texas to further understand how the multiple variables required for AERMOD can be effectively used to correctly model emission probability for future traffic projects.

References

Adar, S. D., Sheppard, L., Vedal, S., Polak, J. F., Sampson, P. D., Diez Roux, A. V., … Kaufman, J. D. (2013). Fine Particulate Air Pollution and the Progression of Carotid Intima-Medial Thickness: A Prospective Cohort Study from the Multi-Ethnic Study of Atherosclerosis and Air Pollution. PLoS Medicine, 10(4), e1001430. https://doi.org/10.1371/journal.pmed.1001430

American Housing Survey (AHS), 2015. AHS 2013 National Summary Tables, U.S. Department of Housing and Urban Development. Retrieved from https://www.census.gov/programs-surveys/ahs/data/2013/ahs-2013-summary-tables/national-summary-report-and-tables---ahs-2013.html, Last Revised: December 4, 2015

Araujo, J.A., 2011. Particulate air pollution, systemic oxidative stress, inflammation, and atherosclerosis. Air Quality, Atmosphere and Health, 4(1):79-93. Retrieved from https://link.springer.com/content/pdf/10.1007%2Fs11869-010-0101-8.pdf

Armijos, R. X., Weigel, M. M., Myers, O. B., Li, W., Racines, M., & Berwick, M., 2015. Residential Exposure to Urban Traffic Is Associated with Increased Carotid Intima-Media Thickness in Children. Journal of Environmental and Public Health, 2015, 1-11. Retrieved from https://www.hindawi.com/journals/jeph/2015/713540/abs/

Barnes, M. J., Brade, T. K., MacKenzie, A. R., Whyatt, J. D., Carruthers, D. J., Strocker, J., … Hewitt, C. N. (2014). Spatially-varying surface roughness and ground-level air quality in an operational dispersion model | Elsevier Enhanced Reader. Environmental Pollution, 185, 44–51. https://doi.org/10.1016/j.envpol.2013.09.039

Cahill, T.A., D.E. Barnes, L. Wuest, D. Gribble, D. Buscho, R.S. Miller, and C. De la Croix. Artificial ultra-fine aerosol tracers for highway transect studies. Atmospheric Environment, 2016. 136: 31–42. Retrieved from https://reader.elsevier.com/reader/sd/pii/S1352231016302540?token=D63766B74B3C9D6CAB2E2323788C8BD1EE7E6AAF56A6FDE6781487504C018BDF10CB850A1F781CC4BBB3807D18320423

Chen, L., Jenison, B.L., Yang ,W., Omaye, S.T., 2000. Elementary school absenteeism and air pollution, Inhal. Toxicol., 12(11): 997-1016. Retrieved from https://reader.elsevier.com/reader/sd/pii/S1352231016302540?token=D9CB1C9E3CBB3EE5C4EB01B37E336F96B43A9A4A2E8F70A45ED16654096C9DD5F20020666816A101ACD0076362561CDD

De Winter, J.L., S.G. Brown, A.F. Seagram, and K. Landsberg. A national-scale review of air pollutant concentrations measured in the U.S. near-road monitoring network during 2014 and 2015. Atmospheric Environment, 2018. 183:94–105. Retrieved from https://www.sciencedirect.com/science/article/abs/pii/S1352231018302280

Gilliland, F.D., Berhane, K., Rappaport, E.B., Thomas, D.C., Avol, E., Gauderman,W.J., London, S.J., Margolis, H.G., McConnell, R., Islam, K.T., Peters, J.M., 2001. The effects of ambient air pollution on school absenteeism due to respiratory illnesses. Epidemiology, 12:43–54. Retrieved from file:///C:/Users/Ivan/Downloads/The_Effects_of_Ambient_Air_Pollution_on_School.9.pdf

Ginzburg, H.1., Liu, X., Baker, M., Shreeve, R., Jayanty, R.K.M., Campbell, D., Zielinska, B., 2015. Monitoring study of the near-road PM2.5 concentrations in Maryland. Journal of the Air & Waste Management Association, 65:1062–1071. Retrieved from https://www.tandfonline.com/doi/full/10.1080/10962247.2015.1056887

Hodan, W. 2004. Evaluating the Contribution of PM2.5 Precursor Gases and Re-entrained Road Emissions to Mobile Source PM2.5 Particulate Matter Emissions. 58. Retrieved from https://www3.epa.gov/ttnchie1/conference/ei13/mobile/hodan.pdf

Holmes, N. S., Morawska, L., 2006. A review of dispersion modelling and its application to the dispersion of particles: An overview of different dispersion models available, Atmospheric Environment, Volume 40, Issue 30, 2006, Retrieved from https://www.sciencedirect.com/science/article/pii/S1352231006006339

Iannuzi, A., Verga, M.C., Renis, M., 2010. Air pollution and carotid arterial stiffness in children. Cardiology in the Young, 20(2):186-190. Retrieved from https://www.cambridge.org/core/services/aop-cambridge-core/content/view/3B476C84CFFB9EA922C3F2E9AA9BE285/S1047951109992010a.pdf/air_pollution_and_carotid_arterial_stiffness_in_children.pdf

Karner, A., D. Eisinger, and D. Niemeier. Near-roadway air quality: Synthesizing the findings from real-world data. Environmental Science & Technology, 2010. 44(14), 5334–5344. Retrieved from https://pubs.acs.org/doi/abs/10.1021/es100008x

Keuken, M.P., M. Moerman, M. Voogt, M. Blom, E.P. Weijers, T. Rockmann, and U. Duset. Source contributions to PM2.5 and PM10 at an urban background and a street location. Atmospheric Environment, 2013. 71:26–35. Retrieved from https://www.sciencedirect.com/science/article/abs/pii/S1352231013000575

Li, W-W, S. Jeon, M. Chavez, I. Ramirez, A. Rangel, A. Urbina, S. Vallamsundar, and R. Farzaneh. 2019. Determination of Background PM2.5 Concentrations at Near-road Air Monitors. Paper submitted to the Transportation Research Record: Journal of the Transportation Research Board.

Li, Wen-Whai, Mayra Chavez, Soyoung Jeon, Adan Rangel, Ivan Ramirez, Alexandria Urbina, Suriya Vallamsundar, and Reza Farzaneh. 2019. Contribution of Traffic Emissions to NearRoad PM2.5 Air Concentrations as Implied by Urban-Scale Background Monitoring. Transportation Research Board 98th Annual Meeting. January 13-17, Washington, D.C., 1–8. https://doi.org/19-01459.

Lin, K. M., Juang, J. Y., Shiu, Y.-W., & Chang, L. F. W. 2016. Estimating the Bowen Ratio for Application in Air Quality Models by Integrating a Simplified Analytical Expression with Measurement Data. Journal of Applied Meteorology and Climatology, 55(4), 1041–1048. https://doi.org/10.1175/JAMC-D-15-0080.1

U.S. Environmental Protection Agency (U.S. EPA), 1985. AP 42, Fifth Edition Compilation of Air Pollutant Emissions Factors, Volume 1: Stationary Point and Area Sources Appendix A. (1985, September). Retrieved from https://www3.epa.gov/ttn/chief/ap42/appendix/appa.pdf

U.S. Environmental Protection Agency (U.S. EPA), 2005. 40 CFR Appendix W to Part 51 - Guideline on Air Quality Models; Fed. Regist. 2005, 70, 68226. Retrieved from https://www3.epa.gov/scram001/guidance/guide/appw_05.pdf

U.S. Environmental Protection Agency (U.S. EPA), 2010. Primary National Ambient Air Quality Standards for Nitrogen Dioxide—Final Rule; Fed. Regist. 2010, 75, 6482. Retrieved from https://www.govinfo.gov/content/pkg/FR-2010-02-09/pdf/2010-1990.pdf

U.S. Environmental Protection Agency (U.S. EPA), 2012. 40 CFR Appendix D to Part 58 - Network Design Criteria for Ambient Air Quality Monitoring. 2012, 71, 249. Retrieved from https://www.govinfo.gov/content/pkg/CFR-2012-title40-vol6/pdf/CFR-2012-title40-vol6-part58-appD.pdf

U.S. Environmental Protection Agency (U.S. EPA), 2016. Revision to the Near-road NO2 Minimum Monitoring Requirements, Pub. L. No. 40 CFR Part 58, 81 791 (2016). Retrieved from https://www.epa.gov/sites/production/files/2016-12/documents/fact_sheet_-_nr_no2_final_rule_12-23-16_final.pdf

U.S. Environmental Protection Agency (U.S. EPA), 2017. Environmental Protection. Revisions to the Guideline on Air Quality Models: Enhancements to the AERMOD Dispersion Modeling System and Incorporation of Approaches to Address Ozone and Fine Particulate Matter, Pub. L. No. 40 CFR Part 51, 54 (2017). Retrieved from https://www3.epa.gov/ttn/scram/appendix_w/2016/Appendix_W-Fact_Sheet.pdf

Vallamsundar, S., and J. Lin. Sensitivity Test Analysis of MOVES and AERMOD models. Presented at 92nd Annual Meeting of the Transportation Research Board, Washington, D.C., 2013. Retrieved from https://www.researchgate.net/profile/Jane_Lin8/publication/262875315_Sensitivity_Test_Analysis_of_MOVES_and_AERMOD_Models/links/580f783c08ae009606bb8735/Sensitivity-Test-Analysis-of-MOVES-and-AERMOD-Models.pdf

Venkatram, A., M. Snyder, V. Isakov, and S. Kimbrough. Impact of wind direction on near-road pollutant concentrations. Atmospheric Environment, 2013. 80: 248-258. Retrieved from https://www.sciencedirect.com/science/article/abs/pii/S1352231013006067

Wendt, J.K, Symanski, E, Stock, T.H., Chan W., Du, X.L., 2014. Association of short-term increase in ambient air pollution and timing of initial asthma diagnosis among Medicaid-enrolled children in a metropolitan area. Environmental Research, 131:50-58. Retrieved from https://www.sciencedirect.com/science/article/pii/S0013935114000401

Weinstock, L., Watkins, N., Wayland, R., Baldauf, R., 2013. EPA's emerging near-road ambient monitoring network: A progress report. Environmental Magazine, 2013(7):6-10. Retrieved from http://pubs.awma.org/gsearch/em/2013/7/weinstock.pdf

Wood, S.R. Performance evaluation of AERMOD, CALPUFF, and legacy air dispersion models using the Winter Validation Tracer Study dataset. Atmospheric Environment, 2014. 89: 707–720. Retrieved from https://reader.elsevier.com/reader/sd/pii/S1352231014001502?token=35BF6CE6938083988741B7C320A221A3C03CFE01F3EA43D38D1BD46F30B357FC88D8D86F6AC891263F29D332809E74A3

Appendix A

Selection of CAMS 1052 UTEP Task 1 Report
Section 4 Near-Road Monitoring Stations
4.1 Background

Traffic-related air pollution has the most profound impact on human health because of the quantity of pollutants emitted and the relatively close proximity between the source and the population. Prior studies have documented the adverse impacts of traffic-related air pollution on cardiovascular health in adults (Hoek et al., 2008; Adar et al., 2013; Hoffman et al., 2007). Emerging evidence suggests that close residential proximity to traffic are particularly harmful to children. Schoolchildren living 30-300 meters from a major roadway had increased arterial stiffness (Iannuzi et al., 2010), increased carotid intima-media thickness (Armijos et al., 2015), decreased academic performance (Gilliland et al., 2001), increased absenteeism (Chen et al., 2000), and increased clinical asthma symptoms (Wendt et al., 2014). According to a recent national household survey (AHS 2013), 16.88 million households in the U.S. lived within 1/2 block from a 4-or-more-lane highway, railroad, or airport in 2011. This implies that approximately 43.5 million of people were exposed to high-level of traffic emissions in 2011, using an average people per household of 2.58 for that year. The numbers are consistent with a widely quoted statistic of 22 million total housing units and 45 million of population living near traffic facilities (U.S. EPA 2010; Weinstock et al 2013).

The U.S. EPA recognized the potentially detrimental effects of air pollution on public health and required national ambient air monitoring networks to i) provide air pollution data to the general public in a timely manner; ii) support compliance with ambient air quality standards and emissions strategy development; and iii) support for air pollution research studies. In 2006, the U.S. EPA finalized a requirement to conduct an assessment of these networks every five years. In 2010, the U.S. EPA further established requirements for a new national air quality monitoring network that include the characterization of nitrogen dioxide (NO_2) in the near-road environment. Specifically, Title 40 CFR Part 58, Appendix D, Section 4.3.2 requires microscale near-road NO_2 monitors for core based statistical areas (CBSAs) with populations of 500,000 or more persons. An additional near-road NO_2 monitoring station is required for any CBSA with a population of 2,500,000 persons or more, or in any CBSA with a population of 500,000 or more persons that has one or more roadway segments with 250,000 or greater annual average daily traffic (AADT) counts to monitor a second location of expected maximum hourly concentrations. The requirement to install near-road nitrogen dioxide (NO_2) monitoring stations in CBSAs having populations between 500,000 and 1 million by January 1, 2017 was removed by EPA in December 30, 2016 (Federal Register, Vol. 81, No. 251 / Friday, December 30, 2016) because i) current near road monitoring shows that air quality levels, in urban areas with larger populations, are well below the National Ambient Air Quality Standards for NO_2 issued in 2010; and ii) near road NO_2 concentrations are not expected to be above the health-based national air quality standards in smaller urban areas. One notices that this action does not change the requirements for near-road NO_2 monitors in more populated areas,

area-wide NO_2 monitoring, or monitoring of NO_2 in areas with susceptible and vulnerable populations.

The near-road NO_2 monitoring stations should be selected by ranking all road segments within a CBSA by AADT and then by identifying a location or locations adjacent to those highest ranked road segments, considering fleet mix, roadway design, congestion patterns, terrain, and meteorology, where maximum hourly NO_2 concentrations are expected to occur and siting criteria can be met in accordance with Title 40 CFR Part 58, Appendix D. In addition, measurements at required near-road NO_2 monitor sites utilizing chemiluminescence FRMs must include at a minimum: NO, NO_2, and NO_X. Appendix D, 4.2.1 and 4.7.1(b)(2) further require that at least one $PM_{2.5}$ monitor and one CO monitor to be collocated at a near-road NO_2 station.

New Near-Road Monitoring in Texas

The Texas Commission on Environmental Quality (TCEQ) conducted annual assessment of the Texas air monitoring network in fulfilment of Title 40 CFR Part 58.10(d) which requires states to submit an annual monitoring network plan to the EPA. This monitoring plan is required to provide the implementation and maintenance framework for an air quality surveillance system. The TCEQ evaluated the existing network of ambient air monitors measuring ozone, carbon monoxide (CO), oxides of nitrogen (NOx), sulfur dioxide (SO_2), lead (Pb), particulate matter of 10 micrometers or less in diameter (PM_{10}), particulate matter of 2.5 micrometers or less in diameter ($PM_{2.5}$), volatile organic compounds (VOCs), carbonyls, semi volatile organic compounds (SVOCs), and speciated $PM_{2.5}$. The assessment also evaluated whether individual monitors within this network should be added, moved, or decommissioned to best understand and evaluate air quality given existing resources.

In response to the EPA's near-road air pollution monitoring requirements, TCEQ first focused on complying with the directly-applicable federal requirements listed in 40 CFR Part 58, Appendix D, Section 4.3.2 by primarily prioritizing potential sites based on AADT ranking (Phase 1). The TCEQ considered road segment fleet equivalent AADT (FE-AADT) rankings, but did not rely solely on FE-AADT in the prioritization of potential sites since FE-AADT is not a specific siting requirement under 40 CFR Part 58, Appendix D, Section 4.3.2 (TCEQ, 2015). The TCEQ then reevaluated each roadway segment and viability in Phase 2.

Currently, there are 6 near-road air monitoring stations selected and operated in Texas by TCEQ. Table 1 lists the 6 near-road air monitoring stations selected and operated in Texas by TCEQ. While NO_x (including NO, NO_2, and NOx, as required by 40CFR Part 58) and CO are recorded hourly, only integrated 24-hr average $PM_{2.5}$ samples are required to be collected every 6^{th} days. Surface meteorological parameters such as wind direction, wind speed, temperature, and atmospheric pressure at these sites are collected hourly at these stations.

Table 1 Summary of the 6 near-road air monitoring sites in Texas

AQS Number	**481131067**	**482011066**	**484531068**	**480291069**	**484391053**	**482011052**
TCEQ CAMS	1067	1066	1068	1069	1053	1052

Site Name	Dallas LBJ Freeway	Houston Southwest Freeway	Austin North Interstate 35	San Antonio Interstate 35	Fort Worth California Parkway North	Houston North Loop
Core Based Statistical Area	Dallas-Fort Worth-Arlington	Houston-The Woodlands-Sugar Land	Austin-Round Rock	San Antonio-New Braunfels	Dallas-Fort Worth-Arlington	Houston-The Woodlands-Sugar Land
2015 Population	7,102,796	6,656,947	2,000,860	2,384,075	7,102,796	6,656,947
Phase	1	1	1	1	2	2
AADT Ranking	15	1	7	21	36	46
FE-AADT Ranking	7	1	10	3	90	46
Pollutants Monitored						
- NO_x	√	√	√	√	√	√
- CO	-	-	-	-	√	√
- $PM_{2.5}$	-	-	-	-	√	√
Distance to Nearest Traffic Lane (m)	24	24	27	20	15	15

4.2.1 Regulation requirements for selected pollutant monitoring

Nitrogen Dioxide (NO_2)

Title 40 CFR Part 58, Appendix D, Section 4.3.2 requires one microscale near-road monitor in each CBSA with a population of 500,000 or more persons to be located near a major road with high annual average daily traffic (AADT) counts. An additional near-road monitor is required in each CBSA with a population of 2,500,000 or more persons. In Texas, these new regulations resulted in the need for eight new near-road monitors. In the first phase, one near-road monitor was placed in each of the designated CBSAs of Houston, Dallas, Austin, and San Antonio by

January 2014. The second phase included an additional near-road monitor in CBSAs of Houston and Dallas by January 2015. The final phase stimulated one near-road monitor to be deployed in each of the CBSAs of El Paso and McAllen-Edinburg-Mission by January 2017. During the selection process, The TCEQ received AADT and Fleet Equivalent (FE) AADT rankings from the Texas Department of Transportation (TxDOT). Because the locations of these sites included requirements in 40 CFR Part 58, TCEQ relied on these criteria to pick site locations. The regulation states "The near-road NO_2 monitoring stations shall be selected by ranking all road segments within a CBSA by AADT and then identifying a location or locations adjacent to those highest ranked road segments, considering fleet mix, roadway design, congestion patterns, terrain, and meteorology, where maximum hourly NO_2 concentrations are expected to occur". Therefore, the TCEQ first sorted the list of road segments provided by TxDOT in descending order by AADT ranking. Through coordination with EPA Region 6, boundaries for ranked road segments were defined as encompassing the area along the roadway of the traffic counting camera up to the point of a major roadway intersection or significant traffic divergence. The TCEQ then conducted a physical site reconnaissance to locate potential sites within that segment. All areas within each defined road segment were considered for the potential to locate a near-road site. Additional logistical considerations required by 40 CFR Part 58, Appendix E were also considered, including distance from obstructions, power availability and sufficient space to accommodate the monitoring station and equipment (AMNP, 2016).

Carbon Monoxide (CO)

Title 40 CFR Part 58, Appendix D, Section 3.0 and Section 5.0 require high sensitivity CO monitors at NCore sites and at one Type 2 PAMS site per ozone nonattainment area. Title 40 CFR Part 58, Appendix D, Section 4.2 also requires the deployment of CO monitors at near-road sites in CBSAs of greater than 1,000,000 people. The TCEQ meets minimum requirements through the operation of seven CO monitors and five high sensitivity CO monitors throughout the state. In compliance with near-road requirements in the Dallas-Fort Worth-Arlington and Houston-The Woodlands-Sugar Land CBSAs, the TCEQ deployed CO monitors at the Fort Worth California Parkway North (AQS 484391053) and Houston North Loop (AQS 482011052) sites in early 2015.

Particulate Matter of 2.5 Micrometers or Less ($PM_{2.5}$)

Title 40 CFR Part 58, Appendix D, Section 4.7 requires $PM_{2.5}$ monitoring in Metropolitan Statistical Areas (MSA) with populations greater than 500,000 people and in MSAs with lower populations if measured $PM_{2.5}$ design values for an MSA are within 85% of the NAAQS of 12 $\mu g/m^3$. Title 40 CFR Part 58.10 (8)(i) requires a minimum of one PM2.5 sampler in each CBSA with a population equal to or greater than 2,500,000 people to be located at a near-road NO_2 monitoring station by January 1, 2015. In addition, 40 CFR Part 58, Appendix D, Section 3.0 requires $PM_{2.5}$ monitoring at NCore sites. This requirement resulted in the need to add a $PM_{2.5}$ federal reference method (FRM) gravimetric sampler at five of the new sites including Houston North Loop CAMS 1052 and Fort Worth California Parkway CAMS 1053 (AMNP, 2015).

4.2.2 Descriptions of the 6 near-road monitoring stations

Descriptions for each of the six newly deployed near-road air monitoring stations are included in this section. Photos showing different views from the stations are also included. Pollutant and meteorological data for 2015 are available at TCEQ's archived database (TAMIS). Surface wind patterns at the six stations are graphically presented in wind roses. "Wind rose" is a graphical presentation of the frequency of occurrence of wind direction and wind speed categories for the purpose of identifying prevailing winds in air pollution study. Each spoke of the wind rose

represents the frequency of occurrence of winds coming from that wind sector, typically a 22.5° wind sector. The colored fractions of each spoke represent frequencies of winds blowing in specific wind speed categories in the same wind sector. Hourly pollutant concentrations for CO or NO_2 are also presented in polar plots for easy visualization.

Houston North Loop (AQS: 482011052; TCEQ CAMS 1052)

Houston North Loop continuous air monitoring station CAMS 1052 (EPA AQS Site Number: 482011052) is located north of the I-45 Highway in Harris County of Houston, Texas and was activated on April 13, 2015. The site is located at 822 North Loop, Houston with coordinates of (29.81453, -95.38769). Samplers at this site include CO, NO/NO_2/NOx, $PM_{2.5}$, temperature, wind direction, wind speed, and peak wind gust. The monitoring objective of all these samplers is to find maximum precursor emissions impact at microscale. The distance of this site to the nearest traffic lane of I-45 is 15 meters and the sampling probe height is 4 meters above the ground. Figure 1 shows the location of the site as well as locations of several regional CAMS sites within a 20-mile radius from CAMS 1052. The relative location of CAMS 1052 to the Interstate Highway I-45 is illustrated in the insert placed at the upper left corner of Figure 1. Wind roses of several CAMS stations are also shown in the figure; they will be explained later in this section.

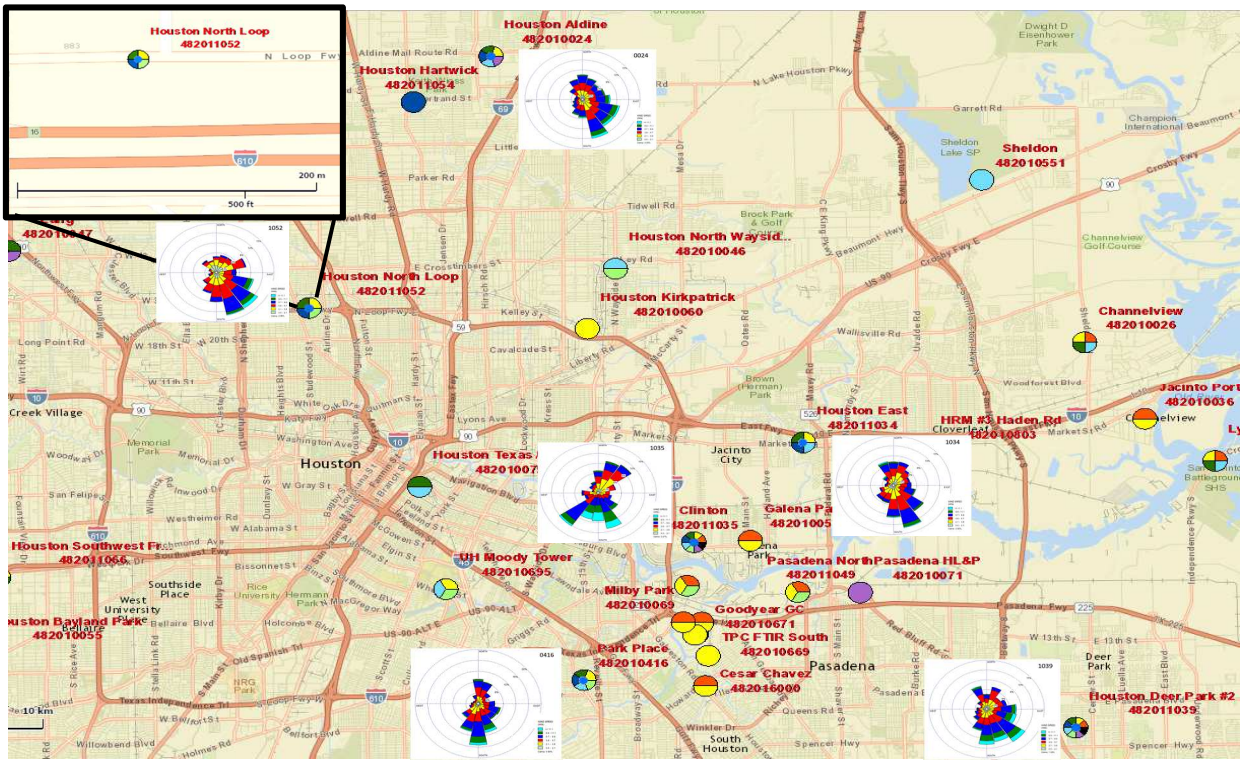

Figure 1: General location of CAMS 1052, Houston, Texas

Figures 2 shows different views from CAMS 1052 looking in different directions. Figure 3 shows the wind rose plot for CAMS 1052 for all data available in 2015. The station was installed in 2014 and began to record air quality data in April, 2015. As visualized in the wind rose plot, southeasterly winds prevailed at the site and the station was downwind of the highway emissions approximately 60 % of the time between April 24 and December 30, 2015. The average wind speed at the site was ~4 mph.

Figure 4 shows in polar plot and in "concentration rose" the hourly CO concentration observed at CAMS 1052 during the same period of time. Similar to the wind rose plot, the concentration rose plot presents the frequency of occurrence of pollutant concentrations categorized by wind direction and pollution concentration. Peak CO concentration was observed on Dec. 6, 2015 between midnight and sunrise (12 AM – 6 AM) when winds were blowing from the northwest, indicating that other CO sources to the north of the site, rather than the highway emissions, are the primary sources of CO pollution at this site. However, hourly CO concentrations (<2.4 ppm) at this station by a busy interstate highway were at no time close to the 35 ppm 1-hour NAAQS or the 8-hour NAAQS of 9 ppm. It is interesting to notice, from the right-hand panel of Figure 4 where a good fraction of the spokes in yellow was observed, that low CO concentrations were frequently observed when CAMS 1052 was downwind of the traffic emissions from I-10. Furthermore, high CO concentrations were observed when the station was upwind of the hot-spot traffic emissions from I-10, as seen in the left-hand panel of Figure 4 where a lot of high CO values scattered in the upper half of the polar plot.

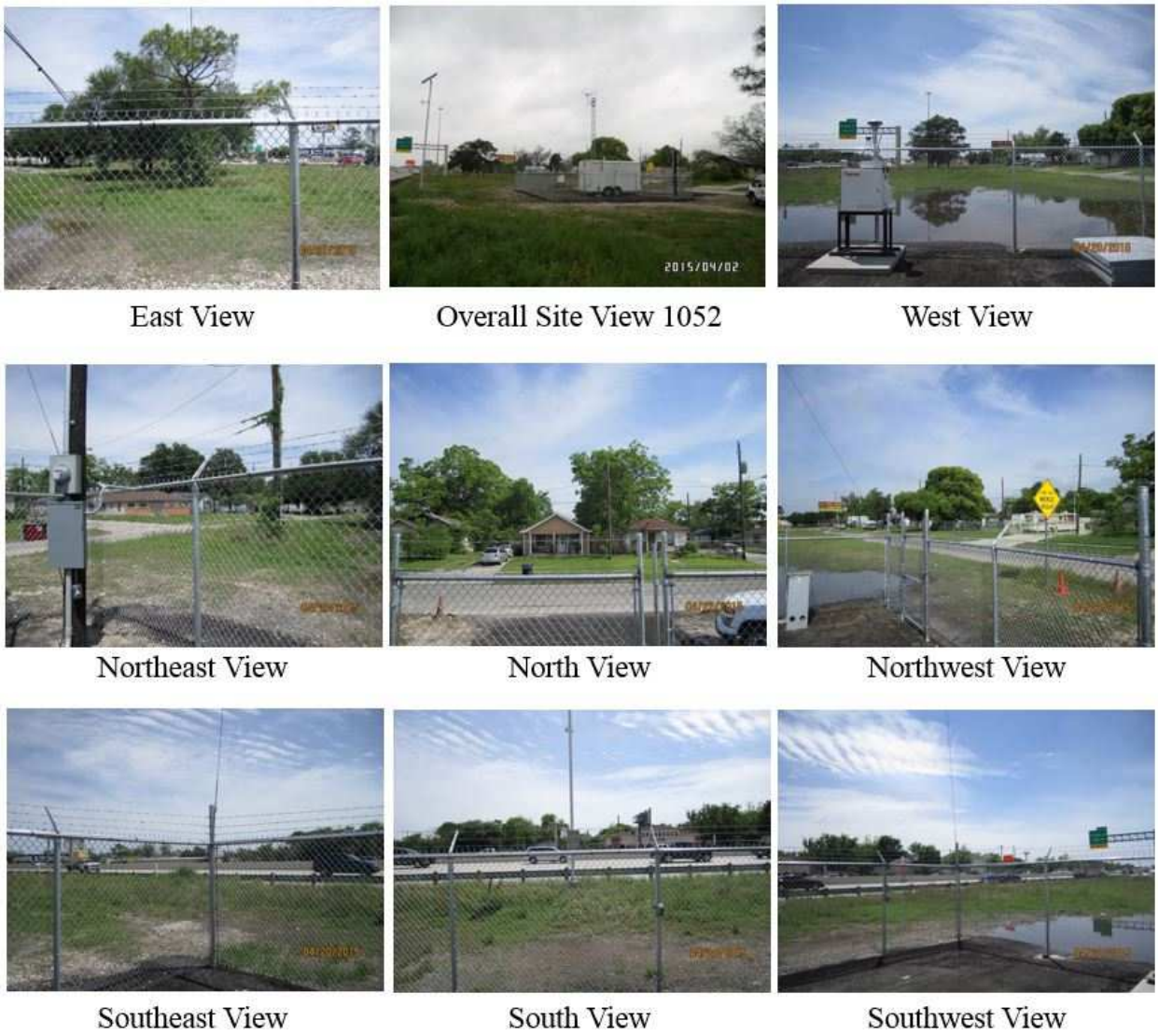

Figure 2: Various views from CAMS 1052 (TCEQ 2017)

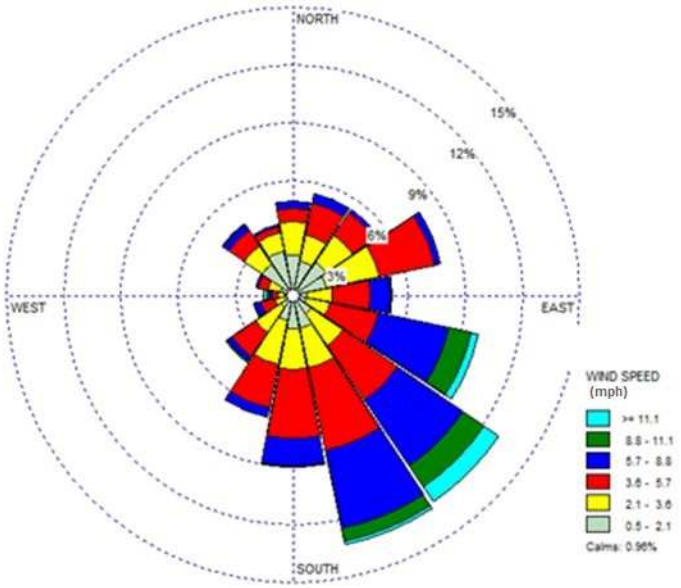

CAMS 1052 Whole Day

Figure 3: Wind rose for CAMS 1052 (year 2015)

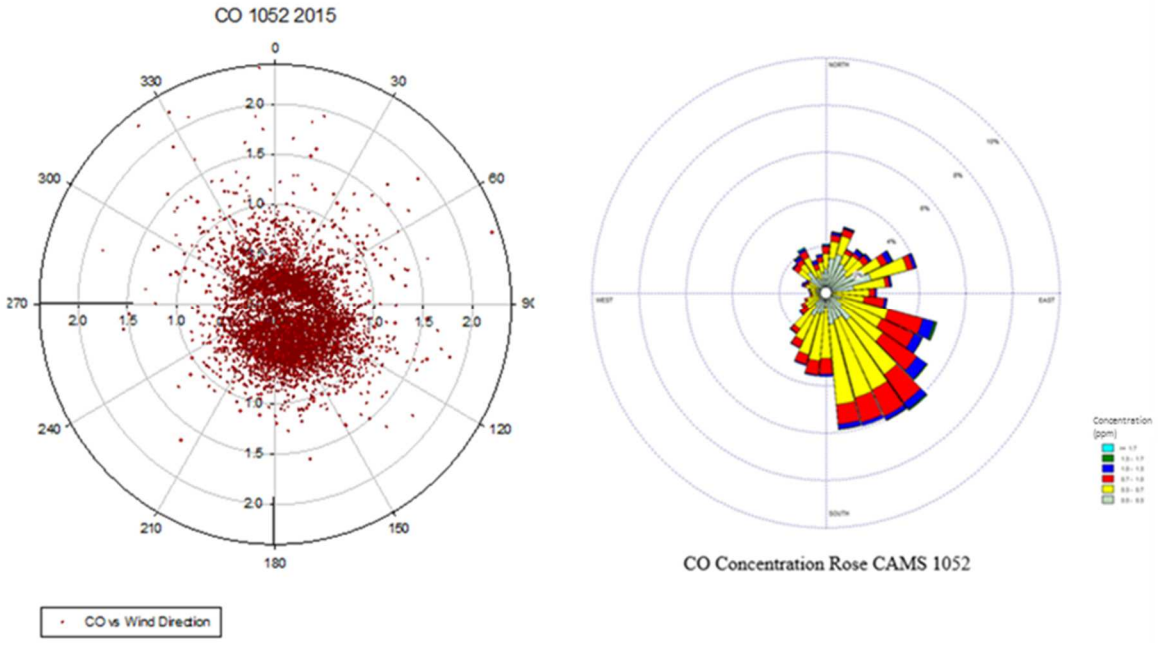

CO Concentration Rose CAMS 1052

Figure 4: CAMS 1052 CO polar plot and concentration rose (year 2015)

Figure 5 shows the hourly NO_2 concentration at CAMS 1052. NO_2 is considered a better marker of traffic emissions. The peak 1-hr NO_2 concentration (68 ppb) in 2015 was well below the NAAQS of 100 ppb. Highway emissions could be the major contributor for the NO_2 concentration

at the site, as the data shows that 96 of the highest 100 1-hr NO_2 readings occurred when the station was downwind of the highway. Furthermore, NO_2 peaked in the evening between 4 to 10 PM. Hourly NO and NO_x concentrations were also monitored at this station. Figure 6 shows the scatter plots for the two co-pollutants in comparison to NO_2. NO peaked in the morning traffic hours when east southeasterly winds prevailed. However, high NO concentrations were also observed during other wind directions indicating that the background NO concentration may be high at this location. NO_x concentration was dominated by the NO concentration and therefore NO_x peaked as NO peaked. Because NO_2 represents a good marker of NO_x and because neither NO or NO_x is regulated by the EPA, presentation and discussion of NO and NO_x data are omitted hereinafter for the other 5 near-road monitoring stations.

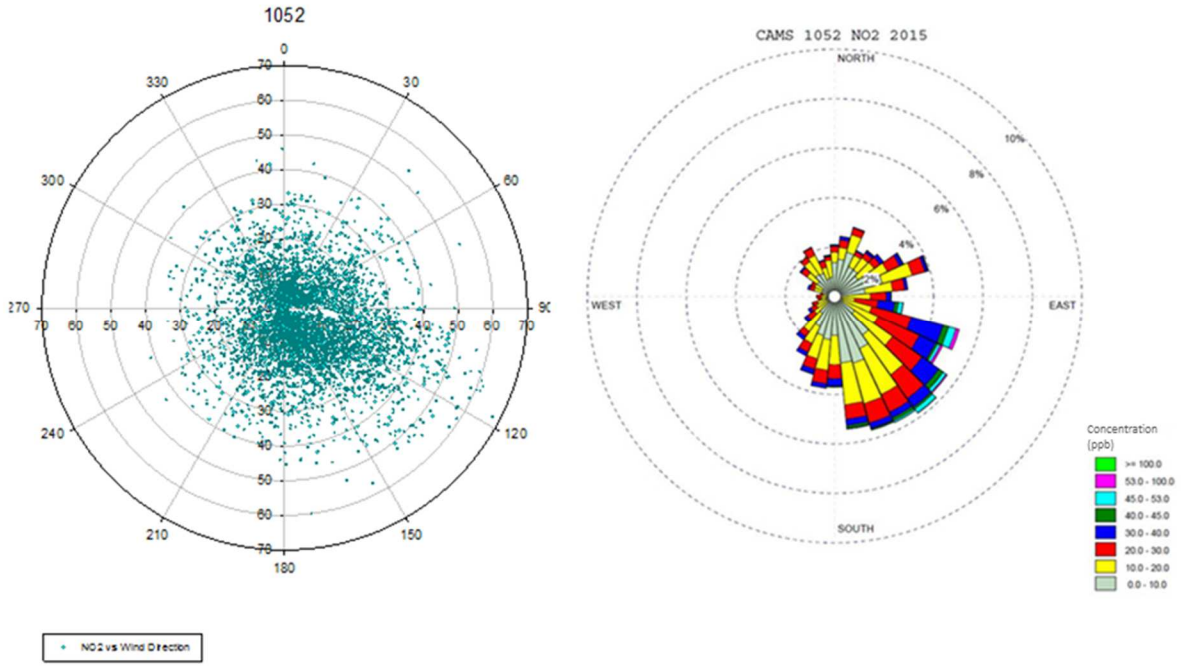

Figure 5 NO_2 polar plot and concentration rose for CAMS 1052 (year 2015)

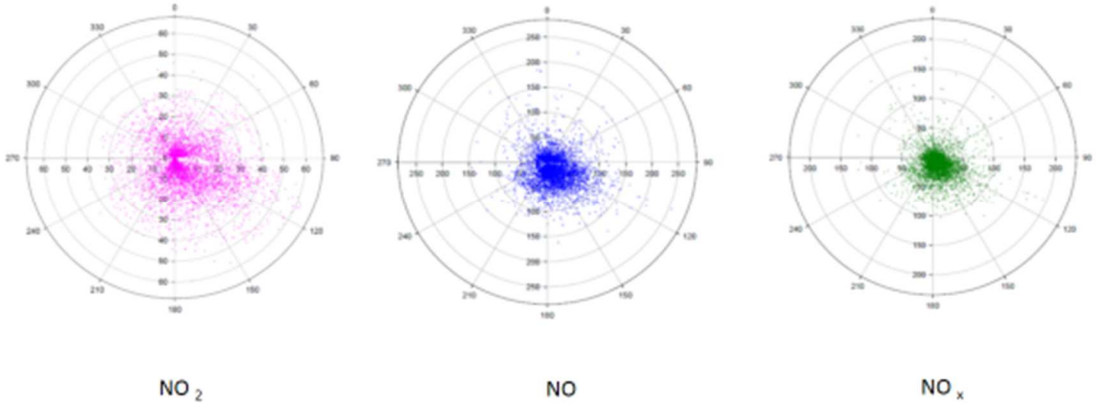

Figure 6 Scatter plots of hourly CAMS 1052 NO_2, NO, and NOx concentrations (year 2015)

Although only one 24-hour integrated $PM_{2.5}$ sample was required to be collected every 6th day at a near-road monitoring station, TCEQ has expanded their sampling program at CAMS 1052 by collecting one 24-hour integrated sample every 3rd day. Figure 7 shows the time series plot of the every-3rd-day 24-hour $PM_{2.5}$ data observed at CAMS 1052. All 24-hour average $PM_{2.5}$ concentrations measured at this station were well below the 24-hour $PM_{2.5}$ NAAQS of 35 $\mu g/m^3$. However, the whole period $PM_{2.5}$ average (form April 15 to December 31, 2015) for this station is 12.5 $\mu g/m^3$ which would exceed the annual average $PM_{2.5}$ NAAQS of 12 $\mu g/m^3$ should this value be treated as an annual average for the station.

Because the upwind-downwind relationship for concentration measurements is severely obscured by the time-varying nature of the surface meteorology, this set of data is not presented in conjunction with the surface wind data. Instead, the impact of traffic emissions on the near-road $PM_{2.5}$ concentration is evaluated based on the comparison with regional $PM_{2.5}$ data observed at other stations. Five regional TCEQ-operated CAMS stations were identified to be located within a radius of 20 miles from CAMS 1052. The locations and wind roses for these CAMS stations are shown in Figure 1. It can be visualized in Figure 1 that the wind patterns are quite similar between CAMS 1052 and other CAMS stations southeast to CAMS 1052, except the Clinton station, indicating that possibly a drainage northwest-southeast wind pattern exists between Houston metropolitan area and Galveston Bay by the Gulf of Mexico. Furthermore, the 24-hour averaged $PM_{2.5}$ concentrations in the Houston urban area exhibit a strong similarity among various CAMS stations in the city (Figure 8) where the near-road $PM_{2.5}$ appears to be greater than that observed at other 5 regional CAMS stations. Hourly $PM_{2.5}$ in the city appears to vary diurnally as $PM_{2.5}$ peaks in the morning and in the afternoon which coincides with the morning and evening traffic congestions (Figure 9).

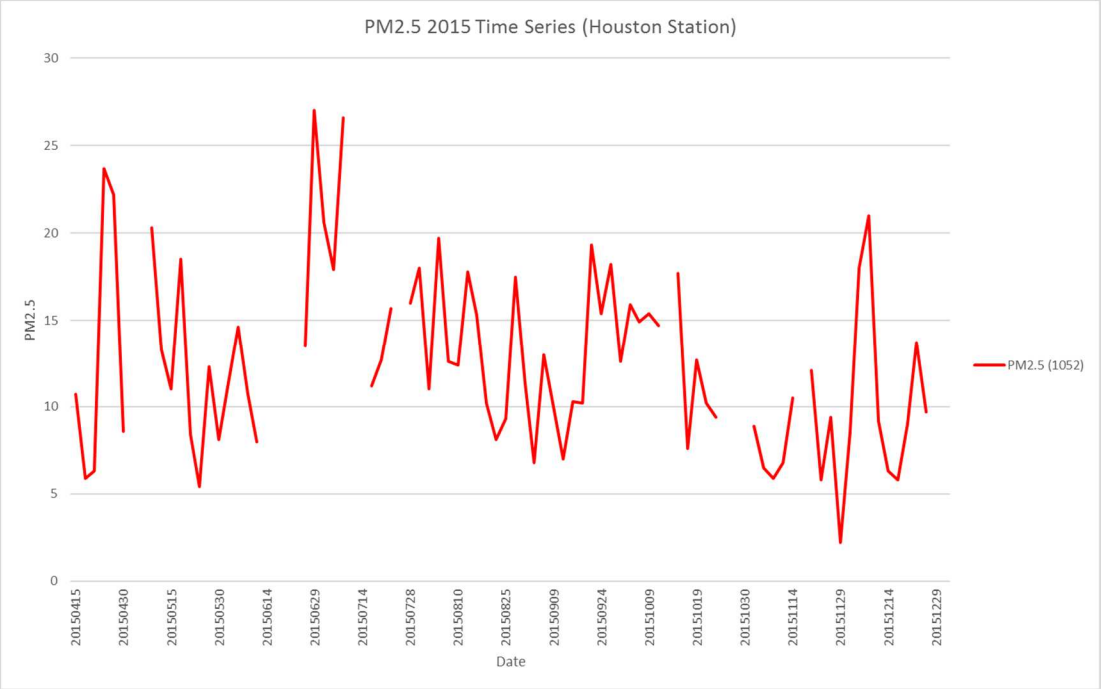

Figure 7 24-hour $PM_{2.5}$ concentrations for CAMS 1052 (starting from April 15, 2015 and collected every 3rd day)

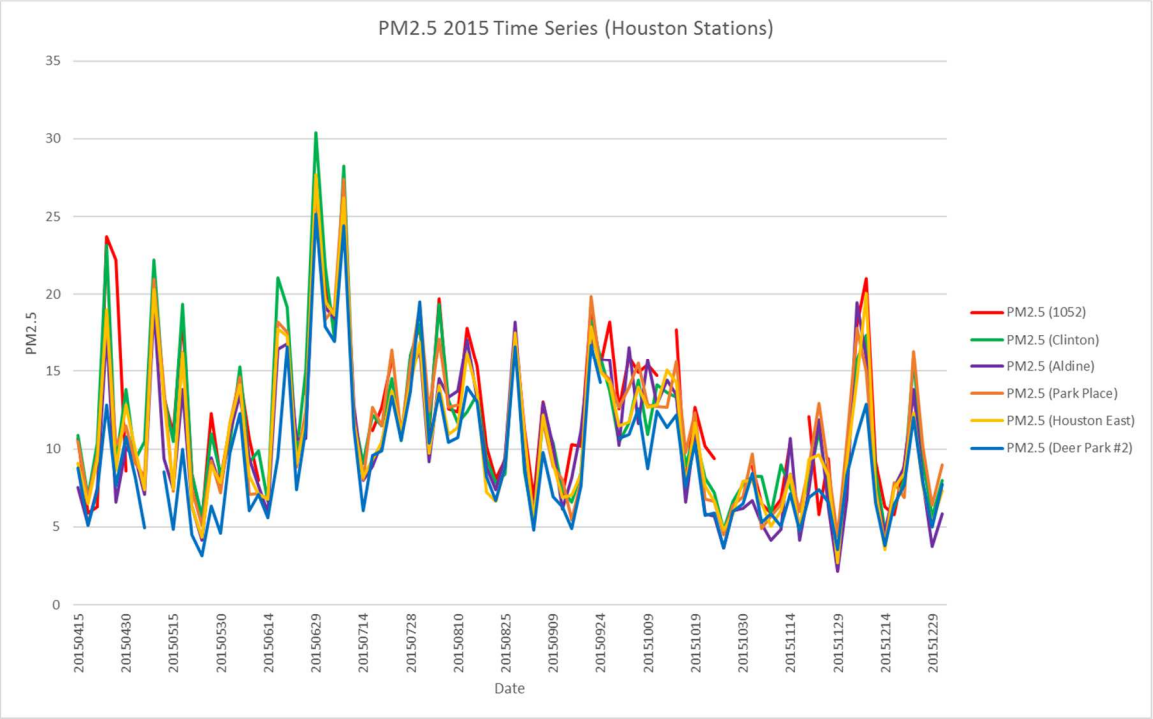

Figure 8 Comparison of 24-hour $PM_{2.5}$ concentrations at CAMS 1052 to that measured at other regional stations (by averaging hourly $PM_{2.5}$ concentrations for the same day at these stations)

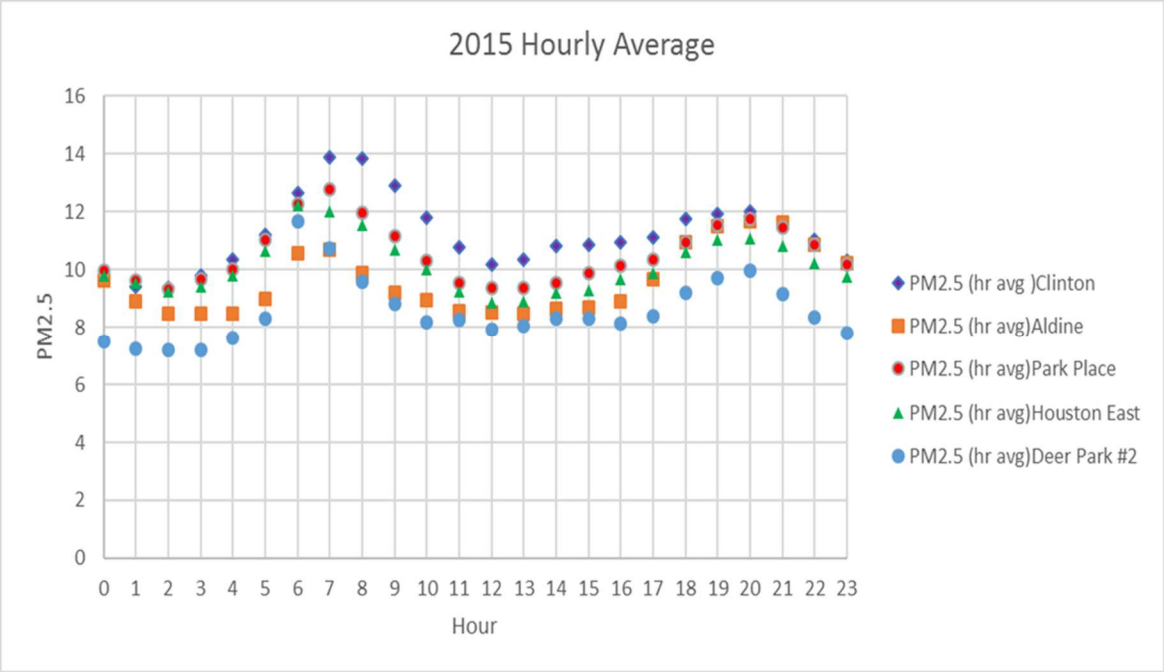

Figure 9 Diurnal variations of average 1-hour $PM_{2.5}$ concentrations at 5 regional background CAMS stations (year 2015)

As indicated in Figures 8 and 9, regional $PM_{2.5}$ concentrations are well correlated temporally and spatially. Figure 10 shows the correlation plots for $PM_{2.5}$ between CAMS 1052 and each of the 5 regional background stations with high correlation coefficients (r^2 >0.75). Furthermore, wind patterns at these stations are well correlated with r^2 >0.85, Figure 11 shows the scatter plot of paired hourly wind directions observed at CAMS 1052 and CAMS 1039 (Deer Park 2). This information will be used in a later section to select a representative regional background station for the near-road CAMS 1052.

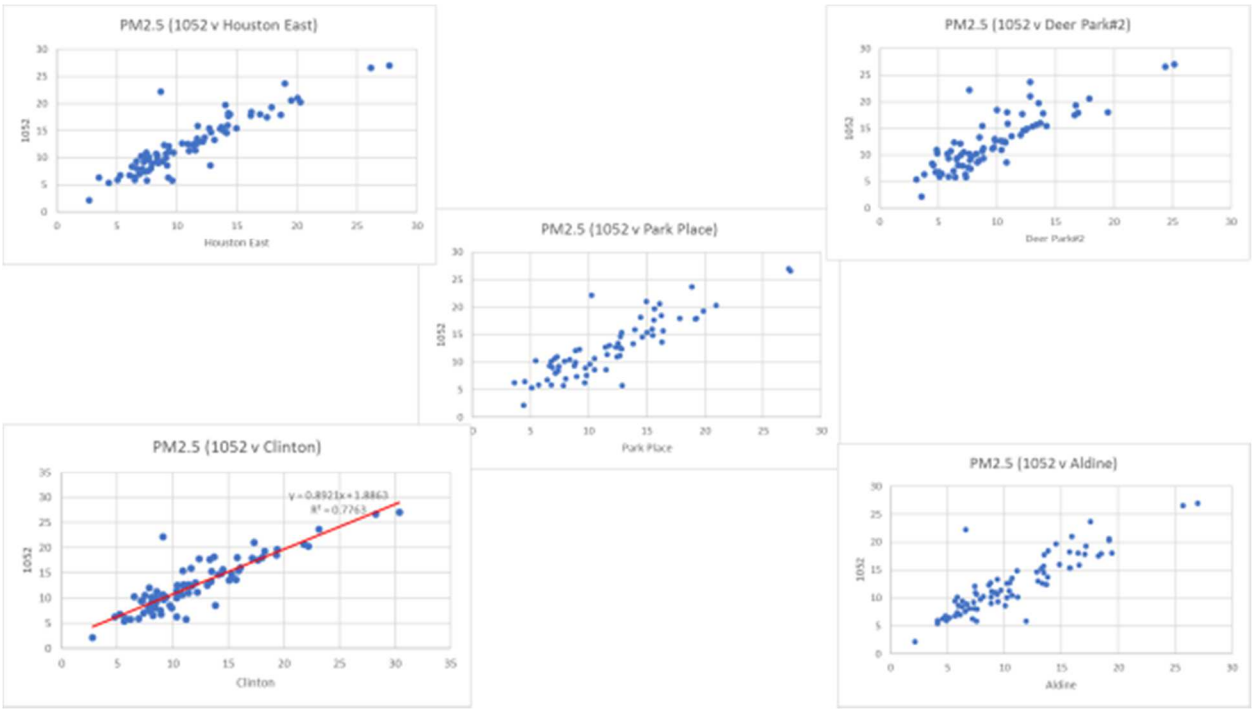

Figure 10 Correlations of 1-hour $PM_{2.5}$ concentrations at CAMS 1052 to that observed at 5 regional background CAMS stations (year 2015)

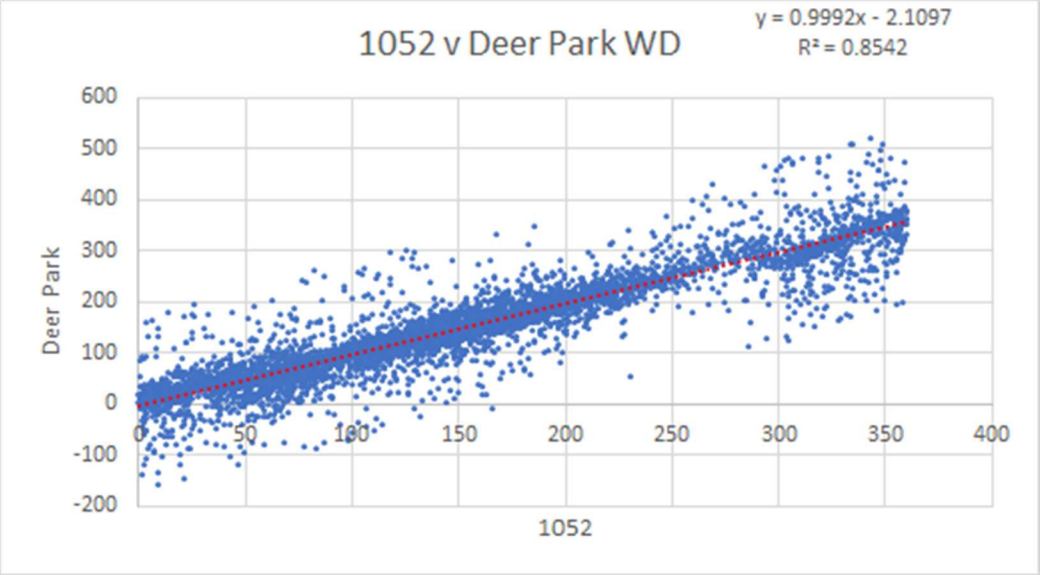

Figure 11 Correlations of paired 1-hour surface wind direction between CAMS 1052 and a regional background station, CAMS 1039 (Deer Park 2)

- *Fort Worth California Parkway North (AQS: 484391053: TCEQ CAMS 1053)*

The Fort Worth California Parkway North CAMS 1053 at 1198 California Parkway North, TX 76115 was activated on March 12, 2015. It has an elevation of 214.9 m and is located at (Latitude 32° 39' 53"N, Longitude -97° 20' 17"W). The station is owned and operated by TCEQ. CAMS 1053 currently monitors CO, NO_X including NO and NO_2, $PM_{2.5}$, temperature, wind speed, wind direction, and peak wind gust. The distance of this site to the nearest traffic lane of I-20 is 15

meters. Figure 12 show the locations of the station and 2 other non near-road regional background stations whereas Figure 13 provides views from the station towards different directions.

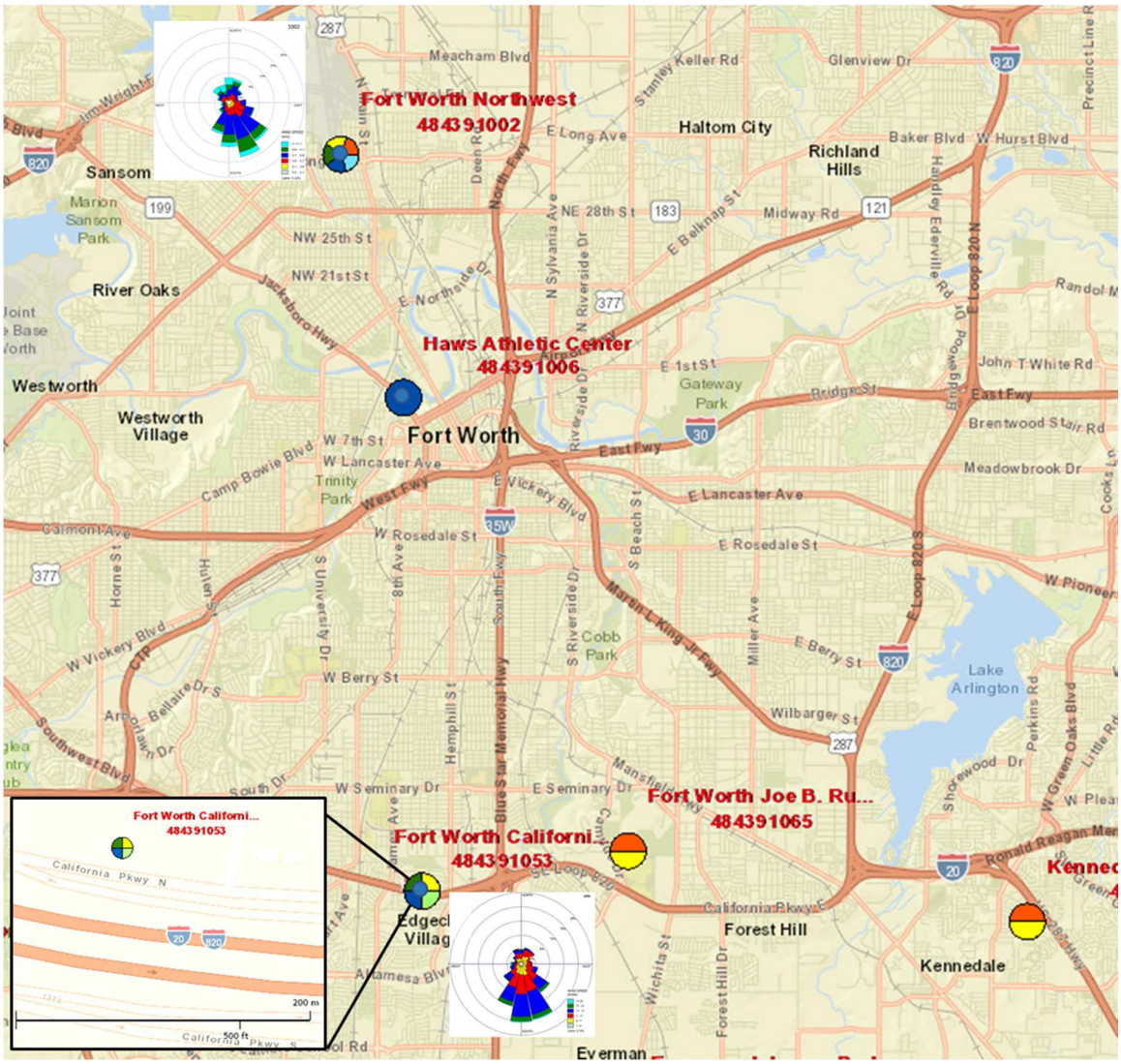

Figure12 General Location of CAMS 1053

Figure 13 Various views from CAMS 1053 (TCEQ 2017)

Figure 14 shows the wind rose plot for CAMS 1053 for all data available in 2015. Southerly winds prevailed at this location and the station was found to be downwind of the highway emissions at least 60 % of the time in 2015. Figure 15 shows the hourly CO concentration observed at CAMS 1053 during the same period of time in polar plot and in "concentration rose". Hourly CO concentrations (<2.0 ppm) at this station were low, far less than the 35 ppm 1-hour NAAQS or the 8-hour NAAQS of 9 ppm for CO.

Figure 16 shows the hourly NO_2 concentration at CAMS 1053. The peak 1-hr NO_2 concentration (<60 ppb) in 2015 was well below the NAAQS of 100 ppb. Similar to CAMS 1052, Figures 15 and 16 show, respectively, no significant increases in CO and NO_2 concentrations when the station is downwind of Interstate Highway I-20, as high concentrations are evenly distributed in all wind directions.

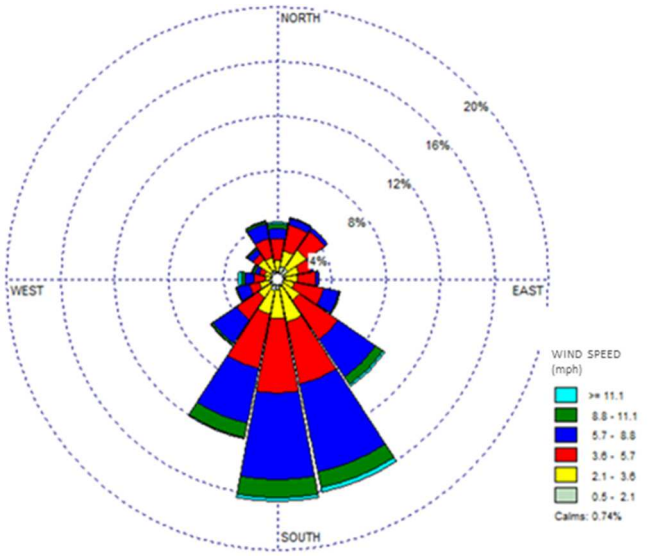

CAMS 1053 Whole Day

Figure 14 Wind rose plot for CAMS 1053 (2015)

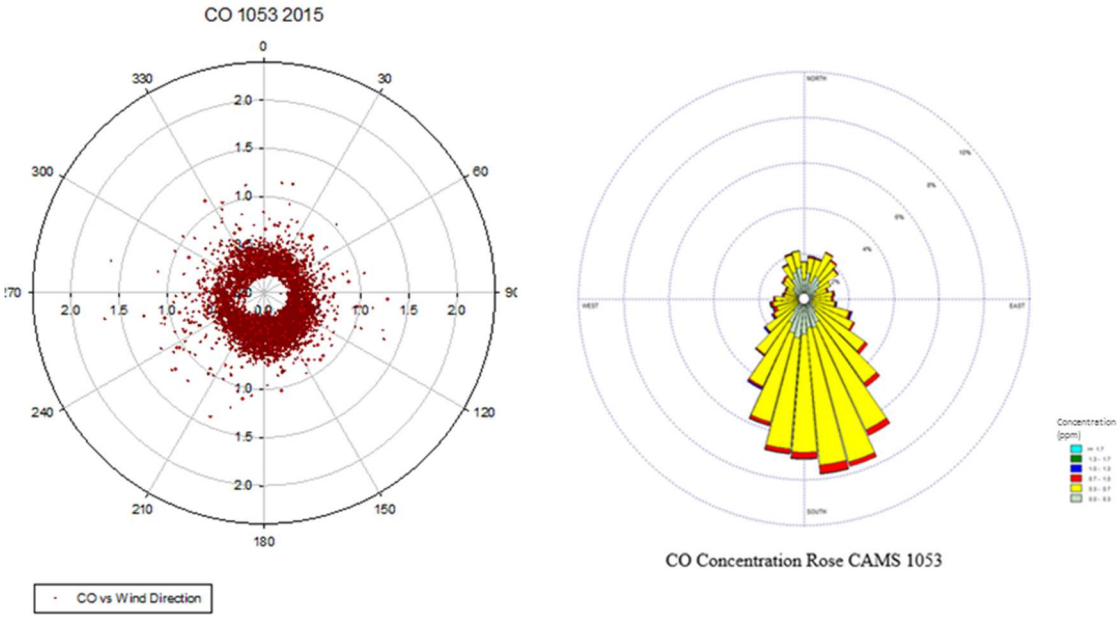

CO Concentration Rose CAMS 1053

Figure 15 CAMS 1053 CO polar plot and concentration rose for 2015

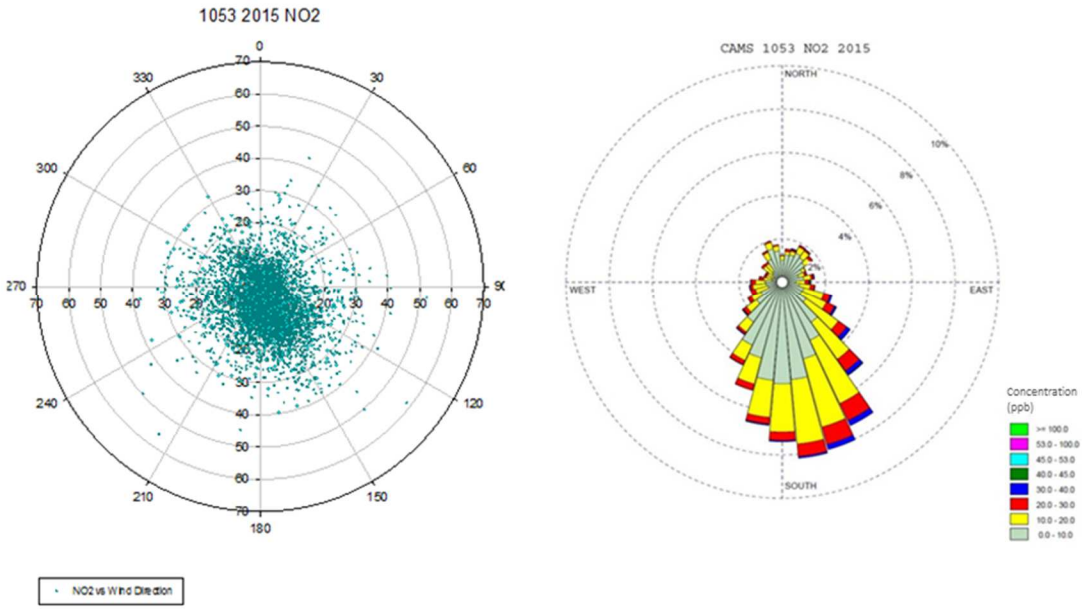

Figure 16 CAMS 1053 NO_2 polar plot and concentration rose for 2015

TCEQ conducted their $PM_{2.5}$ sampling program at CAMS 1053 by collecting one 24-hour integrated sample every 3rd day. Figure 17 shows the time series plot for the 24-hour $PM_{2.5}$ data observed at CAMS 1053. All 24-hour average $PM_{2.5}$ concentrations measured at this station were well below the 35 µg/m^3 NAAQS for 24-hour $PM_{2.5}$. The whole period $PM_{2.5}$ average (form March 12 to December 31, 2015) for this station is 9.3 µg/m^3, which is well below the 12 µg/m^3 NAAQS for annual average $PM_{2.5}$.

The impact of traffic emissions on the near-road $PM_{2.5}$ concentration at CAMS 1053 is evaluated based on the comparison with values observed at 2 regional background stations. The 2 regional TCEQ-operated CAMS stations are located within a radius of 20 miles from CAMS 1053. The locations and wind roses for these CAMS stations are shown in Figure 12. Wind rose plot for one of the 2 stations is not presented because TCEQ does not monitor surface meteorology at this station. Wind patterns are quite similar between CAMS 1053 and the other background CAMS station which is located approximately 20 miles north of CAMS 1053, indicating that wind pattern in the great Dallas-Fort Worth area is quite similar. The 24-hour averaged $PM_{2.5}$ concentration in the Dallas-Fort Worth urban area exhibits good similarity between CAMS 1053 and the two selected background stations in the city (Figures 18 and 19) where a close correlation was observed, with r^2 = 0.71 and 0.61 for the Fort Worth Northwest and Haws Athletic Center sites, respectively.

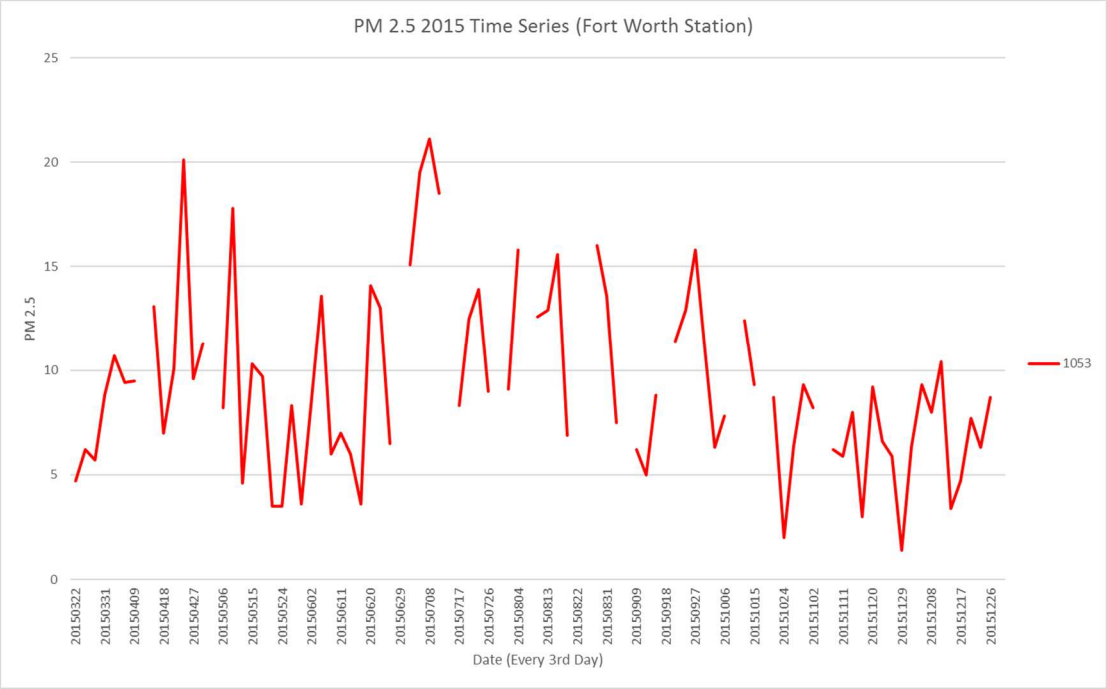

Figure 17 24-hour $PM_{2.5}$ concentrations for CAMS 1053 (every 3rd day samples starting from March 12, 2015)

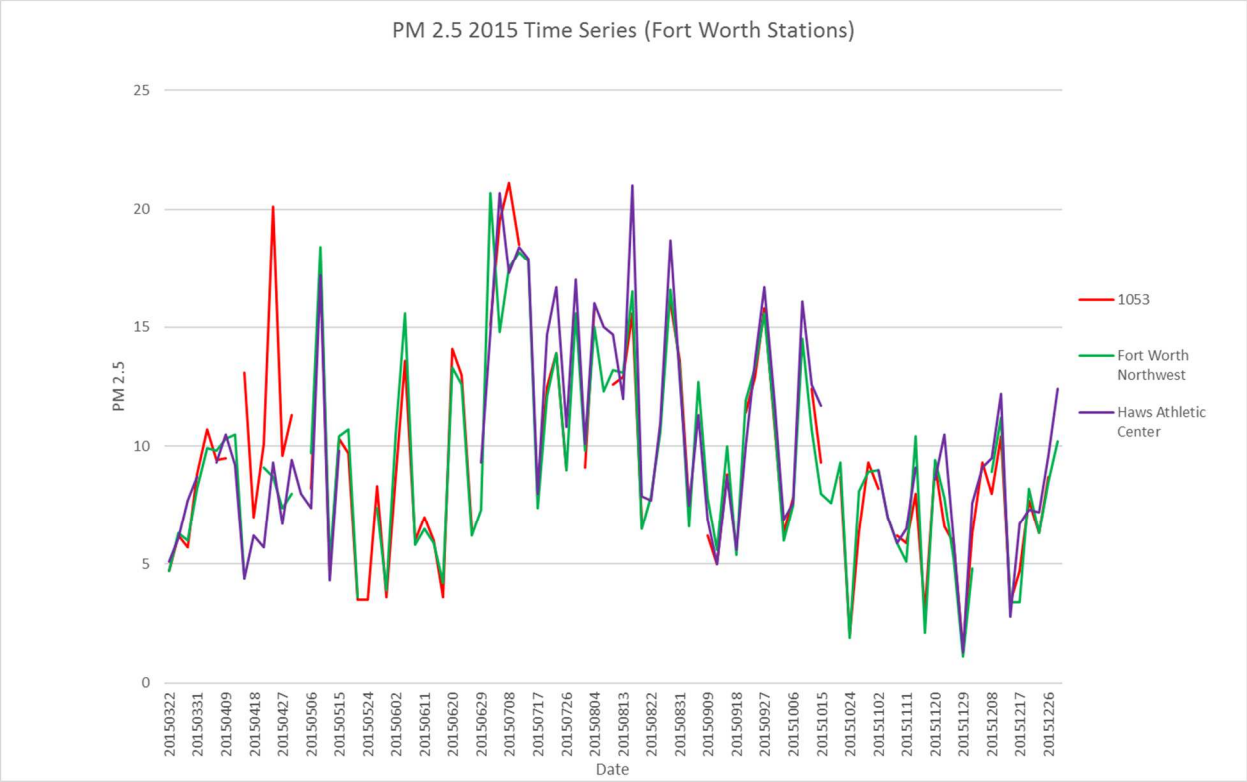

Figure 18 Comparison of 24-hour $PM_{2.5}$ concentrations at CAMS 1053 to that measured at 2 regional background stations (by averaging hourly $PM_{2.5}$ concentrations for the same day at the background station)

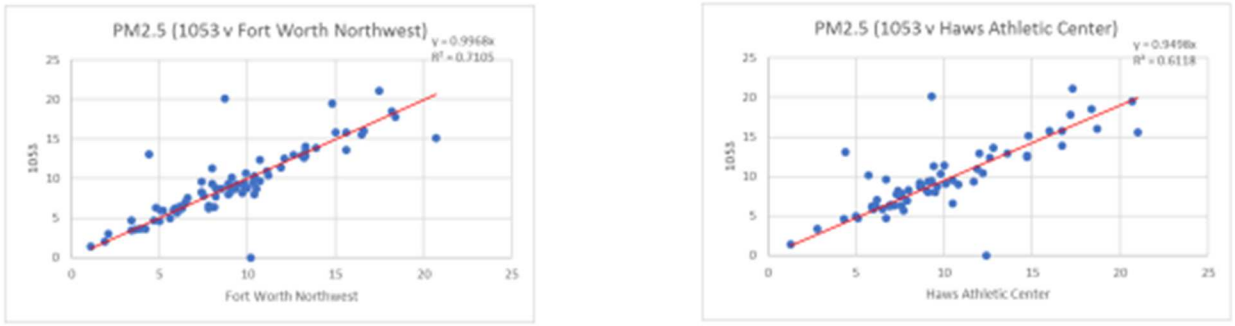

Figure 19 Correlations of 1-hour $PM_{2.5}$ concentrations at CAMS 1053 to that observed at 2 regional background CAMS stations (year 2015)

Houston Southwest Freeway (AQS: 482011066; TCEQ CAMS 1066)

The Houston Southwest Freeway CAMS 1066 station at 5617 Westward Avenue, TX 77081 was activated in January 22, 2014. It's 13 m above the sea level, located at (Latitude 29° 43' 18"N, Longitude -95° 29' 34"W), and owned and operated by TCEQ. The station currently monitors NO_X including NO and NO_2, temperature, wind speed, wind direction, and peak wind gust. The distance of this site to the nearest traffic lane of I-59 is 24 meters. The site is near the intersection of I-59 and Westpark Tollway (Figure 20) beneath elevated several highway facilities including ramps and elevated road segments, as seen in Figures 20. Figure 21 shows views from the station towards different directions.

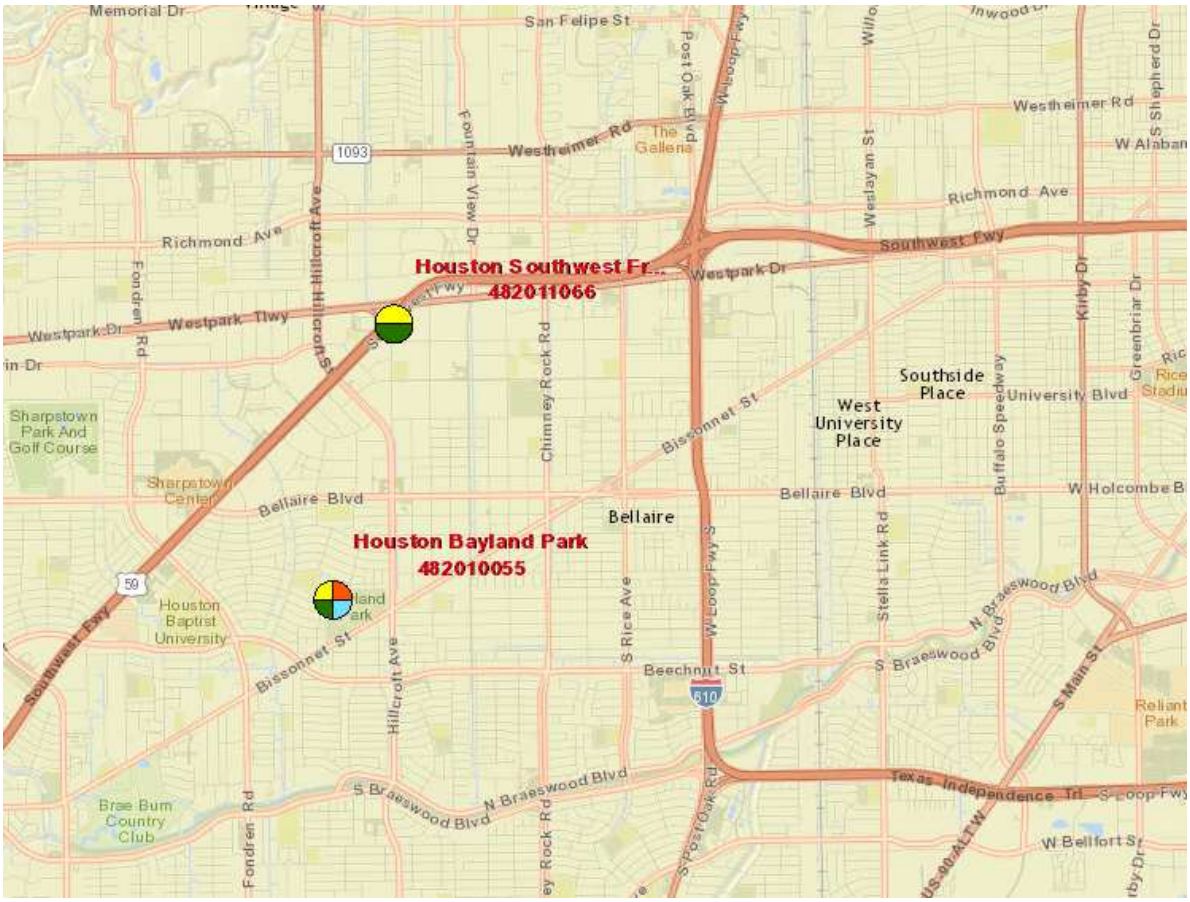

Figure 20 General location of CAMS 1066

Figure 22 shows the wind rose plot for CAMS 1066 for 2015. East to southeasterly winds prevailed at this location and the station was found to be downwind of the highway emissions for approximately 45 % of the time in 2015. Only hourly NO_x concentrations are measured at this station and Figure 23 shows the hourly NO_2 concentrations and concentration rose observed at this station. The peak 1-hour NO_2 concentrations (<70 ppb) observed in 2015 was well below the NAAQS of 100 ppb. No significant increases in NO_2 concentration in any wind direction. This could be caused by the turbulence induced by the artificial complex terrain of elevated highway facilities or simply the consequence similar to that observed in Stations 1052 and 1053 where high concentrations were evenly distributed in all wind directions.

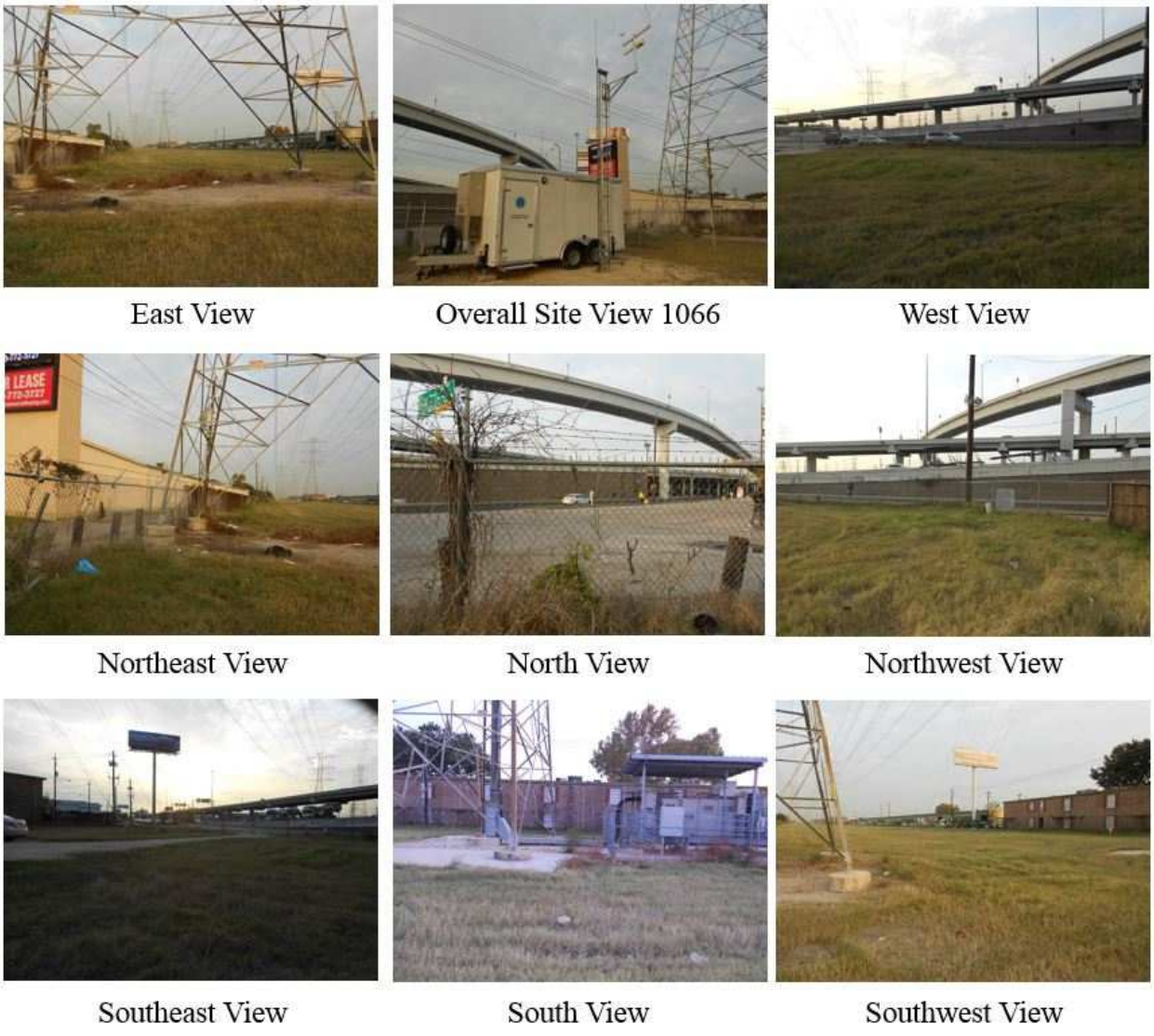

Figure 21 Various Views from CAMS 1066 (TCEQ 2017)

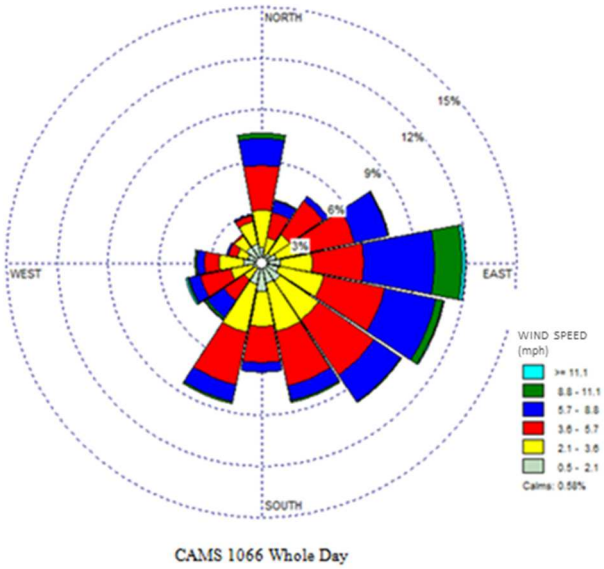

Figure 22 Wind rose for CAMS 1066 (2015)

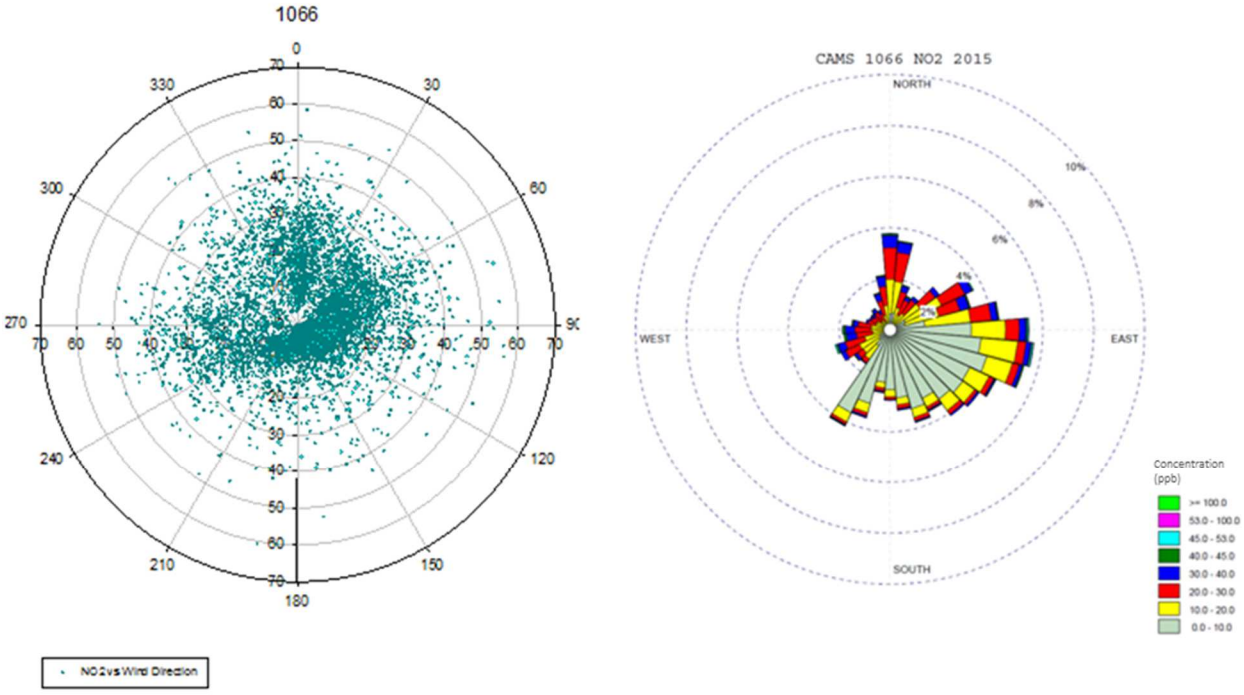

Figure 23 NO_2 concentration plot and concentration rose for CAMS 1066 for 2015

Dallas LBJ Freeway (AQS: 481131067; TCEQ CAMS 1067)

The Dallas LBJ Freeway CAMS 1067 station at 8652 LBJ Freeway, TX 75243 was activated in April 01, 2014. The station has an elevation of 177 m and is located at (Latitude 35° 55' 16"N, Longitude -96° 45' 13"W), owned and operated by TCEQ. CAMS 1067 currently monitors NO_X including NO and NO_2, temperature, wind speed, wind direction, and peak wind gust. The distance of this site to the nearest traffic lane of I-635 is 24 meters. Figure 24 shows the location of the station whereas Figures 25 shows views from the station towards different directions.

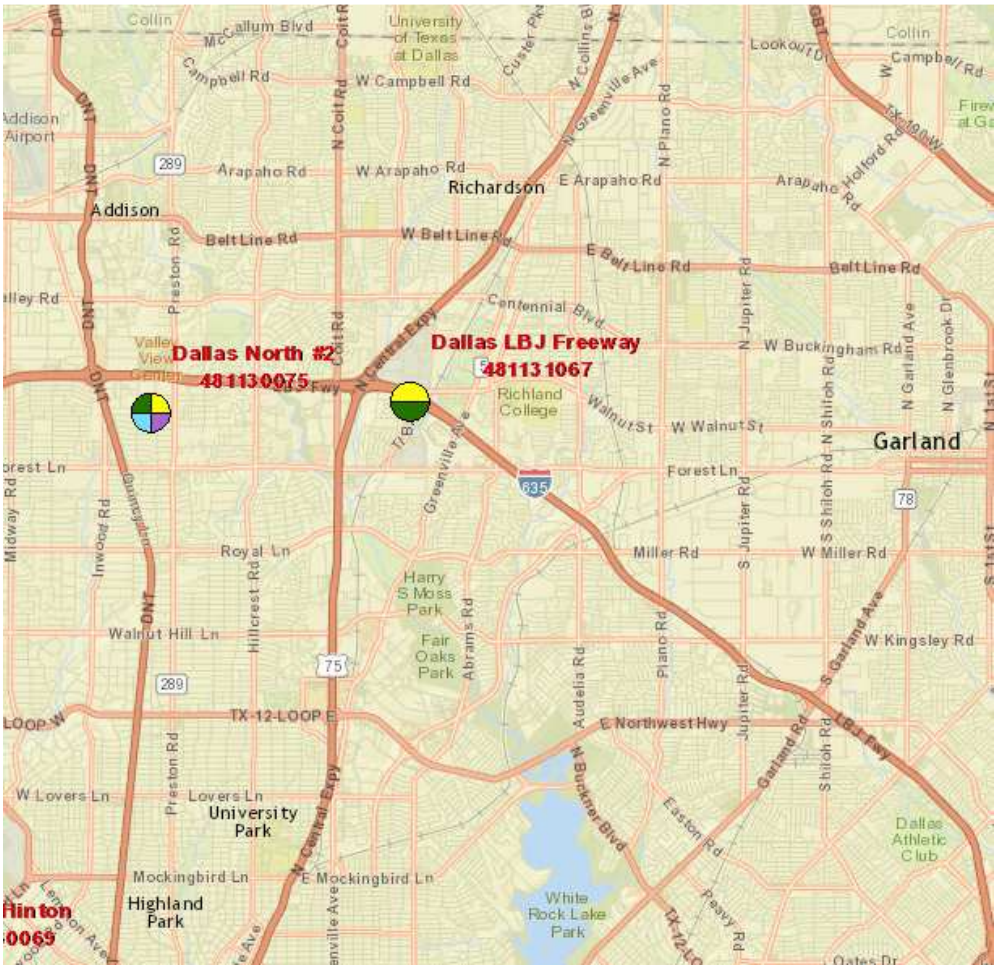

Figure 24 General location of CAMS 1067

Figure 25 Various views for CAMS 1067 (TCEQ 2017)

Figure 26 shows the wind rose plot for CAMS 1067 for 2015. Southerly winds prevailed at this location for at least 70 % of the time in 2015. Only hourly NO_x concentrations are measured at this station and Figure 27 shows the hourly NO_2 concentrations and concentration rose observed at this station. The peak 1-hour NO_2 concentrations (<60 ppb) observed in 2015 was well below the NAAQS of 100 ppb. High NO_2 concentrations were observed at various times regardless the upwind and downwind geometry between the near-road monitor and the highway segment, which is only 24 meters away although slightly elevated.

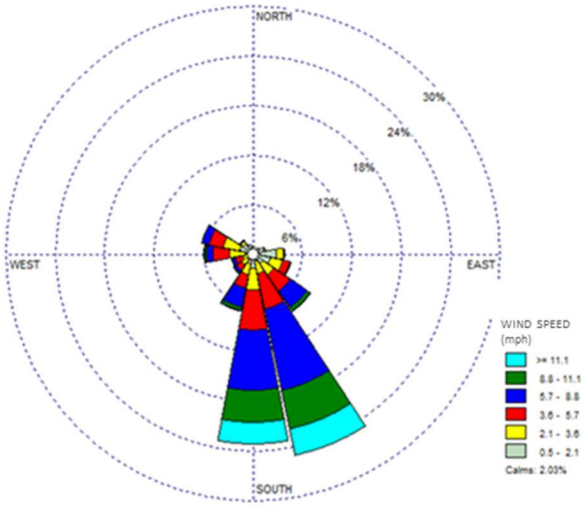

CAMS 1067 Whole Day

Figure 26 Wind rose for CAMS 1067

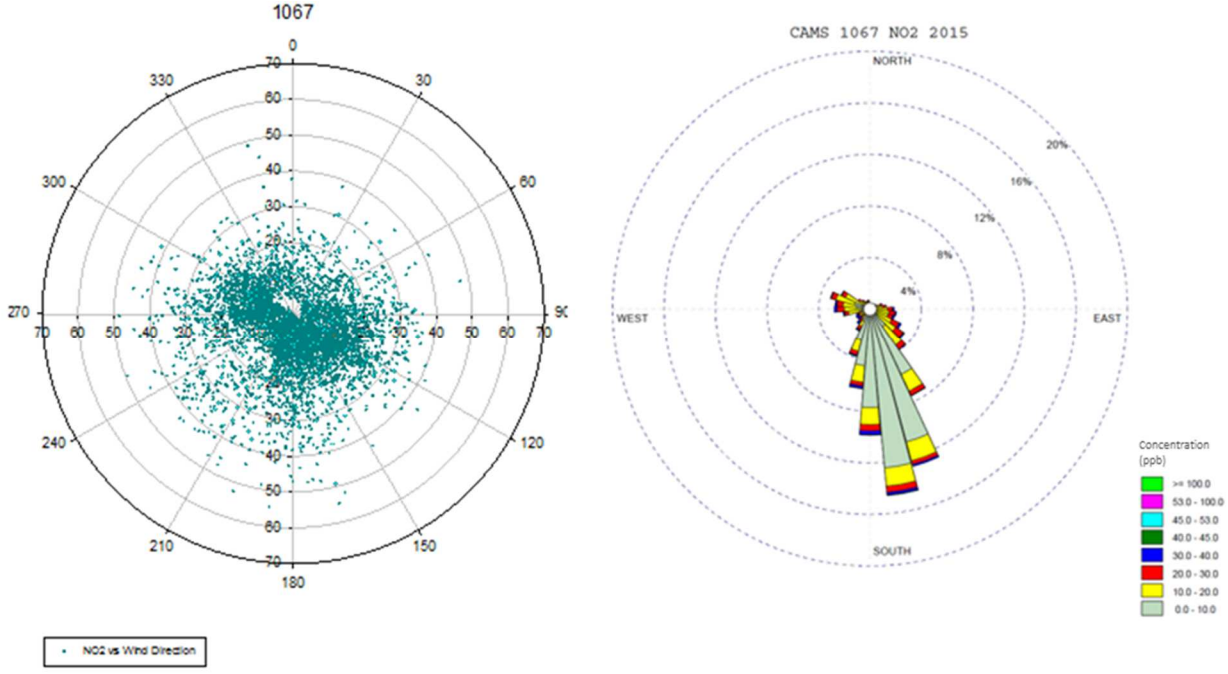

Figure 27 NO_2 concentrations at CAMS 1067 (2015)

Austin North Interstate 35 (AQS: 484531068; TCEQ CAMS 1068)
The Austin North Interstate CAMS 1068 at 8912 N IH-35 SVRD SB, TX 78753 was activated in April 16, 2014. The station has an elevation of 205 m and is located at (Latitude 30° 21' 14"N, Longitude -97° 41' 30"W). It is owned and operated by TCEQ. The CAMS currently monitors NO_X including NO and NO_2, temperature, wind speed, wind direction, and peak wind gust. The

distance of this site to the nearest traffic lane of I-35 is 27 meters. Figure 28 shows the location of the station and Figures 29 displays views from the station towards different directions.

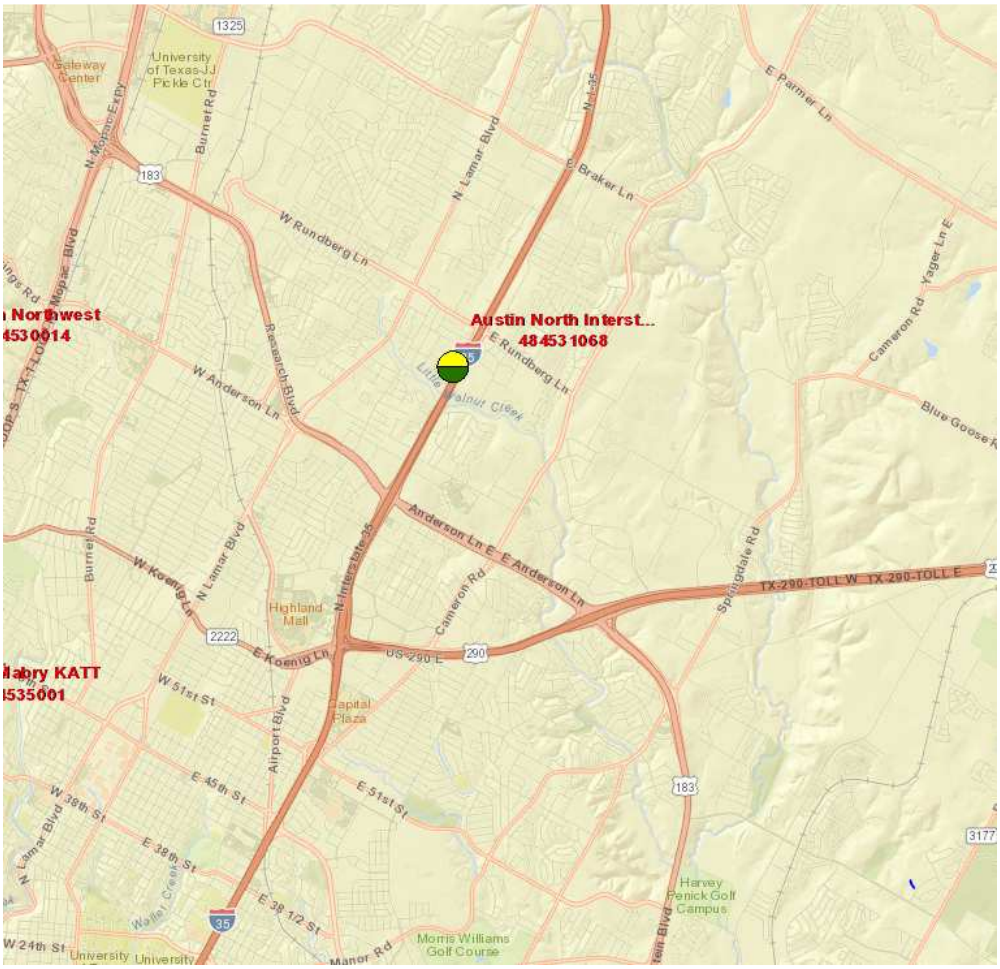

Figure 28 General location of CAMS 1068

Figure 29 Various views from CAMS 1068 (TCEQ 2017)

Figure 30 shows the wind rose plot for CAMS 1068 for 2015. North-south winds prevailed at this location for at least 80 % of the time in 2015. Only hourly NO_x concentrations are measured at this station and Figure 31 shows the hourly NO_2 concentrations and concentration rose observed at this station. The peak 1-hour NO_2 concentrations (<60 ppb) observed in 2015 was well below the NAAQS of 100 ppb. High NO_2 concentrations were observed at various times regardless the upwind and downwind geometry between the near-road monitor and the highway segment.

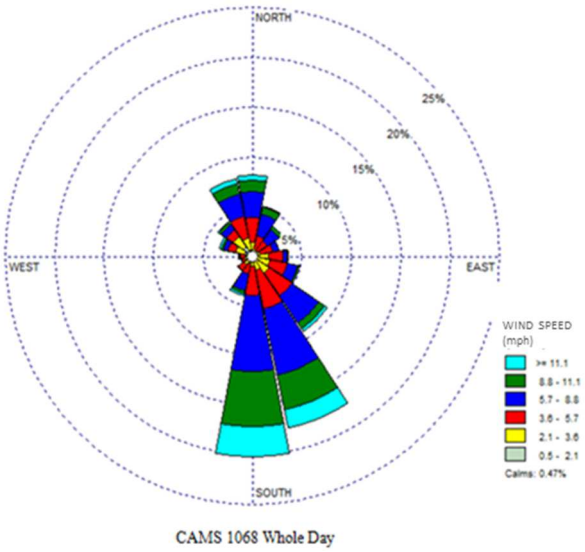

Figure 30 Wind rose for CAMS 1068 (2015)

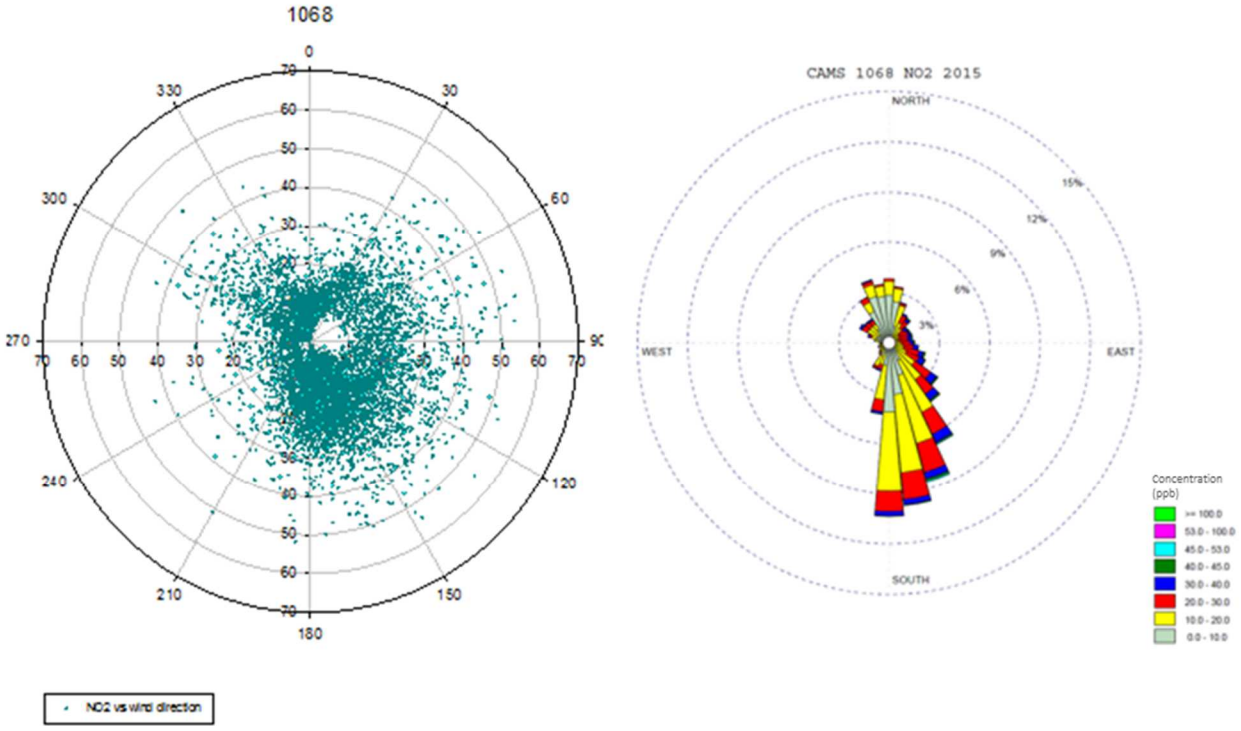

Figure 31 CAMS 1068 NO_2 polar plot and concentration rose 2015

San Antonio Interstate 35(AQS: 480291069; TCEQ CAMS 1069)

The San Antonio Interstate 35 CAMS 1069 at 9904 IH 35 N, TX 78233 was activated in January 08, 2014. The station has an elevation of 284.3 m and is located at (Latitude 29° 31' 46"N, Longitude -98° 23' 29"W). It is owned and operated by TCEQ. CAMS 1069 currently monitors NO_X including NO and NO_2, temperature, wind speed, wind direction, and peak wind gust. The

distance of this site to the nearest traffic lane of I-35 is 20 meters. Figure 32 shows the location of the station whereas Figures 33 show views from the station towards different directions.

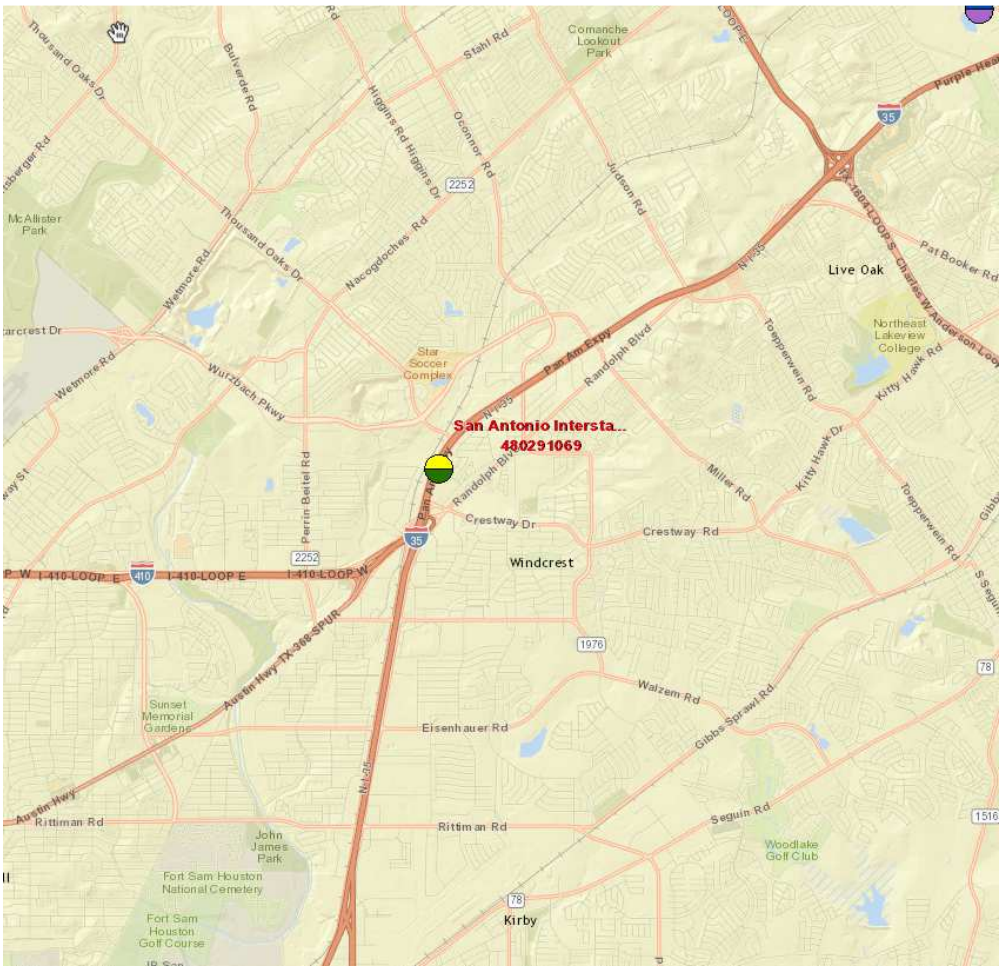

Figure 32 General location of CAMS 1069 in San Antonio, Texas

Figure 33 Various views from CAMS 1069 (TCEQ 2017)

Figure 34 shows the wind rose plot for CAMS 1069 for 2015. Southeasterly winds prevailed at this location for approximately 50 % of the time in 2015. Only hourly NO_x concentrations are measured at this station and Figure 35 shows the hourly NO_2 concentrations and concentration rose observed at this station. The peak 1-hour NO_2 concentrations (<55 ppb) observed in 2015 was well below the NAAQS of 100 ppb. Again, high NO_2 concentrations were observed at various times regardless the upwind and downwind geometry between the near-road monitor and the highway segment which is only 24 meters away.

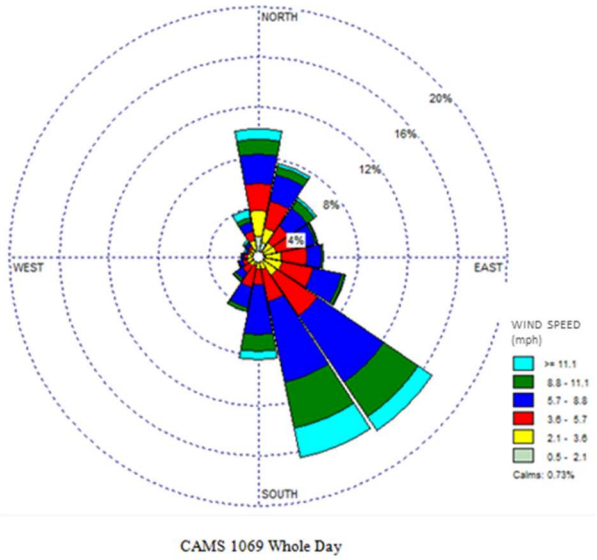

Figure 34 Wind rose for CAMS 1069 (2015)

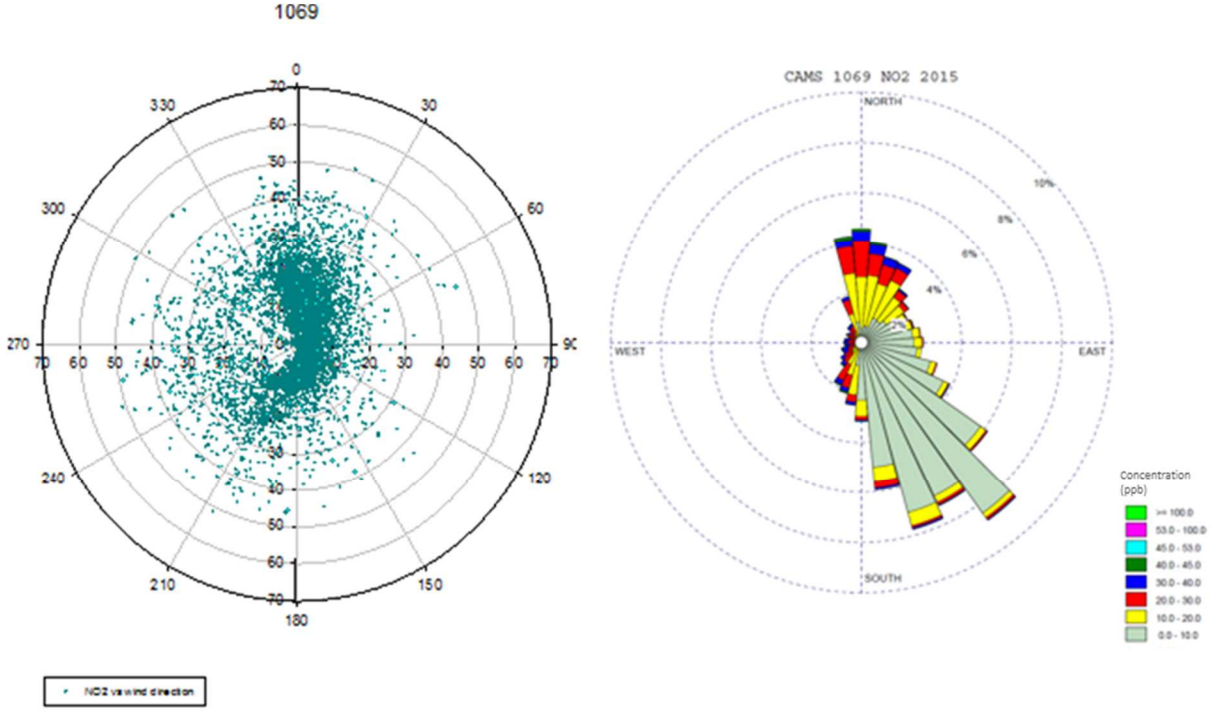

Figure 35 CAMS 1069 NO_2 polar plot and concentration rose 2015

4.2 Near-road Pollutant Concentrations

Near-road air pollution has gained increased attention since February 2010 when the U.S. EPA promulgated new minimum requirements for NO_2 monitoring and required the state and local air monitoring agencies to install near-road NO_2 monitors. Initially, the monitoring priority focused on NO_2 as the primary pollutant of traffic emissions, but the priority quickly extended to cover

two other criteria pollutants, $PM_{2.5}$ and CO, which are both strong markers of traffic emissions. Pollutant concentrations at near-road monitoring stations are affected by a number of factors related to transportation (such as traffic volume, vehicle fleet, vehicle age and maintenance, speed, emission control device), local meteorology (such as wind direction, wind speed, temperature, pressure), and terrain topography (such as roadway-receptor configuration, road condition, source and receptor elevations). Attempts have been made with little success to develop a quantitative relationship between a pollutant concentration and the affecting factors.

The U.S. EPA initiated a near-road pilot study immediately after the promulgation of the 2010 NO_2 monitoring requirements to better understand the selection of monitoring sites and distribution of pollutant concentrations. The pilot study concluded that near-road NO_2 concentrations tended to be highest at locations nearest the roadway and near those roads with highest traffic (Pasch et al 2011). The study also discovered that near-road NO_2 concentrations in 5 studied cities were all less than the 1-hour NAAQS for NO_2 and that the average near-road NO_2 concentrations were higher than the background concentrations observed at non near-road sites (Figure 36). The State of Maryland was more aware of the $PM_{2.5}$ impact on near-road receptors from traffic emissions and conducted a 3½-year study at a Maryland State Highway Administration (SHA) monitoring site (Ginzburg et al 2015). The study concluded that there were no exceedances of the 24-hr or annual NAAQS for $PM_{2.5}$ during the studied period and that the near-road $PM_{2.5}$ concentrations were consistently higher than that measured at background locations. The Maryland study also suggested that $PM_{2.5}$ impacts of traffic emissions are not immediately noticeable at a distance of 150 m (500 feet) from the roadway and that approximately 14% of $PM_{2.5}$ collected at the near-road site could be attributed to the roadway sources, based on source apportionment analysis and AERMOD air dispersion modeling. The contribution of roadway emissions to the near-road $PM_{2.5}$ concentrations apparently could vary significantly due to the uncertainties and variabilities involved in local meteorology, traffic count, vehicle fleet, source-receptor geometry, time, day and season of the year. For instance, Vallamsundar and Lin (2013) estimated that only approximately 5% of the near-road $PM_{2.5}$ can be attributed to the emissions from the road segment, based on a project-level MOVES-AERMOD emission and air dispersion modeling analysis. Near-road PM monitoring sites are exposed not only to the traffic emissions from the immediately adjacent road segments but also to the PM emissions from other point, area, and mobile sources in the regional, urban, local environments. A recent study conducted in Netherlands aiming at this effect suggested that the urban background of $PM_{2.5}$ and PM_{10} is dominated by the regional background, and that primary and secondary PM emission by urban sources contribute less than 15 % to the near-road sites (Keuken et al 2013).

Near-road air quality data became more available in the U.S. since 2014 when state and local air pollution control agencies began to collect NO_2, CO, and $PM_{2.5}$ data and reported to the EPA's Air Quality System (AQS) database. At the request of Washington State Department of Transportation, Sonoma Technology (2016) gathered, processed, and conducted a national-scale review of near-road air pollutant concentrations using the 2014-2015 AQS data. The data represent the best available and most complete data for near-road monitors in the U.S. since they were quality-controlled by the air monitoring agencies and certified by the states. Sonoma Technology also gathered state-reported annual average daily traffic (AADT) of the major roads associated with each of the official near-road monitoring sites in an attempt to understand how concentrations varied by factors such as location, distance to roadway, and traffic volume at the near-road

monitors. It was discovered that CO concentrations were typically 1 ppm or less, although several comparatively high CO concentrations (greater than 4 ppm) were observed at near-road locations in 3 cities. All of the 1-hr values were well below the CO 1-hr NAAQS of 35 ppm. Of the 66 locations with sites reporting NO_2 data to AQS, only three 1-hr daily maximum NO_2 concentrations and 5 hourly observations were above the NAAQS of 100 ppb for NO_2. For $PM_{2.5}$ data, sites in Denver, Colorado; Houston, Texas; Long Beach, California; Ontario, California; and Phoenix, Arizona, recorded $PM_{2.5}$ annual averages for 2015 greater than 12 $\mu g/m^3$. However, of these sites, only Long Beach and Ontario reported a full year of data for 2015, while Houston had three quarters of the year of data. There were 33 days in 2015 at 12 near-road locations that had 24-hr $PM_{2.5}$ concentrations above 35 $\mu g/m^3$. Only three of the sites, Denver, Ontario and Long Beach, had a 98th percentile of 24-hr $PM_{2.5}$ concentrations greater than 35 $\mu g/m^3$. Phoenix had a 98th percentile of 34.5 $\mu g/m^3$.

It becomes obvious that CO concentrations at near-road monitoring sites were consistently detected at levels well below the NAAQS and do not pose any adverse health concern to the public, as demonstrated in the Washington State's study and near-road air monitoring data reported by TCEQ in Section 4.2. Similarly, near-road NO_2 concentrations, although many sites do not yet have full years of data available and with a few marginal readings (less than 1% of the data) that exceeded the NAAQS of 100 ppb, do not appear to have high concentrations at a frequency sufficient enough to violate the NAAQS and raise public health concern. $PM_{2.5}$, on the other hand, does appear to have relatively higher readings and thus require additional evaluation. It is thus important to understand how these high near-road $PM_{2.5}$ concentrations relate to traffic, urban-scale concentrations and meteorology, and what the predictors of high near-road concentrations are (Sonoma Technology 2016).

Karner and coworkers (2010) analyzed 41 roadside monitoring studies between 1978 and 2008 and concluded that almost all pollutants decay to background levels at a distance 115 m to 570 m from the edge of the road and the decay rate varies from one pollutant to another (Figure 37) except $PM_{2.5}$ which achieved the background level by 990 m. $PM_{2.5}$, as seen in the right-hand panel of Figure 37, does not display any trend of rapid decrease from the road edge as the distance from edge increases. This may not seem to agree well with the estimates derived from a typical Gaussian line source model, especially for $PM_{2.5}$. Venkatram et al (2013) examined the effect of wind direction on near-road concentration observations by analyzing data from three near-road pollution measurements and by using the AERMOD dispersion model. Using the line source algorithm built in the AERMOD model, Venkatram et al (2013) showed that the concentration of an inert pollutant decays rapidly to less than 1/5 of its initial strength in 100 m in the direction normal to the roadway. For a short-lived pollutant (due to evaporation, photolysis, chemical reaction, deposition, among other mechanisms), the off-road concentration would be reduced to 1/10 of its initial strength. Recently, Cahill and co-workers (2016) conducted a near-road air quality study using the highway safety flare as a unique source tracer for the fine PM emissions from a highly travelled roadway. Figure 38 shows the downwind PM concentrations measured at distances downwind of the highway edge. The downwind concentrations estimated from a Gaussian line source model are shown in the figure. Fine PM was found to be essentially undiluted at distances well beyond 200 m. The discrepancy was attributed to many uncontrollable factors, such as the existence of sound walls for at-grade freeways, elevated or filled section of a freeway, canopy vegetation, and

classification of atmospheric stability condition. Nevertheless, this gross mismatch between the downwind concentrations and the model estimates shows the need for further model improvement.

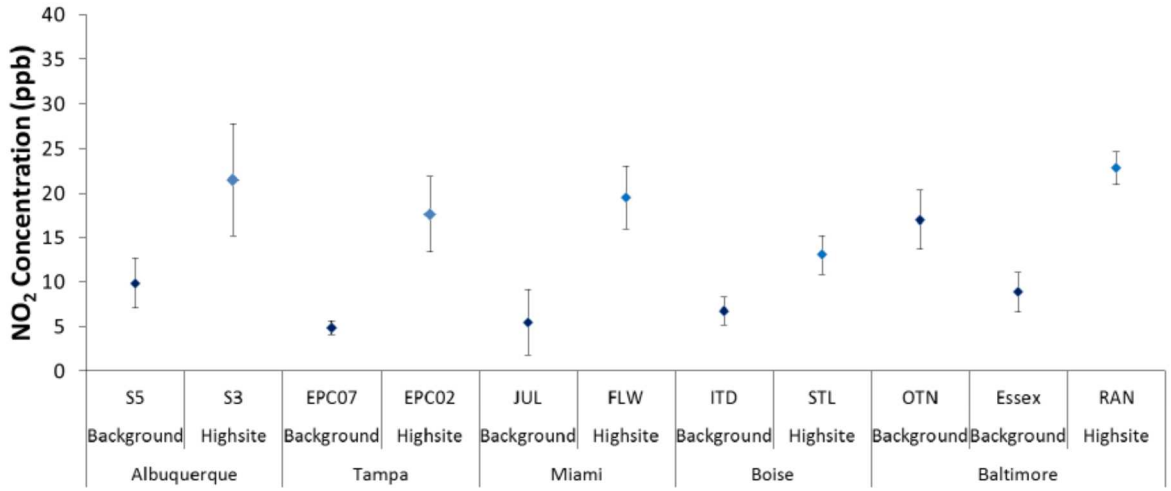

Figure 36 Average NO_2 concentrations at the background and highest-concentration sites by CBSA (Figure 3-12, Pasch et al, 2011)

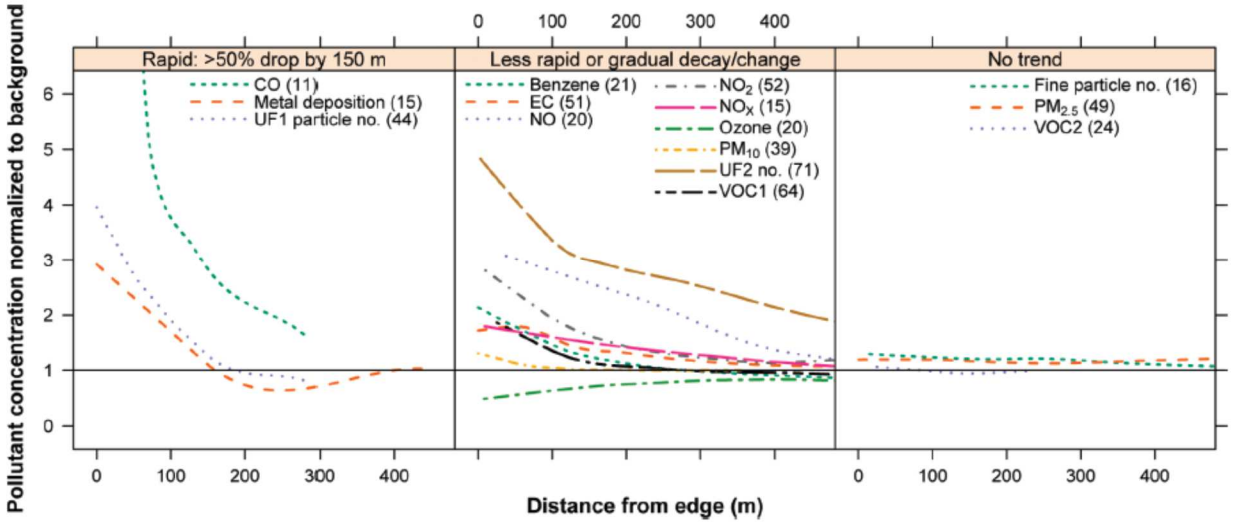

Figure 37 Local regression of edge normalized concentrations on distance (Figure 3 of Karner et al., 2010).

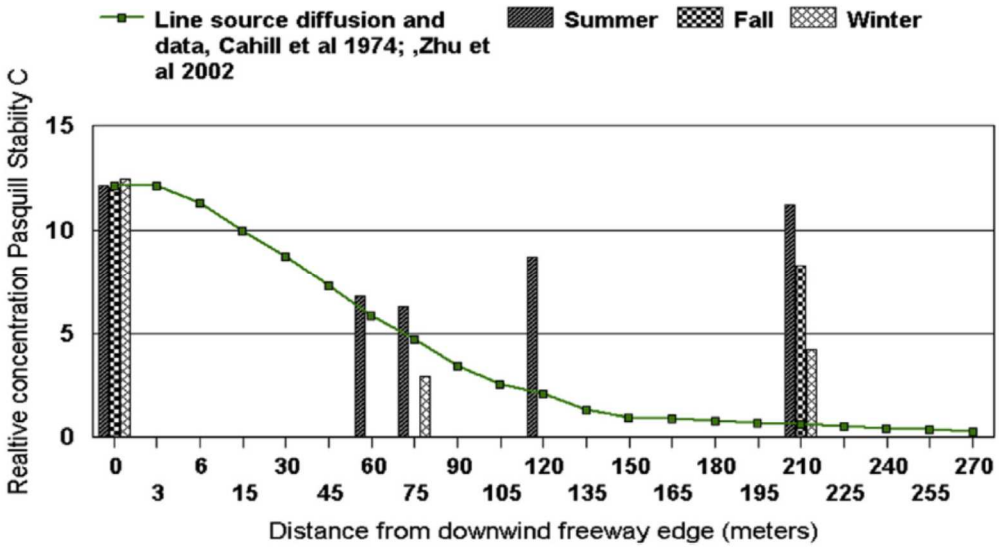

a) 35th Avenue

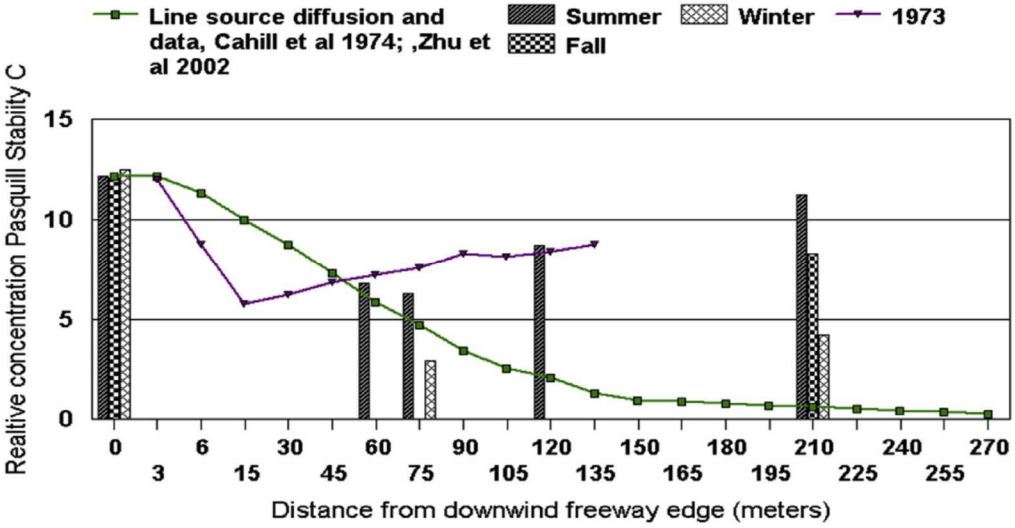

b) 10th Avenue

Figure 38 PM concentrations downwind of a busy highway on a) 35th Avenue; and b) 10th Avenue, Sacramento, CA

4.3 Overview of Regional Ambient $PM_{2.5}$ Monitors in Texas

In accordance to Title 40 CFR Part 58, Appendix D, Section 4.7, the TCEQ installed 21 24-hour $PM_{2.5}$ FRM monitors and 47 continuous $PM_{2.5}$ monitors in 2015 and expected to expand the total number of FRM monitors to 25 throughout the state (TCEQ 2015). The distribution of these monitors in Texas is graphically shown in Figure 39 and listed in Table 2. Six of the 25 FRM monitors are near-road monitors, as summarized previously in Table 1. A review of the locations of existing TCEQ CAMS stations is currently underway to identify additional near-road monitors and monitors that can be used as regional background monitors for $PM_{2.5}$.

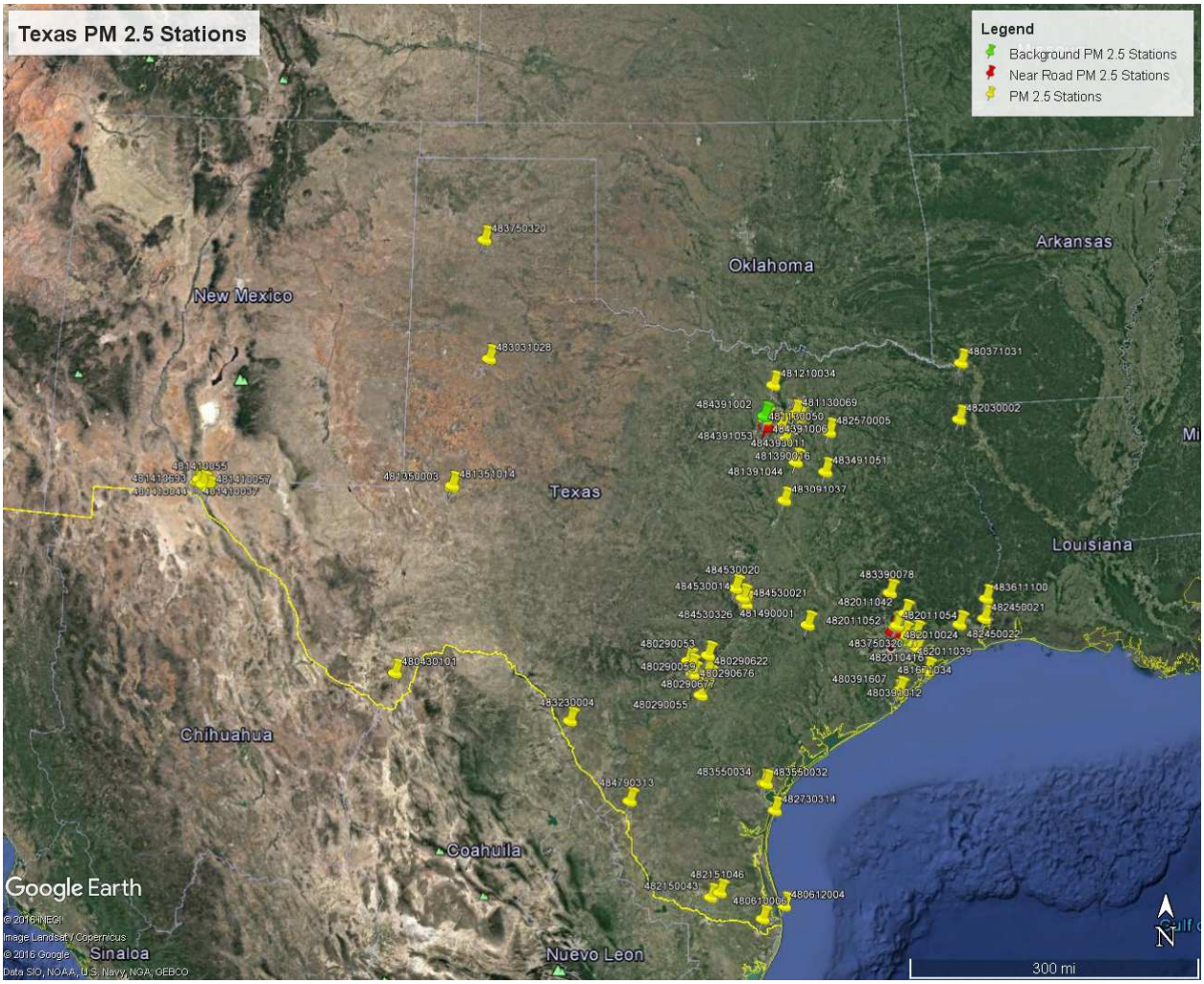

Figure 39 Locations of PM monitoring stations operated by TCEQ

Table 2 Distribution of Texas PM2.5 Monitors (Appendix I of TCEQ 2015)

		2012-2014 Design Value (µg/m³)		Percent of NAAQS		FRM Samplers		Speciation		Continuous	
Metropolitan Statistical Area	2014 Population Estimates[1]	Annual	24-Hour	Annual[2]	24-Hour[3]	Required Monitors[4]	Existing Monitors[5]	Required Monitors[6]	Existing Monitors[5]	Required Monitors[6]	Existing Monitors[5]
Dallas-Fort Worth-Arlington	6,954,330	10.7	24	89	69	4	5	1	2	3	8
Houston-The Woodlands-Sugar Land	6,490,180	11.6	24	97	69	4	5	2	4	3	9
San Antonio-New Braunfels	2,328,652	8.5	21	71	60	2	2	0	0	1	6
Austin-Round Rock	1,943,299	9.4	24	78	69	2	2	0	0	1	3
El Paso	836,698	11.2	34	93	97	3	2	1	1	2	4
McAllen-Edinburg-Mission	831,073	10.2	25	85	71	2	1	0	0	1	1
Corpus Christi	448,108	10.1	31	84	89	1	2	1	1	1	2
Killeen-Temple	424,858	N/A	N/A	N/A	N/A	0	0	0	0	0	0
Brownsville-Harlingen	420,392	N/A	N/A	N/A	N/A	1	0	0	0	1	2
Beaumont-Port Arthur	405,427	N/A	N/A	N/A	N/A	0	0	0	0	0	4
Lubbock	305,644	N/A	N/A	N/A	N/A	0	0	0	0	0	1
Laredo	266,673	N/A	N/A	N/A	N/A	0	0	0	0	0	2
Waco	260,430	N/A	N/A	N/A	N/A	0	0	0	0	0	1
Amarillo	259,885	N/A	N/A	N/A	N/A	0	0	0	0	0	1
Odessa	153,904	N/A	N/A	N/A	N/A	0	0	0	0	0	2
Wichita Falls	151,536	N/A	N/A	N/A	N/A	0	0	0	0	0	0
Texarkana	149,235	10.2	22	85	63	1	1	0	0	1	0
Marshall[7]	67,336	9.5	22	79	63	0	1	0	1	0	1

Section 5: Data Analysis

5 Model Performance Measures

- Modeled and Observed Pollutant Concentrations

It is understood that the Gaussian air dispersion models, such as AERMOD or CALINE3, are performed to provide estimates of the increased pollutant concentrations in space and time resulting from various sources of emissions. Depending on the purposes of the assessment, it may not be critical to accurately account for the spatial and temporal variations in the prediction (Wood 2014). For example, the focus of a transportation air quality compliance assessment is to determine whether the incremental impacts due to traffic emissions will result in noncompliance of NAAQS for the criteria pollutants. Under such circumstance, a model is deemed more appropriate than others if it can conservatively, yet realistically, predicts the worst 1-hr, 8-hr, 24-hr, or annual averages that do not exceed the NAAQS. On the contrary, an unbiased prediction of pollutant concentrations in space and time would be of pivotal importance for a health exposure assessment.

Air pollution data recorded at an air monitoring station includes the contribution from all other sources of emissions in the area. This contribution may be so ubiquitous that it can be deducted as the background concentration or so specific to certain sources that a source apportionment analysis is needed to segregate the contribution.

- Performance Objectives

As stated in the project statement, the primary objective of the project is to evaluate the model performance of AERMOD and CALINE3 with near-road air quality monitoring data to provide insights into the differences between modeling results and monitoring data. Therefore, the model performance objectives are to select a model that provide i) spatially and temporally accurate estimates and ii) conservative, yet realistic, estimates for transportation conformity analysis.

- Performance Metrics

Performance measures for air quality models are well documented in the literature (Cox and Tikvart 1990; Chang and Hanna, 2004). The following measures will be used in the evaluation of model estimates and field observations.

- *Common Variables:*

M = predicted concentration

O = observed concentration

X = predicted or observed concentration

σ = standard deviation

- *Mean Bias, Mean Error, and Root Mean Square Error (ppb)*

$$\text{Mean Bias} = \frac{1}{n}\sum_{1}^{n}(M - O)$$

$$\text{Mean Error} = \frac{1}{n}\sum_{1}^{n}|M - O|$$

Root Mean Square Error = $\sqrt{\frac{\sum_{1}^{n}(M-O)^2}{n}}$

- *Normalized Mean Bias and Error (unitless)*

Normalized Mean Bias = $\frac{\sum_{1}^{n}(M-O)}{\sum_{1}^{n}(O)}$

Normalized Mean Error = $\frac{\sum_{1}^{n}|M-O|}{\sum_{1}^{n}(O)}$

- *Fractional Bias and Error (unitless)*

Fractional Bias = $\frac{1}{n}\left(\frac{\sum_{1}^{n}(M-O)}{\sum_{1}^{n}\left(\frac{(M+O)}{2}\right)}\right)$

Fractional Error = $\frac{1}{n}\left(\frac{\sum_{1}^{n}|M-O|}{\sum_{1}^{n}\left(\frac{(M+O)}{2}\right)}\right)$

- *Correlation Coefficient (unitless)*

Correlation = $\frac{1}{(n-1)}\sum_{1}^{n}\left(\left(\frac{O-\overline{O}}{\sigma_o}\right)*\left(\frac{M-\overline{M}}{\sigma_m}\right)\right)$

- *Standard Deviation (ppb)*

Standard Deviation (σ) = $\sqrt{\frac{1}{n}\sum_{1}^{n}(X-\bar{X})^2}$

- *Coefficient of Variation (unitless)*

Coefficient of Variation = $\frac{\sigma}{\overline{X}}$

Adar, S.D., Sheppard, L., Vedal, S.L., Polak, J.F., Sampson, P.D., Diez Roux, A.V., Budoff, M., Jacobs, Araujo, J.A., 2011. Particulate air pollution, systemic oxidative stress, inflammation, and atherosclerosis. *Air Quality, Atmosphere and Health*, 4(1):79-93

American Housing Survey (AHS), 2015. AHS 2013 National Summary Tables, U.S. Department of Housing and Urban Development and, https://www.census.gov/programs-surveys/ahs/data/2013/ahs-2013-summary-tables/national-summary-report-and-tables---ahs-2013.html, Last Revised: December 4, 2015

Armijos, R. X., Weigel, M. M., Myers, O. B., Li, W., Racines, M., & Berwick, M., 2015. Residential Exposure to Urban Traffic Is Associated with Increased Carotid Intima-Media Thickness in Children. *Journal of Environmental and Public Health,2015*, 1-11.

Cahill, T.A., Barnes, D.E., Wuest, L., Gribble, D., Buscho, D., Miller, R.S., De la Croix, C., 2016. Artificial ultra-fine aerosol tracers for highway transect studies, *Atmospheric Environment*, 136 (2016): 31-42

Chang, J.C., Hanna, S.R., 2004. Air quality model performance evaluation, *Meteorol. Atmos. Phys*. 87: 167-196.

Chen, L., Jenison, B.L., Yang ,W., Omaye, S.T., 2000. Elementary school absenteeism and air pollution, *Inhal. Toxicol*., 12(11): 997-1016

Cox, W.M., Tikvart, J.A., 1990. A statistical procedure for determining the best performing air quality simulation model. *Atmospheric Environment* 24A, 2387-2395.

Gilliland, F.D., Berhane, K., Rappaport, E.B., Thomas, D.C., Avol, E., Gauderman,W.J., London, S.J., Margolis, H.G., McConnell, R., Islam, K.T., Peters, J.M., 2001. The effects of ambient air pollution on school absenteeism due to respiratory illnesses, *Epidemiology*, 12:43–54

Ginzburg, H.1., Liu, X., Baker, M., Shreeve, R., Jayanty, R.K.M., Campbell, D., Zielinska, B., 2015. Monitoring study of the near-road PM2.5 concentrations in Maryland, *Journal of the Air & Waste Management Association,* 65:1062–1071

Hoek, G., Beelen, R., de Hoogh, K., Vienneau, D., Gulliver, J., and Fischer, P., 2008, A review of land-use regression models to assess spatial variation of outdoor air pollution. *Atmospheric Environment*, 42:7561–7578

Hoffmann, B., Moebus, S., Möhlenkamp, S., Stang, A., Lehmann, N., Dragano, N., Schmermund, A., Memmesheimer, M., Mann, K., Erbel, R., Jöckel, K.H., Heinz, N., 2007. Residential exposure to traffic is associated with coronary atherosclerosis. *Circulation*, 116(5):489-496

Iannuzi, A., Verga, M.C., Renis, M., 2010. Air pollution and carotid arterial stiffness in children. *Cardiology in the Young,* 20(2):186-190

Karner, A; Eisinger, D; Niemeier, D., 2010. Near-roadway air quality: Synthesizing the findings from real-world data; *Environ. Sci. & Technol.* , *44*(14), 5334-5344

Keuken M.P., Moerman, M. Voogt, M., Blom, M., Weijers, E.P., Rockmann, T.,Duset, U., 2013. Source contributions to $PM_{2.5}$ and PM_{10} at an urban background and a street location, Atmospheric Environment, 71:26-35

Pasch, A.N., Hafner H.R., Vaughn, D.L., O'Brien T.E., 2011. Summary of Results from Near-Road NO2 Monitoring Pilot Study. Final Report STI-910308-4211-FR, Sonoma Technology,

Inc., Final report prepared for the U.S. Environmental Protection Agency, Research Triangle Park, NC.

Sonoma Technology, Inc., 2016. National Near-Road Data Assessment: Draft Report No. 2 With 2015 Data, Draft report 2 prepared for Washington State Department of Transportation, Settle, WA., Aug. 2016.

Texas Commission on Environmental Quality (TCEQ), 2013. *2013 Annual Monitoring Network Plan.* P.O. Box 13087, Austin, Texas 78711-3087

Texas Commission on Environmental Quality (TCEQ), 2014. *2014 Annual Monitoring Network Plan.* P.O. Box 13087, Austin, Texas 78711-3087

Texas Commission on Environmental Quality (TCEQ), 2015. *2015 Annual Monitoring Network Plan.* P.O. Box 13087, Austin, Texas 78711-3087

Texas Commission on Environmental Quality (TCEQ), 2015. *Texas Five-Year Ambient Monitoring Network Assessment.* P.O. Box 13087, Austin, Texas 78711-3087

Texas Commission on Environmental Quality (TCEQ), 2016. *2016 Annual Monitoring Network Plan.* P.O. Box 13087, Austin, Texas 78711-3087

Texas Commission on Environmental Quality (TCEQ), 2017. *TCEQ Daily Summary Report by Site,* https://www.tceq.texas.gov/cgi-bin/compliance/monops/select_month.pl?region=12, accessed January 2017.

U.S. Environmental Protection Agency (U.S. EPA), 2010. Primary National Ambient Air Quality Standards for Nitrogen Dioxide—Final Rule; *Fed. Regist.* 2010, *75*, 6482

U.S. Environmental Protection Agency (U.S. EPA), 2012. Near-road NO2 Monitoring Technical Assistance Document, Office of Air Quality Planning and Standards, EPS-454/B-12-002.

Vallamsundar, S. and Lin, J., 2012. Using MOVES and AERMOD models for PM2.5 Conformity Hot-Spot Air Quality Modeling, 91st Annual Meeting of the Transportation Research Board, Washington, DC

Venkatram, A., Snyder, M., Isakov, V., Kimbrough, S., 2013. Impact of wind direction on near-road pollutant concentrations, *Atmospheric Environment*, 80: 248-258

Wendt, J.K, Symanski, E, Stock, T.H., Chan W., Du, X.L., 2014. Association of short-term increase in ambient air pollution and timing of initial asthma diagnosis among Medicaid-enrolled children in a metropolitan area, *Environmental Research*, 131:50-58

Weinstock, L., Watkins, N., Wayland, R., Baldauf, R., 2013. EPA's emerging near-road ambient monitoring network: A progress report, *Environmental Magazine*, 2013(7):6-10

Wood, S.R., 2014. Performance evaluation of AERMOD, CALPUFF, and legacy air dispersion models using the Winter Validation Tracer Study dataset, *Atmospheric Environment,* 89 (2014): 707-720

Appendix A

Meteorological Data

According to the EPA's Guideline on Air Quality Models (40 CFR Appendix W to Part 51), "the meteorological data used as input to an air quality model should be selected on the basis of spatial and climatological (temporal) representativeness as well as the ability of the individual parameters selected to characterize the transport and dispersion conditions in the area of concern". The use of 5 years of adequately representative (off-site) NWS meteorological data or at least 1 year of site-specific meteorological data is required. As a result, both off-site 5 consecutive years (2012-2016) of surface meteorological data using nearby NWS airport data and on-site 2 years (2015-2016) surface meteorological data using site-specific TCEQ CAMS data were developed for this study.

Five consecutive years (2012-2016) of off-site NWS surface meteorological data were retrieved from the WBAN website for Station IAH, located at the International Airport of Houston, for use in the dispersion modeling of the Houston North Loop site. WBAN is the Weather-Bureau-Army-Navy numbers used by NCDC to identify its weather monitoring stations. Similarly, five consecutive years (2012-2016) of the off-site NWS surface meteorological data were retrieved from the WBAN station FTW, located at the Fort Worth Meacham Airport which is the closest off-site airport, for the dispersion modeling of our Fort Worth California Parkway North site. There are two systems reporting surface meteorological data at these airport sites: Automated Surface Observing System (ASOS) or Automated Weather Observing System (AWOS) and the Integrated Surface Data system (ISD). In addition, the Local Climatological Data (LCD) is a summary which provides a synopsis of climatic values for a single weather station. This NCDC generated summary is a product of surface observations from both manual and automated (AWOS, ASOS) stations with source data taken from the National Centers for Environmental Information's ISD dataset. LCD data was chosen over ISD for its greater degree of completeness and inclusion of ceiling height and sky cover for use in generating meteorological files for CAL3QHCR modeling. The ISD data was processed in conjunction with ASOS 1-minute data in AERMET, as recommended by EPA (U.S. EPA, 2016), to provide meteorological data files for AERMOD modeling. On-site surface meteorology is available at the Houston North Loop (TCEQ C1052) and the Fort Worth California Parkway North (TCEQ C1053) sites. Thus, two years (2015-2016) of site-specific meteorological parameters (such as dry bulb temperature, wind direction, and wind speed) from these two sites were obtained for use in the performance evaluation of the air dispersion models. Table 1 lists the locations of the sources used for processing the necessary meteorological files for air dispersion modeling at the two selected sites.

Table 1 Locations of Sources for Meteorological Data Acquisition Stations

Selected Dispersion Model	**Site Source Type**	**Houston North Loop**			**Fort Worth California parkway**		
		Upper Air Data	**Surface Observation**	**Automated Minute Data**	**Upper Air Data**	**Surface Observation**	**Automated Minute Data**
AERMET	**5-yr Offsite**	Lake Charles, LA	*Houston Intercontinental Airport*	*Houston Intercontinental Airport*	Fort Worth, TX	Meacham International Airport, Fort Worth, TX	Meacham International Airport, Fort Worth, TX
	1-yr Onsite	Lake Charles, LA	*Houston Intercontinental Airport and C 1052*	*Houston Intercontinental Airport*	Fort Worth, TX	Meacham International Airport, Fort Worth, TX and C1053	Meacham International Airport, Fort Worth, TX

CAL3QHCR	**5-yr Offsite**	Lake Charles, LA	*Houston Intercontinental Airport*	Not Required	Fort Worth, TX	Meacham International Airport, Fort Worth, TX	Not Required
	1-yr Onsite	Lake Charles, LA	*Houston Intercontinental Airport and C1052*	Not Required	Fort Worth, TX	Meacham International Airport, Fort Worth, TX and C1053	Not Required

A. Meteorological Data for AERMOD

AERMOD requires two meteorological input files, a surface meteorology and a wind profile file, which are created using AERMET. AERMET processes the input files in three different stages. The first stage extracts the input data from raw surface, upper air, and minute data and processes them through various quality checks. The second stage merges all the inputs and creates a single merge file. Stage three creates both the surface and profile files to be used in AERMOD. According to the EPA (U.S. EPA, 2016), AERMET shall be used to preprocess all meteorological data, be it observed or prognostic, for use with AERMOD in regulatory applications and the AERMINUTE processor, in most cases, should be used to process 1-minute ASOS wind data for input to AERMET when processing NWS ASOS sites in AERMET.

A.1 Meteorological Files Required by AERMET

A total of five input files are required by AERMET to create the meteorological files for AERMOD modeling. These files are called Surface, Onsite, Upper Air, AERMINUTE and AERSURFACE.

A.1.1 Surface Input

The surface input file is acquired from NCDC of NOAA. The hourly surface data for all available years is placed in a file transfer protocol server at the link ftp://ftp.ncdc.noaa.gov/pub/data/noaa/. The users can identify the desired stations and years of data by looking up the table in the file, isd_history.txt, located in the ftp site.

A.1.2 Onsite Input

The onsite input file has to be created from scratch based on what parameters are desired in accordance to input requirements as specified by EPA (EPA, 2016). Each column of the created dataset should represent one parameter. For this project, the parameters to be used are day, month, year, hour, precipitation amount, temperature, dew point temperature, wind speed, wind direction, standard deviation of horizontal wind, and relative humidity. The data for these parameters can be retrieved, as a CSV file, from NOAA's Local Climatological Data at the link https://www.ncdc.noaa.gov/cdo-web/datatools/lcd. The Texas Commission on Environmental Quality (TCEQ) also provides a number of selected years of site-specific onsite data for many Texas air monitoring stations and the parameters can also be found at their TAMIS website.

A.1.3 Upper Air Input

Upper air data is recorded at unevenly, sparsely distributed locations throughout the U.S. Selection of the closed upper air data for use in air dispersion modeling requires special attention as only certain stations record data at a certain time so the closest upper air station to the point of interest can be far away from the modeling domain. The data can be retrieved from NOAA's Radiosonde Database at https://ruc.noaa.gov/raobs/. The data format required from Breeze's AERMET, a window-based version of EPA AERMET software commercially developed for easy use by environmental professionals, is FSL.

A.1.4 AERMINUTE Input

It is usually necessary to run the program AERMINUTE in order to supplement the ISD surface data for a more complete surface meteorological file to be used in the air dispersion modeling. As mentioned by O'Donnell (2014), a potential concern related to the use of ISD meteorological data for air dispersion modeling is the often high incidence of calms and variable wind conditions. In the reporting of surface weather data, a calm wind is defined as a wind speed less than 3 knots and is assigned a value of 0 knots. In addition, the wind direction may be reported as missing if the wind direction varies more than 60 degrees during the 2-minute averaging period for the observation (O'Donnell, 2014). To reduce the number of calms and missing winds in the surface data, the 1-minute ASOS wind data is used to calculate hourly average wind speed and directions, which are used to backfill the missing data and calms in the ISD data. This ASOS minute data can be found in the NCDC database, the same link as the previously discussed surface data. The ASOS data contains both TD 6405 and TD 6406 formatted files. For the purpose of creating a MET file, the data starts with 6405 followed by the desired year should be used. As the ASOS minute files are unusually large they need to be downloaded separately based on the months required

A.1.5 AERSURFACE Input

The AERSURFACE processor is developed to compute surface characteristic values such as albedo, Bowen ratio, and surface roughness length, in a modeling domain for use in AERMET (U.S. EPA, 2013). Much like AERMINUTE the data from AERSURFACE can be created or simplified by dividing the area of study into different sectors and giving each sector an albedo, Bowen ratio, and surface roughness, which can be helpful when the area of study can be measured for said parameters. For the sake of this project the AERSURFACE program was run using National Land Cover Data from 1992 (NLCD 92) from the United States Geological Survey at the following link; https://www.mrlc.gov/viewerjs/.

A.2 Meteorological Files Generated by AERMET

Five consecutive years (2012-2016) of off-site surface meteorological data were generated for use in the dispersion modeling of the Houston North Loop site, and the same five years for the Fort Worth California Parkway North site. Two years (2015-2016) of site-specific meteorological parameters for the Houston North Loop and the Fort Worth California Parkway site were generated from AERMET by using the on-site data from TCEQ's CAMS C1052 and C1053 in conjunction with respective upper air, ISD, and ASOS data, as listed in Table 1. Each file is named with index codes in the following fashion:

File Name:	Site_Surface_Upper_Year_SR.File
Site =	Onsite or offsite
Surface =	Station ID for surface data
Upper =	Station ID for upper air data
Year =	year of data in 2 digits
SR =	Surface Roughness (High: 10 cm; Medium: 5 cm; or Low: 1 cm)

File = File extension, PFL for profile data and SFC for surface data

For example, File ONSITE_IAH_LCH_15H.SFC is the site-specific (ONSITE) hourly surface data (SFC) for the year of 2015 using upper air data from Lake Charles (LCH), surface data from Houston International Airport (IAH), and surface roughness of 10 cm (H) for AERMOD modeling.

Meteorological Data for CAL3QHCR

CAL3QHCR is a U.S. Environmental Protection Agency (EPA) Gaussian air dispersion model and an enhanced version of CAL3QHC, a CALINE3 based model with queuing and hot spot calculations and with a traffic model to calculate delays and queues that occur at signalized intersections (Eckhoff and Braverman, 1995). A major change between models includes CAL3QHCR's ability to process up to a year of hourly meteorological data. A meteorological file for CAL3QHCR must include wind vector (degrees), wind speed (meters/sec), ambient temperature (K), stability class, and mixing heights. These files can also be created using available EPA auxiliary meteorological processors and downloaded meteorological data.

Data from the National Weather Service (NWS) or National Climatic Data Center (NCDC) formatted data can be processed through EPA's meteorological processors and accessory programs such as, the Meteorological Processor for Regulatory Models (MPRM), PCRAMMET, or RAMMET programs, as recommended by the EPA (U.S. EPA, 1999). Unfortunately, the NCDC has ceased to process NWS or NCDC formatted data for use in any of the meteorological processors. Therefore, it becomes incumbent to the research team to process the necessary meteorological data for use in the CAL3QHCR modeling.

Among the EPA recommended meteorological processors, PCRAMMET is selected for this study because it has been widely used by EPA in preparing National Weather Service (NWS) data for use in the Agency's short term air quality dispersion models such as CAL3QHCR, ISCST3, CRSTER, RAM, MPTER, BLP, SHORTZ, and COMPLEX1 (U.S. EPA, 1999). The minimum input data requirements to PCRAMMET are the twice-daily mixing heights, hourly surface observations of wind speed and wind direction, dry bulb temperature, opaque cloud cover, ceiling height, and station pressure, if calculating dry deposition. These parameters can be obtained from the NCDC database with the exception of the twice-daily mixing heights. Since the NCDC no longer provides the mixing height data, it needs to be independently processed by using the EPA's Mixing Height Program (MIXHGT) program in conjunction with surface data and radiosonde upper air files (U.S. EPA, 1998).

B.1 HUSWO Surface Meteorological Data

Both PCRAMMET and MIXHGT can read surface meteorological data in either HUSWO, SCRAM, or CD-144 formats. Because the NCDC does not provide meteorological data in these readable formats, data must be arranged in one of these formats using a text editor or other methods. The HUSWO format was selected in this study to process on-site and off-site surface meteorological data.

LCD data was chosen over ISD for i) its greater degree of completeness and inclusion of ceiling height and sky cover, required inputs for MIXHGT and because ii) the ISD data consists of a high percentage of missing values. The more robust LCD data allows the MIXHGT program to calculate more mixing heights.

Two years (2015-2016) of site-specific meteorological parameters (such as dry bulb temperature, wind direction, and wind speed) for the Houston North Loop site were obtained from the TCEQ CAM stations C1052 to develop site-specific meteorological files, and from C1053 for the Fort Worth California Parkway site. Table 2 shows the HUWSO format parameters in the

meteorological data file, units, and the source and station code used to download meteorological data. Some parameters are not used in CAL3QHCR or MIXHGT but must be included in the HUSWO format chosen; these parameters are preserved in the file but filled with missing data identifiers. PCRAMMET assumes the HUSWO data was retrieved in English units. Therefore, wind speeds in HUSWO are converted from miles per hour to meters per second (m/s). Wind speeds below 1.0 m/s (calms included) are set to 1.0 m/s before computations are made in PCRAMMET (U.S. EPA, 1999). Missing temperature, wind direction, and wind speed values from the CAM stations are replaced by the averages of the adjacent values, the previous and next hour of data. This method is recommended by the U.S EPA for data sets that are less than 90% complete (Atkinson and Lee, 1992). For off-site meteorological files using NCDC airport data, large amounts of missing data were supplemented by using meteorological data from a nearby TCEQ CAM station; this was the case for the off-site file required for the Fort Worth California Parkway location, replacing missing NCDC with values from CAM station C1002 Fort Worth Northwest.

Table 2 HUSWO Meteorological Data File

	Parameter	Units	Data Source	Data Source Station
1	Station ID	Station Number (WBAN)	NCDC	IAH, FTW
2	Time	Year-Month-Day-Hour	NCDC	IAH, FTW
3	Global Radiation	Nearest Tenth Watt Per Meter Squared	-	-
4	Direct Radiation	Nearest Tenth Watt Per Meter Squared	-	-
5	Total Sky Cover	Amount of Sky Dome (In Tenths) Covered by Clouds. 99 = Missing	NCDC	IAH, FTW
6	Opaque Sky Cover	Amount of Sky Dome (In Tenths) Covered by Clouds. 99 = Missing	NCDC	IAH, FTW
7	Dry Bulb Temperature	Degrees Fahrenheit	TAMIS	C1052, C1053
8	Dew Point Temp	Degrees Fahrenheit	NCDC	IAH, FTW
9	Relative Humidity	Percent	NCDC	IAH, FTW
10	Station Pressure	Hundredths Of Inches	NCDC	IAH, FTW
11	Wind Direction	Degrees	TAMIS	C1052, C1053
12	Wind Speed	Miles Per Hour (Mph)	TAMIS	C1052, 1053
13	Visibility	Miles	NCDC	IAH, FTW
14	Ceiling Height	Feet	IEM	IAH, FTW
15	Present Weather	Code	NCDC	IAH, FTW
16	ASOS Cloud Layer 1	Sky Condition Code 00-09	-	-
17	ASOS Cloud Layer 2	Sky Condition Code 00-09	-	-
18	ASOS Cloud Layer 3	Sky Condition Code 00-09	-	-
19	Hourly Precipitation	Hundredths Of Inches	NCDC	IAH,FTW
20	Snow Depth	Inches	NCDC	IAH, FTW

B.2 MIXHGT Mixing Height Data

MIXHGT requires two input files, the HUSWO surface file and a separate radiosonde upper air data file which can be obtained from the National Oceanic and Atmospheric Administration (NOAA) database. The output of MIXHGT provides the mixing height data file needed for use in PCRAMMET. Missing mixing height values were found with the previously stated method of averaging the adjacent values from the previous and next entry of data.

B.3 Meteorological Files Generated by PCRAMMET

Meteorological files generated by PCRAMMET for CAL3QHCR modeling are named the same way as discussed in Section A.2 with additional identifier in the extension.

File Name: Site_Surface_Upper_Year_SR.File
Site = Onsite or offsite
Surface = Station ID for surface data
Upper = Station ID for upper air data
Year = year of data in 2 digits
SR = Surface Roughness (N: not requires)
File = File extension, ISC for surface data and ADJ for adjusted wind data.

For example, File ONSITE_IAH_LCH_15_N.ISC is the site-specific (ONSITE) hourly surface data (ISC) for the year of 2015 using upper air data from Lake Charles (LCH), surface data from Houston International Airport (IAH), and no specified surface roughness (N) for CAL3QHR modeling.

It was discovered during the cross check of the surface meteorological data files generated by PCRAMMET and AERMET for using in AERMOD and CAL3QHR modeling that the hourly wind direction and wind speed do not agree with each other completely. As understood, ASOS 1-minute data is used to supplement the ISD surface hourly meteorological data in AERMINUTE because ISD hourly surface meteorological data often includes high incidence of calms and variable wind conditions (O'Donnell, 2014). Although using the same ISD and ASOS data for the same site, the algorithms used by NCDC (for processing the LCD file) and by EPA (for processing the SFC file) to process the data are likely different and would be the primary cause for the discrepancies in wind direction and wind speed. In order to evaluate the sensitivities of non-meteorology related parameters (e.g., source characterization, time-varying emission) on the downwind concentrations estimated by AERMOD and CAL3QHR, additional set of ISC data files were generated by replacing the wind speed and wind direction in the ISC files with the corresponding values in SFC files. These ISC files are named with a new extension ADJ and can also be used in CAL3QHCR to assess the uncertainties resulted from the use of different meteorological data.

References

Atkinson, D., and Lee, R.F. 1992. Memo: Procedures for Substituting Values for Missing NWS Meteorological Data for Use in Regulatory Air Quality Models. NC: U.S. Environmental Protection Agency.

Eckhoff, P.A., and Braverman, T.N. 1995. User's Guide to CAL3QHC Version 2.0 (CAL3QHCR User's Guide), Research Triangle Park, NC: U.S. Environmental Protection Agency.

O'Donnell M., 2014. Course #296 Health Risk Assessments and Dispersion Modeling, California-EPA Air Resources Board Compliance Training Section, http://docplayer.net/54555831-Course-296-health-risk-assessments-and-dispersion-modeling.html

United States Environmental Protection Agency (U.S. EPA). 1998. User Instructions: Computing Twice-Daily Mixing Heights from Upper Air Soundings and Hourly Temperatures. Office of Air Quality Planning and Standards Emissions, Monitoring, and Analysis Division Research. Triangle Park, NC.

United States Environmental Protection Agency (U.S. EPA). 1999. PCRAMMET User's Guide. EPA-454/B-96-001. Office of Air Quality Planning and Standards Emissions, Monitoring, and Analysis Division Research. Triangle Park, NC.

United States Environmental Protection Agency (U.S. EPA). 2016. User's Guide for the AERMOD Meteorological Preprocessor (AERMET). EPA-454/B-03-002. U.S. Environmental Protection Agency, Research Triangle Park, NC.

United States Environmental Protection Agency (U.S. EPA). 2013. AERSURFACE User's Guide. EPA-454/B-08-001. Office of Air Quality Planning and Standards Emissions, Monitoring, and Analysis Division Research. Triangle Park, NC.

Vita

Ivan M. Ramirez was born in El Paso, Texas, on March 2, 1994. He attended school in Ciudad Juarez, Chihuahua up to 2nd grade, he then started 3rd grade in El Paso, Texas until he graduated from Americas High School in 2012. The following August after his high school graduation he started his Civil Engineering career at The University of Texas at El Paso, where he received his Bachelor of Science degree in 2017. In August 2017 he began pursuing his degree of Masters of Science in Environmental Engineering which was received in June 2021.